Understanding Properties of Zwitterionic Materials from Their Molecular Structures

Qing Shao

A dissertation

Submitted in partial fulfillment of the

Requirements for the degree of

Doctor of Philosophy

University of Washington

2014

Reading Committee:

Shaoyi Jiang, Chair

Jim Pfaendtner

Valerie Daggett

Program Authorized to Offer Degree:

Chemical Engineering

University of Washington

Abstract

Understanding Properties of Zwitterionic Materials from Their Molecular Structures

Qing Shao
Chair of the Supervisory Committee:
Professor Shaoyi Jiang
Department of Chemical Engineering

Materials that resist nonspecific protein adsorption in complex media are important for many biological and chemical applications, such as surface coatings of biosensors, marine coatings, drug delivery, and therapeutic protein protection. Zwitterionic materials have shown unique properties for this purpose. But two critical questions about zwitterionic materials remain unsolved. First, why are zwitterionic materials different from non-ionic materials? Second, what are the differences among zwitterionic materials? This work aims to answer the two questions and design new zwitterionic materials based on the solutions. To study the differences between zwitterionic and non-ionic materials, this work investigated the effects of carboxybetaine (CB) and oligo(ethylene glycol) (OEG) moieties on protein structure and hydrophobic interactions. Non-ionic OEG moieties present amphiphilic features. They mask the hydrophobic domains of protein surfaces and impede hydrophobic associations in aqueous solutions. Zwitterionic CB moieties present superhydrophilic features. They do not influence hydrophobic substrates

and hydrophobic associations. To study the differences among zwitterionic materials, this work studied hydration, ionic interactions, and self-associations of CB and sulfobetaine (SB) moieties; and the influences of carbon spacer length on hydration and ionic interactions of CB moieties. This work employed quantum mechanics, molecular dynamics simulations, free energy perturbation methods and well-tempered metadynamics simulations. Finally, properties of 12 zwitterionic moieties were studied to look for new nonfouling zwitterionic materials. The work suggests three criteria for assessing protein-resistant zwitterionic materials: strong hydration, few or moderate self-associations, and few specific interactions with proteins.

TABLE OF CONTENTS

List of Figures

List of Schematics

List of Tables

Acknowledgements

The author would like to give acknowledgment to financial support through the Office of Naval Research (N00014-10-1-0600), Defense Threat Reduction Agency (HDTRA1-10-1-0074), National Science Foundation (CBET-0854298, CBET-126477, CMMI-0758358, and CBET-0854298), and American Chemical Society, Petroleum Research Fund(ACS PRF #48096-AC7). The author would like to thank the members of Jiang research group, especially Dr. Yi He, Andrew White and Luo Mi for helpful discussions. The author would also like to thank Professor Jim Pfaendtner and the members of the Pfaendtner group for helpful discussion about molecular simulation techniques. The work in this thesis was also supported in part by the National Science Foundation through TeraGrid resources provided by NICS and TACC under grant number TG-CHE110006. The work in this thesis was facilitated through the use of the advanced computational, storage, and networking infrastructure provided by the Hyak supercomputer system, supported in part by the University of Washington eScience. Finally, the author thanks Professor Shaoyi Jiang for discussion, advisement and funding for all presented works.

Chapter 1. Introduction

Materials that resist biofouling are important in biological and chemical applications, including surface coatings of biosensors[1-2], scaffolds for tissue engineering[3], contact lenses, marine coatings[4], vehicles for drug delivery[5-7], and polymeric protection of therapeutic proteins[8]. The materials need to resist biofouling in complex media[9], and are required to not influence any critical processes unintentionally. In regard to these two criteria, zwitterionic materials have shown excellent performance[10]. Zwitterionic materials possess moieties with both cationic and anionic groups. They resist non-specific protein adsorption in 100% blood serum[11], prevent the formation of capsule *in vivo* for up to three month[12], and protect the chymotrypsin against denaturing effects of heating and urea without scarifying the activity of the protein[8].

The first successful synthesis of zwitterionic materials was reported in 1950s[13]. After that, many studies have been carried out on the synthesis and solution properties of zwitterionic materials, and their applications. The review of Lowe et al. has well summarized the synthesis and solution properties of zwitterionic materials[14].

Ishihara et al.[15] showed that zwitterionic 2-methacryloyloxyethyl phosphorylcholine (MPC) polymers could function as a protein-adsorption-resistant additive. The ability of MPC materials to reduce protein adsorption was initially attributed to the fact that they have the same chemical groups as cell membranes[15] do. The study of Chen et al.[16] showed that the key is the zwitterionic feature that results in strong hydration of materials via electrostatic interactions. The simulation study of Yi et al.[17] also showed that the hydration of zwitterionic self-assembled monolayers (SAMs) is stronger than the hydration of PEG materials. Strong hydration is critical to the nonfouling properties of

materials[18]. Therefore, the strong hydration brought by the zwitterionic feature was determined to be the reason of the excellent nonfouling properties of zwitterionic materials.

After the nonfouling mechanism was revealed, carboxybetaine (CB) and sulfobetaine (SB) materials showed super low fouling properties first time and have been extensively used since then[19-20]. The zwitterionic moieties of CB and SB materials are similar to some naturally occurring osmolytes, but the nonfouling properties of these two materials should be due to their strong hydration. As stated above, both of these two materials showed nonfouling properties in complex media. In addition, SB materials are stimuli responsive[21] and CB materials are functionalizable[22]. The excellent nonfouling properties and the capability to couple with other desired properties make zwitterionic materials good platforms to develop biological and chemical applications.

However, two fundamental questions about zwitterionic materials remain unsolved. First, why do zwitterionic materials perform differently from non-ionic materials? Second, what are the differences among various zwitterionic materials? The answers to these two questions will not only explain the current applications of zwitterionic materials, but also help to design new zwitterionic materials. This thesis presents experimental and computational simulation studies to answer the two questions above and design new nonfouling zwitterionic materials beyond CB and SB materials. Chapters 2 and 3 will present the studies about the differences of zwitterionic CB and non-ionic OEG moieties in their influences on protein structure and hydrophobic interactions. These two chapters will provide insights in the different performance between zwitterionic and PEG materials. CB and SB materials are the most widely used

zwitterionic materials today. Chapters 4 to 6 will present the studies about the differences between CB and SB moieties in their hydration, ionic interactions, and self-associations among zwitterionic moieties. These studies, in line with experimental observations, will provide insights in the structure-property relationship of zwitterionic materials. Chapter 7 will present the influence of carbon spacer length on hydration and ionic interactions of CB moieties. Chapter 8 will present a computational design of new zwitterionic moieties beyond CB and SB moieties. Chapter 9 will summarize all the studies above.

Chapter 2. Different Effects of Carboxybetaine and Oligo(ethylene glycol) Molecules on Protein Structure

This chapter presents a molecular simulation study on the different effects of zwitterionic carboxybetaine (CB) and non-ionic oligo(ethylene glycol) (OEG) moieties on the structure of a chymotrypsin inhibitor 2 (CI2). We studied the radial distribution functions between the two solutes and the Cα atoms of the 64 residues of CI2, the average numbers of solute-protein and water-protein hydrogen bonds, the root mean square deviation (RMSD) of the Cα atoms of the protein, and the solvent accessible surface area (SASA) of the protein. CB moieties have a minimal effect on the protein due to the shared zwitterionic nature of CB and protein whereas non-ionic OEG moieties alter the flexibility and SASA of hydrophobic domains of the protein.

2.1. Introduction

Protein-solute interactions are attracting increasing attention because of their critical roles in protein structure and function[23-25]. The structure and bioactivity of a protein can be altered by exposing to different solutes[26-30].

Solutes with different chemical structures can share similar effects on proteins. For instance, trimethylamine N-oxide (TMAO), glycine betaine, sorbitol, trehalose and glycerol are all recognized as protein stabilizers[25], and their mechanisms of action have been extensively studied experimentally[31-32] and theoretically[33-40]. Molecular dynamics simulations[34-37, 40] have shown that these five solutes, despite their different chemical structures, share the common feature that they do not accumulate near the protein surface. Instead, the solutes distribute throughout the solvent, enhance the water structure, and slow water mobility. The low water mobility and enhancement of water structure is

suggested to be responsible for protecting the native structure of a protein [41]. The protein is surrounded by slower solvent molecules while the solute molecules are excluded from the protein surface. This phenomenon implies that protein stabilizers may be potential candidates to develop non-specific protein resistant materials because they do not associate with proteins[42]. This hypothesis was tested with a number of materials based on the protein stabilizers. Anand et al.[43] also showed that the self-assembly of TMAO on CH_3-self assembled monolayers can form a low protein-adsorbing surface.

However, because of the chemical heterogeneity of proteins, solutes with different chemical features may interact distinctly with proteins, even though they share common properties. Identifying the difference among various solutes is critically important for both fundamental understanding and practical applications. Recent experiments of Keefe et al.[8] showed that polycarboxybetaine (PCB) can stabilize the chymotrypsin as well as polyethylene glycol (PEG), but without sacrificing the enzymatic activity. This indicates that CB and EG may share some common properties to protect a protein, but interact with the protein differently.

CB and EG moieties have different characteristics. CB is a zwitterionic moiety possessing both cationic and anionic groups. Its structure is similar to naturally occurring glycine betaine. OEG is a neutral moiety with a structure similar to polyols, which can protect proteins. It is also interesting to note that EG-type solutes can stabilize[44-45] or destabilize[44, 46] proteins, depending on the structure of the protein, the molecular weight and concentration of the solutes, and other environmental factors such as temperature and presence of other solutes. Our previous study[47] has shown that the local hydration structure of a CB moiety differs from that of an OEG moiety, though both are highly

hydrated. The hydration free energy of the former is lower than the one of the latter[48], indicating that the CB moieties may be more hydrophilic. This also indicates that these two solutes may interact with proteins differently. A thorough comparison of the effects of CB and OEG moieties on proteins is therefore critical to not only distinguish these two solutes and provide insights in how solutes with different chemical structures can interact with a protein, but also provide a guide for the rational design of biomaterials.

In this work, we studied the interactions of CB and EG moieties with CI2, a model protein, using molecular dynamics simulations. We selected EG_4 moieties as the representative OEG moieties[47-48]. The main objective is to explore the common and different effects of these two solutes on a protein by comparing the spatial distribution of solutes around the protein, protein flexibility, and surface areas of different domains.

2.2. Simulation Details

The structures of CB and EG_4 moieties are shown in Figure 2.1. We selected chymotrypsin inhibitor 2 (CI2) (pdb ID: 1ypc) as the model protein since its protein-solute interactions have been extensively studied[34]. All atom models were used in this work. The SPC/E model[49] was used to represent water molecules because of its good representation of the dipole moment, dielectric constant and diffusion properties of water molecules.

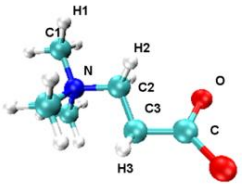

(a)

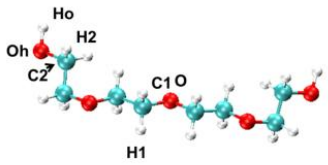

(b)

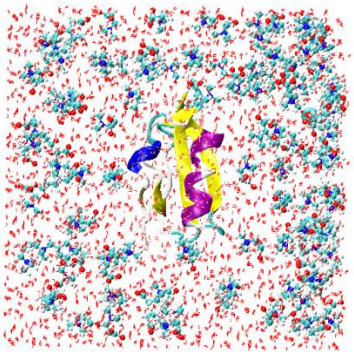

(c)

Figure 2.1. Structures of carboxybetaine and OEG moieties and the initial configuration of the simulation system. (a) CB; (b) EG_4 and (c) the initial configuration of CB1 case.

The potential energy of intermolecular interactions is calculated as a combination of a Lennard-Jones (L-J) 12-6 potential and a Coulombic potential, as shown in Equation 2.1

$$U(r_{ij}) = 4\varepsilon_{ij}\left[\left(\frac{\sigma_{ij}}{r_{ij}}\right)^{12} - \left(\frac{\sigma_{ij}}{r_{ij}}\right)^{6}\right] + \frac{q_i q_j}{r_{ij}} \qquad (2.1)$$

where r_{ij} is the distance between atoms i and j, q_i is the partial charge assigned to atom i, and ε_{ij} and σ_{ij} are energy and size parameters obtained by Jorgensen combining rules.

In simulations of zwitterionic molecules, the proper description of their partial charges is particularly important. To obtain the partial charges of the CB molecule, we carried out quantum calculations with DFT-B3LYP/6-31G** and CHELP with Gaussian 09[50]. The calculations were carried out using GridChem system[51]. The L-J parameters were obtained from the OPLS all atom force field[52] developed by Jorgensen group because of

the force field's good representation of small organic molecules. The bond interaction parameters were also derived from OPLS all atom force field. Table 2.1 lists the L-J parameters and partial charges for EG_4 molecule and CB molecule. The parameters for protein were derived from OPLS all atom force field[52].

Table 2.1. Force field parameters of EG_4 and CB molecules as labeled in Figure 2.1

	σ (nm)	ε (kJ·mol^{-1})	q (e)		σ (nm)	ε (kJ·mol^{-1})	q (e)
EG_4				CB			
O	0.290	0.5858	-0.4000	N	0.325	0.7113	0.3516
C1	0.350	0.2761	0.1400	C1	0.350	0.2761	-0.3226
H1	0.250	0.1255	0.0300	H1	0.250	0.0628	0.1514
C2	0.350	0.2761	0.1450	C2	0.350	0.2761	0.0200
H2	0.250	0.1255	0.0600	H2	0.250	0.0628	0.0660
Oh	0.312	0.7113	-0.6830	C3	0.350	0.2761	-0.1262
Ho	0.000	0.0000	0.4180	H3	0.250	0.1255	0.0360
				C	0.375	0.4393	0.9070
				O	0.296	0.8786	-0.8756

The simulation system was a periodic solvent box containing water molecules, solute molecules, one protein molecule and two Cl^- anions as counter ions. We noticed that the EG_4 and CB molecules have different molecular weights and volumes. To compare them fairly, we used one EG_4 simulation system and three CB simulation systems, as listed in Table 2.2. The recent investigation of Silow et al.[44] showed that EG solute types increase the folding rate of CI2 at concentrations < 4 M, and the EG_4 system used in this work is within this concentration and thus should not destabilize the protein. The three CB simulation systems have the same mole, mass or volume of CB solutes with the

corresponding values of the EG_4 system. The numbers of water molecules are consistent in these four simulation cases. We also simulated a case with only CI2 and counterions in pure water as the reference, which is also listed in Table 2.2. Figure 2.1(c) shows the initial configuration of the CB1 case, which was produced with the Visual Molecular Dynamics program (VMD)[53].

Table 2.2. Five simulation cases

Name	Solute type	Solute number	Water number	Molar con. (M)	Mass con. (%)	VDW solute vol. (nm^3)
Water	N/A	N/A	3250	N/A	N/A	N/A
EG4	EG_4	100	5500	1.0	15.3	19.7
CB1	CB	100	5500	1.0	11.0	13.9
CB2	CB	140	5500	1.4	14.8	19.5
CB3	CB	150	5500	1.5	15.6	20.9

Molecular dynamics (MD) simulations were performed using Gromacs-4.5.1[54] in an isobaric-isothermal (NPT) ensemble. After energy minimization and a 100.0 ns MD run with an integral step of 1.0 fs for equilibrium, another 100.0 ns MD run was carried out to collect data. The coordinates were saved every 2.0 ps. Long-range electrostatic interactions were computed with the particle mesh Ewald method[55] with periodic boundary conditions in all three dimensions. The short-range van der Waals interactions were calculated with a cutoff distance of 1.1 nm. For each simulation case, the first 100 ns MD simulation was maintained at 298 K (0.1 ps time constant) and 100.0 KPa with the Berendsen algorithm[56] (with a compressibility of 4.5×10^{-5} bar^{-1} and a 1 ps time constant). For the next 100 ns for data collection, temperature was maintained at 298 K with Nose-Hoover thermostat[57-58], and pressure was coupled with Parrinello-Rahman method[59]. Intramolecular bonds of molecules involved hydrogen atom were kept constrained with the LINCS algorithm during simulations[60].

2.3 Results and Discussion

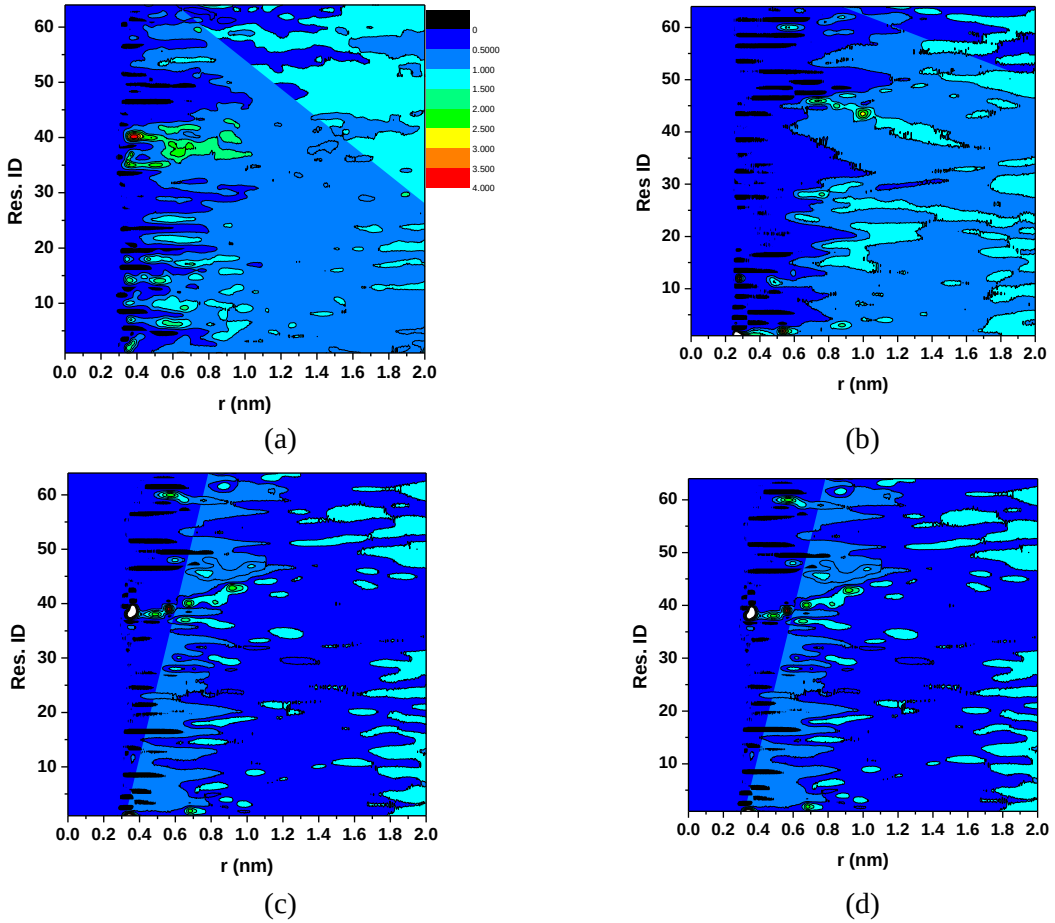

Figure 2.2. Radial distribution functions (RDFs) between the oxygen atoms of the solutes and the Cα atoms of each residue in CI2. (a) EG4, (b) CB1, (c) CB2 and (d) CB3.

To investigate whether CB or EG_4 molecules are concentrated or expelled from the protein surface, we analyzed the radial distribution functions (RDFs) between the solute molecules and the CI2. Because of the chemical heterogeneity of the protein, we investigate the RDFs of the selected atoms of solute molecules and the Cα atoms of the 64 residues of CI2 instead of the RDFs between the centers of mass of the solutes and protein. We selected the two oxygen atoms in CB molecules because of their importance in the hydration of CB[48] and the five oxygen atoms of EG_4 molecules. Figure 2.2 shows the RDFs of the oxygen atoms of CB and EG_4 molecules and the Cα atoms of 64 residues

in the CI2. As shown in Figure 2.2(a), for most residues, the RDFs of EG4 case are less than 1.5. This indicates that the EG_4 molecules do not significantly associate with the protein, consistent with the observations of trehalose and glycerol[37, 40]. From Figures 2.2(b)-(d), we can find that, for most residues, the RDFs of CB cases are less than 1.5. Thus the CB molecules also do not concentrate near the protein either, similar with the behavior of TMAO[7] and glycine betaine[8]. The RDF results here showed that both EG_4 and CB molecules do not accumulate near the protein surface, similar to protein stabilizers.

Nevertheless, the RDFs show that EG_4 and CB molecules associate specifically with certain residues of the CI2. As shown in Figure 2.2(a), EG_4 molecules mainly associate with six nonpolar and polar residues. Among them, the nonpolar Ala40 residue has the highest peak with a value around 4.0 and the Gly35, Thr36, Ile37, Val38, and Thr39 residues have peaks around 2.0. However, the CB molecules only associate with Thr39, as shown in Figures 2.2(c) and 2.2(d). This is probably because CB is superhydrophilic and EG_4 is amphiphilic. A recent MD simulation study[40] showed that methanol and trifluoroethanol bound to non-polar side chains of a peptide, while more hydrophilic glycol and glycerol were excluded from its nonpolar side chains. This trend agrees well with what is observed for CB and EG_4 in this work. The different behavior implies that CB and EG_4 may influence the protein structure differently. Because EG_4 approaches more nonpolar residues, it may have more effect on the hydrophobic domain.

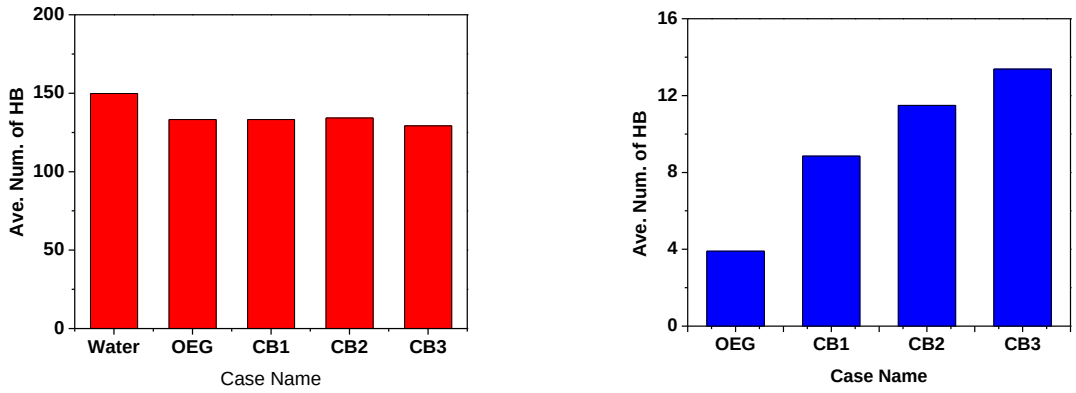

(a) (b)

Figure 2.3. Average numbers of hydrogen bonds. (a) protein-water and (b) protein-solute for five different solutes. Protein is CI2.

To further explore the protein-solute interactions, we investigated the hydrogen bonds (HBs) between them. We used the criteria of Luzar et al.[61] to define a hydrogen bond. Figure 2.3 shows the average numbers of water-protein, EG_4-protein and CB-protein hydrogen bonds per protein for five simulated cases. Bennion et al.[34] have shown that even with a concentration of TMAO as high as 4 M, the number of the protein-TMAO hydrogen bonds is still overwhelmed by the protein-water hydrogen bonds. The observation here for EG_4 and CB agrees well with this observation.

As shown in Figure 2.3b, the number of EG_4-protein hydrogen bonds (4.0) is less than the numbers of CB-protein hydrogen bonds in the CB1 (8.8), CB2 (11.5) and CB3 (13.4) cases. Shao et al.[40] showed that different hydrogen bonding interactions played a crucial role in the different effects of alcohol molecules on a polypeptide BBA5. The different hydrogen bond numbers between EG_4-protein and CB-protein implies that these two solutes may affect the protein structure differently.

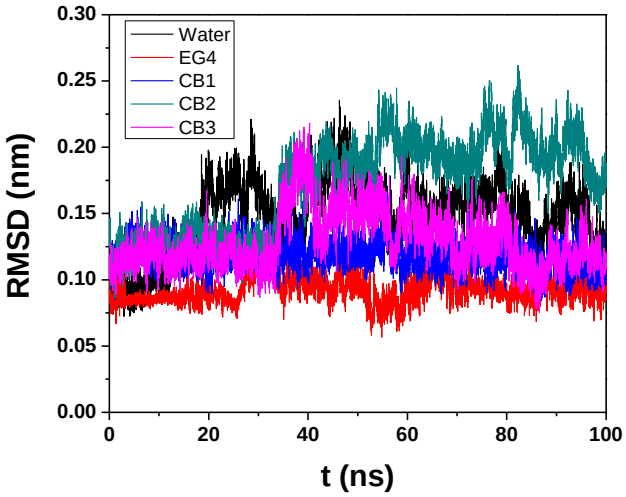

Figure 2.4. RMSD of the Cα atoms of CI2 in five simulated cases.

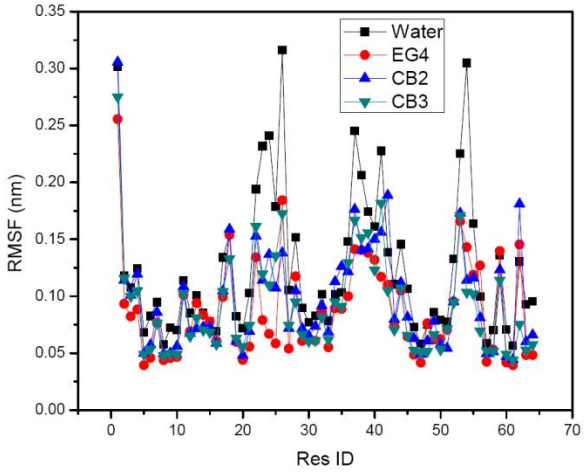

Figure 2.5. RMSF of the Cα atoms of CI2 in simulated cases.

The analysis of protein structure reveals the different effects of EG_4 and CB. Protein structure was first investigated with the root mean square deviation (RMSD) of the C-α atoms of CI2. Figure 2.4 shows the RMSD as a function of time for the five cases. In the simulation of Bennion *et al.*[34], an unfolded CI2 denatured by urea has RMSD as high as 0.6 nm and the one denatured by high temperature has RMSD around 0.5 nm; the folded protein has RMSD around 0.2 nm. In this work, the CI2 has RMSD around 0.2 nm in water case, agreeing well with the results of Bennion *et al.*[34]. From Figure 2.4, the

RMSDs of three CB cases are also around 0.2 nm during the 100-ns MD simulations, and their fluctuations are in the same scale of that of the water case. This similarity indicates that CI2 maintains its native structure and flexibility in the CB solutions just as in water. However, the RMSD of the EG4 case is around 0.09 nm, much lower than the RMSD of the water case. In addition, the RMSD fluctuation of the EG4 case is much less than that of the water case. Liu et al.[37] showed a similar RMSD reduction for CI2 in 0.5 M trehalose and glycerol solutions in their simulations. This implies that, although still folded, the protein in the EG_4 solution has structure closer to the crystal structure than the native one in water, and its flexibility decreases. In other words, the structure of protein in EG_4 solution deviates from the one in water more than the ones in the CB solutions. In addition, the protein in EG_4 solution is more rigid. The root mean square fluctuation (RMSF) in Figure 2.5 also indicates that the protein is more rigid in the EG_4 solution. Because the flexibility is critical to certain functions such as binding and catalysis [62-64], such a reduction in flexibility may influence protein's activity.

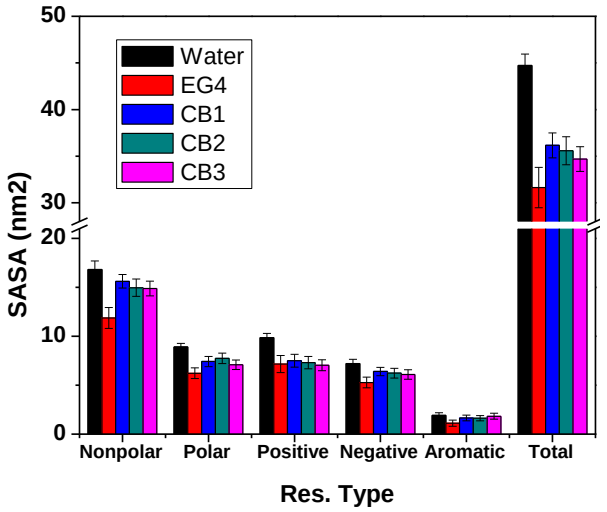

Figure 2.6. Solvent accessible surface area (SASA) of the nonpolar, polar, positive, negative and aromatic residues and their sum in the five simulation cases.

The difference between CB and EG_4 was also observed from the solvent accessible surface area (SASA) of CI2. We analyzed the SASA of CI2 with a probe of 0.14 nm radius. In the four cases of EG_4 or CB, the SASA calculations were carried out considering the solute molecules. To provide insights into the effects of these two solutes on different types of residues, we categorized the 64 residues of the CI2 into five types: nonpolar, polar neutral, positive charged, negative charged and aromatic based on their side chains. Figure 2.6 shows the SASAs of these five residue types in the five simulation cases.

As shown in Figure 2.6, the total SASA of CI2 decreases for both EG_4 and CB solutions. The SASA of a protein is expected to decreases when solute is added[65]. However, EG_4 and CB influence differently the SASA of nonpolar residues, while they influence similarly the SASAs of other four types of residues. The SASA of the nonpolar residues for the EG4 case is 11.87 ± 1.07 nm^2, considerably less than the corresponding SASA for the water case (16.82 ± 0.89 nm^2). However, the SASA of the nonpolar residues for the three CB cases are 15.62 ± 0.7, 14.96 ± 0.89 and 14.88 ± 0.75 nm^2, comparable to the one for the water case.

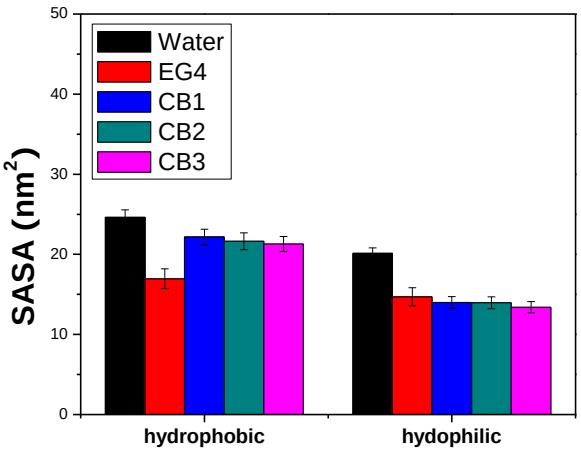

Figure 2.7. SASAs of hydrophobic and hydrophilic domains in the five simulation cases

Figure 2.7 shows the SASA of the hydrophobic and hydrophilic domains of the CI2 in the five cases. The hydrophobic domains were defined by all atoms with partial charges from -0.2 to 0.2. We can observe that the EG4 case has SASA of hydrophobic domains decreased much more than the CB cases. As shown in Figure 2.6, the SASAs of the hydrophobic domains of the three CB cases (22.16 ± 0.98 nm^2, 21.63 ± 1.06 nm^2 and 21.29 ± 0.94 nm^2) are 90.08%, 87.93% and 86.55% of the SASA of the water case (24.60 ± 0.96 nm^2), whereas the SASA of hydrophobic domains in the EG4 case (16.95 ± 1.24 nm^2) is only 68.90% of that of the water case. This means that nearly 1/3 of the hydrophobic domains originally accessible in the water solvent become inaccessible in the EG_4 solution, whereas the corresponding loss in the CB solution is only around 1/10.

This difference is due to that CB moieties consist of two charged groups and are superhydrophilic, whereas EG_4 moieties are amphiphilic with hydrophobic nature. The EG_4 moieties used in this work are capped with hydrophilic –OH groups to decrease their hydrophobicity. However, even with hydrophilic-group capped EG_4 moieties, nearly 1/3

of the hydrophobic domain of the protein is covered. Thus, we expect that the hydrophobic-group capped EG_4 molecules will cover more hydrophobic domain. The hydrophobic domain is generally recognized to play an essential role in the protein bioactivity (e.g., substrate binding or catalysis), and aggregation. Chennamsetty et al.[41] showed a correlation between the domain with high hydrophobicity and the known aggregation domain using the spatial aggregation propensity (SAP) analysis they developed. Thus, different effects of CB and EG_4 solutes on the SASA of the hydrophobic domain signal the dramatic differences between these two types of materials on protein bioactivity and aggregation. As shown in Figure 2.6, the SASA of hydrophilic domains decreases with both EG_4 and CB to a similar degree. The effect of CB on the SASA of domain is not sensitive to concentration variation. From CB1 case to CB3 case, as the concentration increases from 1.0 to 1.5 M, the SASA of the respective domain is nearly the same.

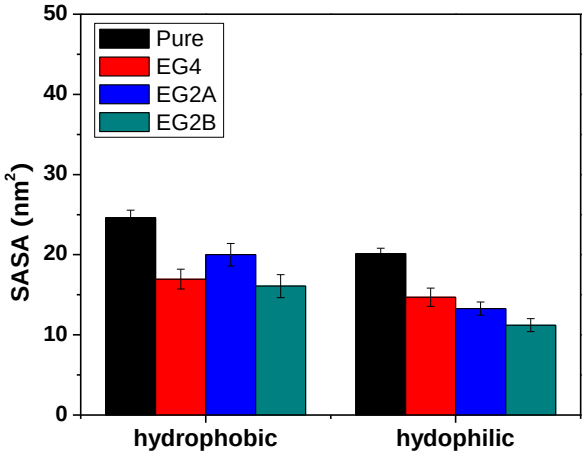

Figure 2.8. SASAs of hydrophobic and hydrophilic domains in the Pure, EG4, EG2A and EG2B cases.

For the results presented above, EG_4 moieties have been used. To investigate if the molecular length and concentration of OEG solutes will affect our findings, we simulated two cases with 100 and 200 EG_2 moieties, named as EG2A and EG2B. The details of the simulation system are exactly the same as the EG4 case. The EG2A case has the same mole, while the EG2B case has the same mass and volume of solutes as the EG4 case. 50 ns MD simulation was performed for each case in the same way as described in section 2.2 and the last 25 ns was used to collect data. Figure 2.8 shows the SASAs of hydrophobic and hydrophilic domains for these two cases. We can observe that, in EG2A case, the SASA of hydrophobic domain is 20.00 ± 1.40 nm^2, larger than that in the EG4 case. This is expected because the volume of solute in EG2A case is only around half of that in the EG4 case. In the EG2B case, which has the same solute volume as the EG4 case, the SASA of hydrophobic domain is 16.08 ± 1.44 nm^2, comparable to that of EG4 case. It is interesting to note that the EG_2 molecule is more hydrophilic than the EG_4 molecule because of the hydrophilic cap we used. Therefore, though the SASA of hydrophobic domains varies with the molecular length and concentration of EG solute, it does not affect the conclusion that OEG molecules affect the hydrophobic domain more than CB molecules.

2.4 Conclusions

In this work, we investigated the similarities and differences in the effect of CB and OEG solutes on CI2 using MD simulations. We analyzed the RDFs between the solutes and the protein, the solute-protein and water-protein hydrogen bonds and the structure properties of CI2 including the RMSD and SASA. The results show that, although their chemical structures are different, these two solutes share a common feature that neither of

them preferentially accumulates near the protein surface, and keeps CI2 in its folded state. However, the EG_4 moieties associate with hydrophobic residues more than the CB moieties, and the later has more hydrogen bonds with the protein. CI2 has different flexibility and SASAs with these two solutes even though the protein is in folded state with both of them. In EG_4 solution, CI2 has reduced structural dynamics whereas the protein with CB solution has flexibility similar to that of CI2 in water. Compared to CI2 in pure water, the SASA of the hydrophobic domain decreases nearly 1/3 in solution of 1M EG_4, whereas the corresponding decrease in solution with CB of the same concentration is only around 1/10. Their effects on the hydrophilic domains are similar.

Chapter 3 Different Effects of Carboxybetaine & Oligo(ethylene glycol) Moieties in Alternating Hydrophobic Interactions

Polycarboxybetaine and poly(ethylene glycol) materials resist non-specific protein adsorption, but differ in influencing biological functions such as enzymatic activity. To investigate this difference, we studied the influence of carboxybetaine and oligo(ethylene glycol) moieties on hydrophobic interactions using molecular simulations. We employed a model system composed of two non-polar plates and studied the potential of mean force of plate-plate association in carboxybetaine, $(ethylene\ glycol)_4$ and $(ethylene\ glycol)_2$ solutions using well-tempered metadynamics simulations. Water, trimethylamine N-oxide and urea solutions were used as reference systems. We analyzed the variation of the potential of mean force in various solutions to study how carboxybetaine and oligo(ethylene glycol) moieties influence the hydrophobic interactions. To study the origin of their influence, we analyzed the normalized distributions of moieties and water molecules using molecular dynamics simulations. The simulation results showed that oligo(ethylene glycol) moieties repel water molecules away from the non-polar plates and weaken the hydrophobic interactions. Carboxybetaine moieties do not repel water molecules away from the plates and therefore do not influence the hydrophobic interactions.

3.1 Introduction

Materials that can resist non-specific protein adsorption are important for applications such as contact lenses[66], implanted medical devices[12] and biosensors[1]. Polycarboxybetaine (PCB) and poly(ethylene glycol) (PEG) are two typical nonfouling materials.[9, 48] They both resist nonspecific protein adsorption through strong hydration of

their moieties.[47-48, 67] Although they both display strong hydration, the two materials have different chemical moieties and some differences have been recently reported. For instance, Keefe and Jiang[8] studied the enzymatic activity of chymotrypsin conjugated by PEG or PCB chains. They found that PCB does not decrease the enzymatic activity as PEG does, indicating that they influence the molecular structure and/or interactions in biological systems differently. A recent simulation study[68] has also described different effects of small solutes, (ethylene glycol)$_4$ (EG_4) and CB moieties on protein structure. EG_4 moieties mask the hydrophobic domain of a protein more than CB moieties.

However, little is known about the differences between PEG and PCB in the ability to change molecular interactions in biological systems. Biological systems utilize a sophisticated balance of interactions to maintain homeostasis among these interactions, and hydrophobic interactions play one of the most important roles.[69-70] The hydrophobic interactions originate from the disruption of water-water hydrogen bonds by nonpolar solute[71], and are important in protein folding[72-73], cell membrane formation[74] and protein-ligand binding[75]. Research has shown that the hydrophobic interactions are susceptible to external influences, including ions, organic osmolytes, temperature and pressure[76-77]. Considering EG and CB have different molecular structures and hydration[48], we expect that the two materials will differently influence hydrophobic interactions.

Here we studied the effects of CB and oligo(ethylene glycol) (OEG) moieties on hydrophobic interactions using molecular simulations. A model system of hydrophobic interactions was chosen: the association of two nonpolar plates. The moiety concentrations in solutions were set to 1.0 M (CB, EG_4 and EG_2) or 2.0 M (EG_2). We used three reference systems: pure water, 1 M trimethylamine N-oxide (TMAO) solution

and 1 M urea solution. Previous studies have shown that TMAO molecules do not influence hydrophobic interactions[78] while urea molecules weaken them[79]. Therefore, water and TMAO systems served as the references for which hydrophobic interactions were not influenced while the urea system served as the reference for which hydrophobic interactions were weakened.

3.2 Simulation Details

3.2.1 Simulation Systems

For well-tempered metadynamics simulations, the simulation system includes two model nonpolar plates that were placed at an initial distance of 1.0 nm, 1126 water molecules and 20 moiety molecules. The initial lengths in *x* and *y* directions are 3.0 nm and the initial length in *z* direction is 4.0 nm. Figure 3.1a shows the configuration of the simulation system for the plates in the 1.0 M CB solution.

Table 3.1 Details of simulation systems

	moiety number	water molecule number	concentration (M)
1M CB	20	1126	1.0
1M EG_4	20	1113	1.0
1M EG_2	20	1113	1.0
2M EG_2	40	1110	2.0
water		1477	
1M TMAO	20	1100	1.0
1M urea	20	1666	1.0

The molecular dynamics (MD) simulations include the same numbers of molecules as the well-tempered metadynamics simulations. The plate-plate distances were set to their desired values. For instance, in a MD simulation to study the distribution of carboxybetaine (CB) moieties around the plates with a plate-plate distance of 0.45 nm, the initial plate-plate distance was set to be 0.45 nm.

3.2.2 Force Field Parameters

Water molecules in this work were represented with the TIP3P model[80]. We used the force field parameters developed by Kast et al.[81] to describe TMAO molecules, and the force filed parameters[82] developed in our previous work to describe CB molecules. EG_4, EG_2, and urea molecules were described by the OPLSAA force field[52].

A model nonpolar plate was composed of a sheet of 4×4 interaction sites. Each interaction site was described by the united-atom OPLS force field parameters for a methane molecule. The distance between nearby interaction sites is 0.3 nm and the *x* and *y* positions of the interaction sites were restrained by a force with a constant of 5000 kJ mol^{-1}.

A combination of a Lennard-Jones (L-J) 12-6 potential and a Coulomb potential (eq. 3.1) was used to calculate the non-bonded potential energy.

$$U(r_{ij}) = 4\varepsilon_{ij}\left[\left(\frac{\sigma_{ij}}{r_{ij}}\right)^{12} - \left(\frac{\sigma_{ij}}{r_{ij}}\right)^{6}\right] + \frac{q_i q_j}{r_{ij}} \qquad (3.1)$$

where r_{ij} is the distance between atoms *i* and *j*, q_i is the partial charge assigned to atom *i*, and ε_{ij} and σ_{ij} are energy and size parameters obtained by Jorgensen combining rules.

3.2.3 Details of Molecular Dynamics Simulation

After energy minimization and a 5.0 ns MD run with an integral step of 1.0 fs for equilibrium, another 10.0 ns run was carried out with integral step of 2.0 fs. The coordinates were saved every 0.2 ps. Long-range electrostatic interactions were computed with the particle mesh Ewald method with periodic boundary conditions in all three dimensions.[55] The short-range van der Waals interactions were calculated with a cutoff distance of 1.0 nm. During the 5.0 ns MD simulation for equilibrium, the system was

maintained at 298 K (0.1 ps time constant) and 100.0 kPa with the Berendsen algorithm[56] (with a compressibility of 4.5 × 10-5 bar^{-1} and a 1 ps time constant). During the 10.0 ns MD simulation for data collection, the system was maintained at 298 K with the Nose-Hoover algorithm[57-58]. Intramolecular bonds of moieties and water molecules involving hydrogen atoms were kept constrained with the LINCS algorithm.[60] The MD simulations were performed using Gromacs-4.5.5[83].

3.2.4 Details of Well-Tempered Metadynamics Simulation

Well-tempered metadynamics simulations[84] were used to calculate the potentials of mean force. This method was developed from traditional metadynamics[85] and improves the convergence of simulations since it rescales the hill weight factor. The collective variable was the distance between the centers of mass (COM) of the plates in the *z* direction. The initial hill height was set to be 1.5 kJ mol^{-1} and the deposition rate of the hill bias terms was set to be 200 fs with a bias factor of 10. The width σ for the hills was set to 0.05. The total production simulation times were 100 ns (water), 120 ns (1.0 M CB, 11.0 M TMAO and 1.0 M urea), 260 ns (1.0 M EG_4 solution), 260 ns (1.0 M EG_2 solution) and 140 ns (2.0 M EG_2 solution) with an output frequency of 200 fs.

The initial configurations used in the well-tempered metadynamics simulations were obtained after an energy minimization and a 5 ns MD simulation in order to equilibrate the systems. The plates were placed with a COM distance of 1.0 nm and the other details of the MD simulations and systems were described in section II.C. All the well-tempered metadynamics simulations were carried out in a NVT ensemble with v-rescale algorithm[86] to control the temperature at 298 K using Plumed-1.3.0[87] implemented Gromacs-4.5.5[83].

3.3 Results and Discussion

3.3.1 Potential of Mean Force

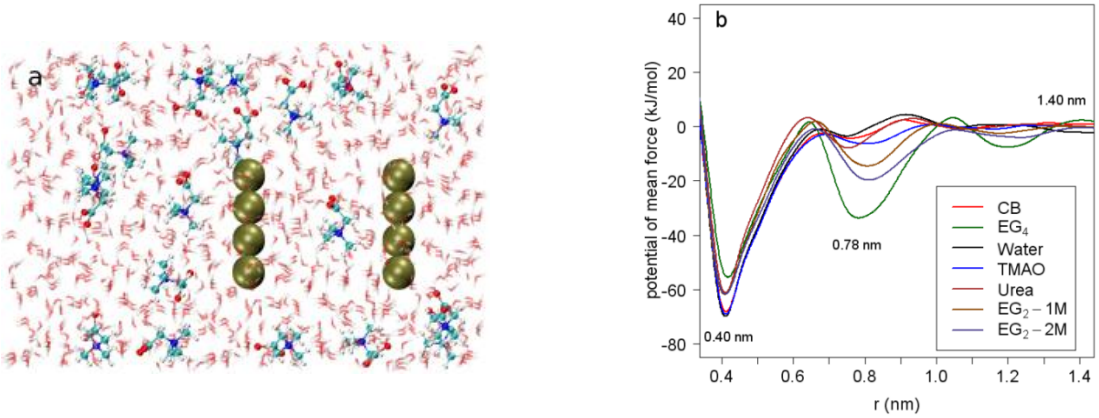

Figure 3.1. (a) Representative configuration of the simulation system of the 1.0 M CB solution. The water molecules are displayed with a line model. The interaction sites of the nonpolar plate are displayed with a tan colored VDW model. The CB moieties are displayed with a CPK model. (b) Potentials of mean force (PMFs) of the plate-plate associations in the CB, EG_4, and EG_2 solutions and the three reference systems (water, 1.0 M TMAO, and 1.0 M urea).

Figure 3.1b shows the potentials of mean force (PMFs) of the plate-plate associations in various solutions as a function of the plate-plate distance *r*. Convergence of metadynamics simulations was investigated through the variation of potentials of mean force as a function of simulation time, as shown in Figure 3.2. The PMFs show the difference between CB and EG_4 in their effects on hydrophobic interactions. The PMF of CB solution is identical to the PMF of water. The PMF profile in the TMAO solution is also similar to the one in water. Athawale et al.[78] studied the effect of TMAO on assembly of a hydrophobic polymer chain. They concluded that TMAO has a negligible effect on hydrophobic interactions based on the similar free energy profiles of assembly in the TMAO solution and in neat water. Thus the similar PMFs of CB solution and water indicate the CB moieties also have a negligible effect on hydrophobic interactions.

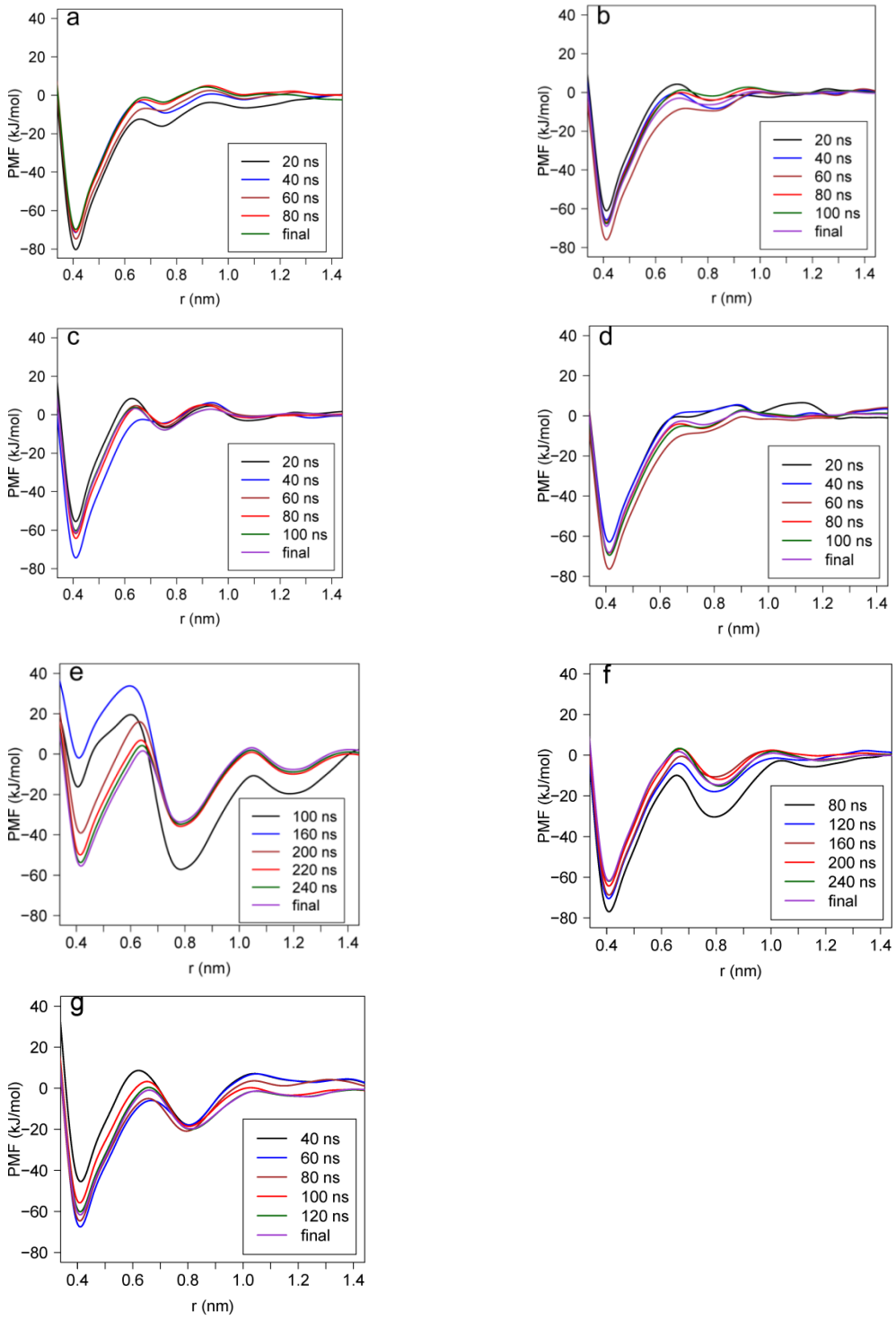

Figure 3.2 Potentials of mean force for plate-plate associations in various solutions as a function of simulation time. (a) water, (b) 1M TMAO, (c) 1M urea, (d) 1M CB, (e) 1M EG_4, (f) 1M EG_2 and (g) 2M EG_2 solutions.

The PMF of EG_4 solution differs from the PMF of water in two aspects: The minimum at 0.4 nm increases by 10 kJ mol^{-1} and a new minimum occurs at 0.78 nm with a value of around -40 kJ mol^{-1}. The minimum at 0.4 nm represents the state that the two plates associate directly, and its value is the free energy of this direct association. The upside movement of minimum therefore means a decrease of association free energy, indicating that the hydrophobic interactions between the two plates weaken. The PMF of urea solution has a similar movement for the minimum at 0.4 nm. Zangi et al.[79] reported that urea weakens the hydrophobic interactions of two nonpolar plates, which was also manifested as a upside movement of the PMF minimum. The minimum at 0.78 nm indicates a new association state. The large *r* of this state implies the two plates may be associating indirectly with some molecules between them. The minimum value indicates that this association state at 0.78 nm may be not as stable as the one at 0.4 nm. However, the association state at 0.78 nm may impede the formation of an association at 0.4 nm because the two plates need energy to dissociate from the state at 0.78 nm to approach closer. The structural detail of this association state will be discussed in the next section.

To study the influence of molecular size, we analyzed the PMFs of EG_4 and EG_2 moieties. As shown in Figure 3.1b, when EG_4 is shortened to EG_2 moieties, the minimum at 0.4 nm is still higher than the one in water. The minimum shifted from 0.78 to 0.80 nm, with a minimum value around -20 kJ mol^{-1}. This observation indicates the influence of OEG moieties mainly depends on their chemical nature. The PMFs of 1.0 M and 2.0 M EG_2 solutions have similar minima at 0.40 nm but different minima at 0.80 nm. As shown in Figure 3.1b, the minimum at 0.80 nm for the PMF of 2.0 M EG_2 solution is lower than

that of 1.0 M EG_2 solution, indicating that hydrophobic interactions are influenced more with more OEG moieties.

3.3.2 Density Distribution

The distinct effects of CB and EG_4 moieties on hydrophobic interactions may be caused by their different effects on the local environments of the plates. The literature[79, 88-89] has shown the importance of local environment to hydrophobic interactions. In order to study the local environments of the plates, we did MD simulations to investigate the distributions of the atoms of moieties and water molecules when *r* is equal to 1.4 nm. Figure 3.3 shows their normalized distributions in the normal direction of the plates in various solutions. The profiles in Figure 3.3 were calculated only for the portion of box delimited by the *x* and *y* values of the plates. The Ow curves were normalized as N(Ow)/N(Ow-bulk), where N(Ow) is the actual number of Ow in the bin and N(Ow-bulk) is the number of Ow in the bin in bulk phase. The curves of atoms for moieties were normalized as N(A)/N(A-ave), where N(A) is the actual number of atom A in the bin and N(A-ave) is the number of atom A in the bin if they distribute evenly at the normal direction of the plate in the system. Table 3.2 lists the peak-plate distances in the CB and EG_4 solutions, and water.

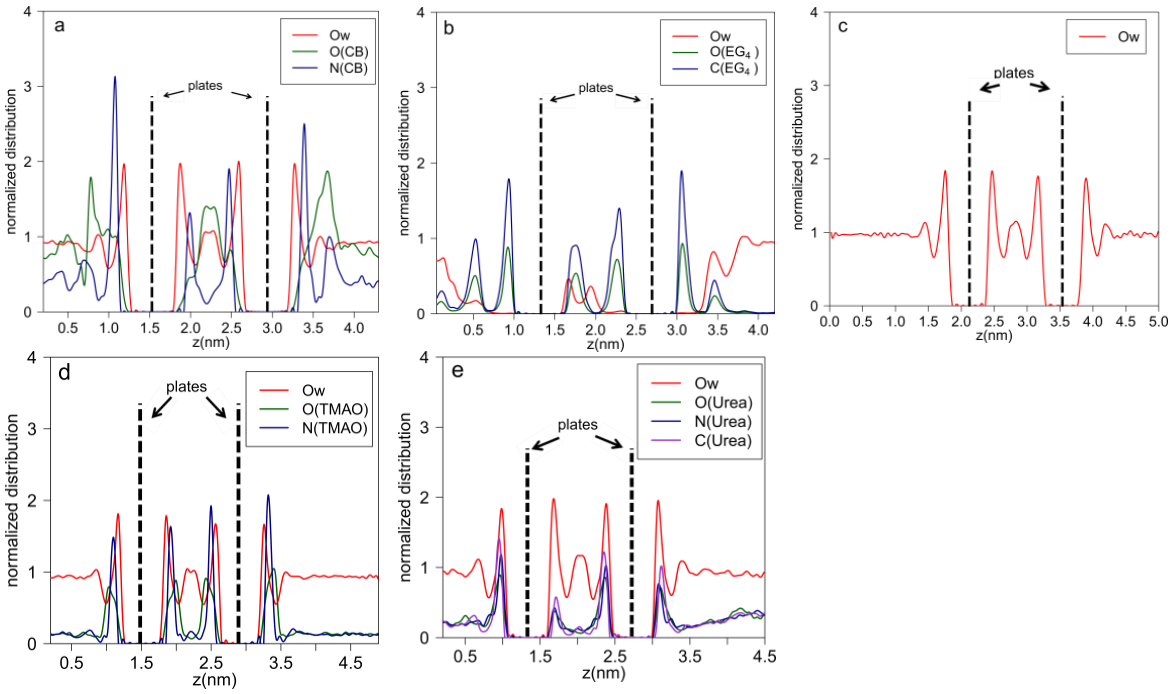

Figure 3.3. Normalized distributions of the atoms of moieties and water molecules in (a) CB, (b) EG4, (c) water, (d) TMAO and (e) urea solutions with r =1.4 nm. The positions of the two plates were also plotted in the figures.

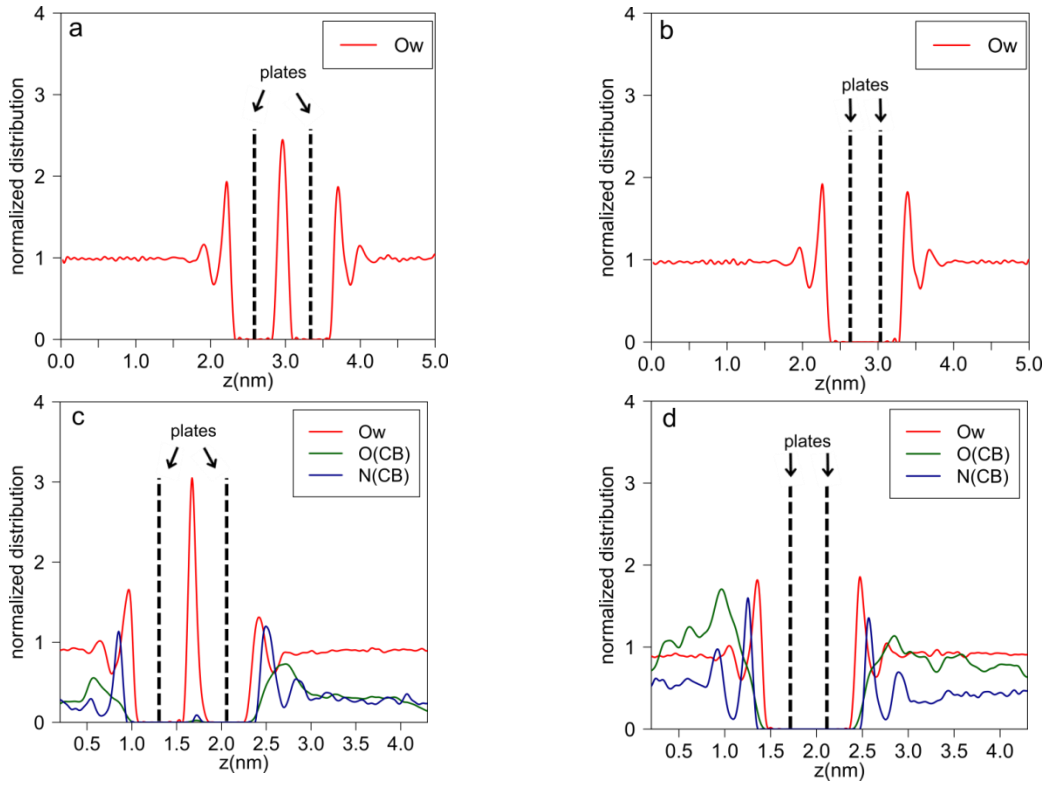

Figure 3.4. Normalized distributions of the atoms of moieties and water molecules in (a) water with r = 0.78 nm, (b) water with r = 0.40 nm, (c) CB solution with r = 0.78 nm and (d) CB solution with r = 0.40 nm. The positions of the two plates are also shown in the figures.

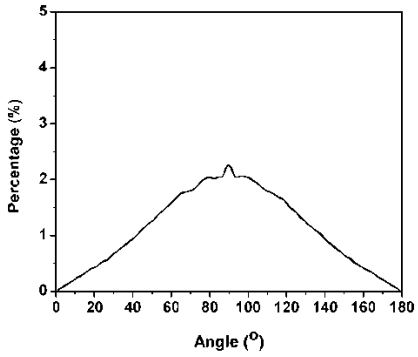

Figure 3.5. Dipole orientation distribution of water molecules between the plates in water when r = 0.78 nm. A value of 90 ° indicates that the dipole momentum of the water molecule is parallel to the plates, and the values of 0 ° or 180 ° indicate that the dipole momentum of the water molecule is perpendicular to the plates.

The normalized distributions in the CB and EG_4 solutions illustrate their hydrophobicities and why they change the hydrophobic interactions differently. Figure 3.2 (a and b) show that the CB moieties are further from the plates than water molecules, while the EG_4 moieties are closer to the plates than water molecules. This EG_4 accumulations demonstrates the hydrophobic feature of EG_4 moieties, which has been discussed previously[90]. The strength of hydrophobic interactions is affected by water-water hydrogen bonds between the two plates. The CB moieties keep the plates in a hydrophilic environment similar to that of water. EG_4 moieties deplete water molecules from the plates and offer a more hydrophobic environment for the plates. In CB solution, when *r* decreases to 0.78 or 0.40 nm, the plates are in a hydrophilic environment similar to that of water (Figure 3.4). Figures 3.2d and 3.2e show the plates are surrounded by water molecules in the TMAO solution and by a urea-water mixture in the urea solution. Zangi et al[79]. also observed that the plates are surrounded by a water-urea mixture in the urea solution, and they attributed the change of hydrophobic interactions to this change of the local environment of plates.

Table 3.2 Peak-Plate distances of atoms in the CB and EG_4 solutions, and water when *r* = 1.4 nm (nm)

	water	moieties		
	Ow	O	C	N
CB	0.34±0.01	0.69±0.06		0.45±0.01
EG_4	0.88±0.20	0.40±0.04	0.40±0.04	
Water	0.36±0.01			

We also did MD simulations with *r* constrained at 0.78 and 0.4 nm in the 1.0 M EG_4 solution in order to investigate the mechanism for the two different association states in the EG_4 PMF profile. Figure 3.6 shows the normalized distributions of the atoms of EG_4

moieties and water molecules in the normal direction of the plates in these two states. As shown in Figure 3.6a, no water molecules but only EG_4 moieties are between the plates when *r* is equal to 0.78 nm, confirming that the two plates associate indirectly through EG_4 moieties. MD simulations showed that there could be only a layer of water molecules between the plates when r is equal to 0.78 nm in water (Figure 3.4a), and the dipole moments of these water molecules prefer to align with the plates (Figure 3.5). The hydrophobic feature[90] of EG_4 moieties made it more energetically favorable to replace layer of water molecules with a layer of EG_4 moieties, which is consistent with the PMF profile. No molecules are between the plates when *r* is equal to 0.40 nm, indicating a direct plate-plate association.

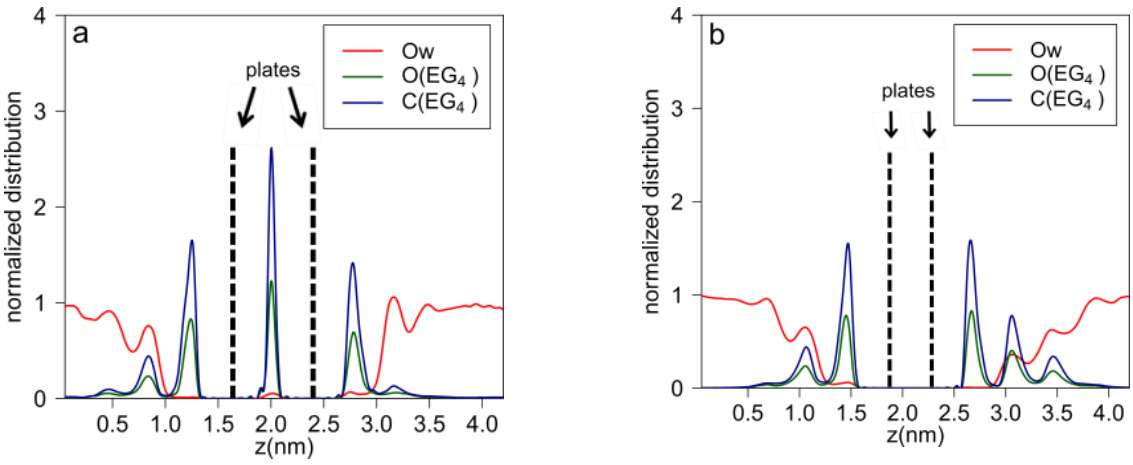

Figure 3.6. Normalized distributions of atoms of EG_4 moieties and water molecules in the EG_4 solution when (a) r = 0.78 nm and (b) r = 0.40 nm. The positions of the two plates are also shown in the figures.

Table 3.3 Peak-Plate distances of atoms of EG_4 moieties and water molecules outside the plates and between the plates at the two association states when r = 0.78 nm and 0.40 nm (nm)

	outside the plates			between the plates		
	water	EG_4		water	EG_4	
r (nm)	Ow	O	C	Ow	O	C
0.78	0.97	0.38	0.38		0.39	0.39
0.40	0.97	0.38	0.38			

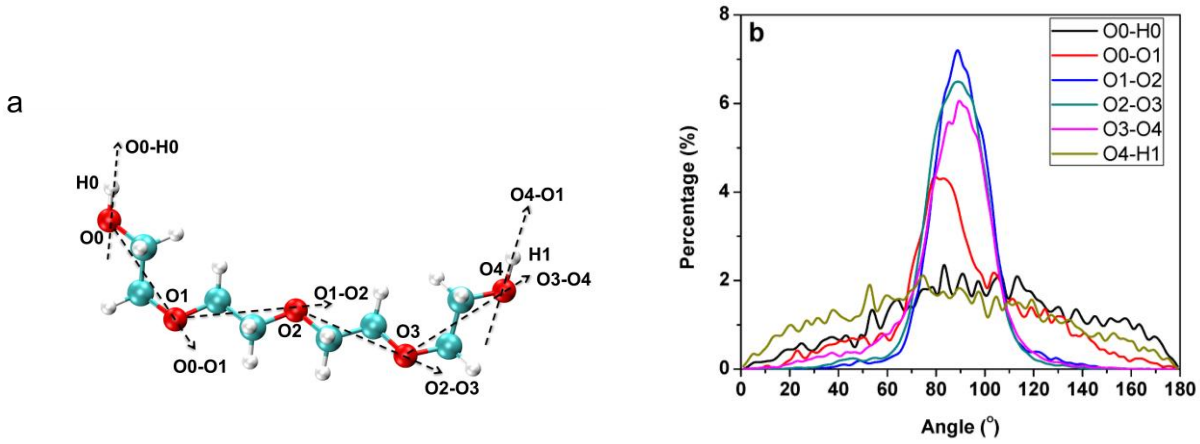

Figure 3.7. The orientation distribution of EG4 moieties between the plates when r = 0.78 nm. (a) The definitions of the angles and (b) the distributions of these angles.

To study the orientation of EG_4 moieties between the plates, we analyzed the distributions of angles between their adjacent oxygen atoms and the normal direction of the plates (Figure 3.7a). We also analyzed the distributions of angles between the hydroxyl groups and the normal direction of the plates. As shown in Figure 3.7b, the four angle distributions of the adjacent oxygen atoms (O0-O1, O1-O2, O2-O3 and O3-O4) were concentrated at around 90 °. This indicates that the EG_4 moieties between the plates were mostly aligned with the plates. This is consistent with the observations in Figure 3.6

where the peak of O(EG_4) is at the same position as the peak of C(EG_4). The hydroxyl groups (O0-H0, O4-H1) have a random orientation distribution.

The difference in altering hydrophobic interactions leads to distinct roles of PEG and PCB materials in biological and chemical applications. As stated before, hydrophobic interactions play an important role in many critical biological processes[72, 74-75, 91]. PEG not only weakens the hydrophobic interactions, but also introduces a new indirect association state that competes with the direct hydrophobic association. In this way, PEG could impede the biological processes driven by hydrophobic interactions. For instance, PEGylated chymotrypsin has a bioactivity drop[8]. Fatima et al. [92] showed that PEG destabilizes thiol proteases. Kubetzko et al.[93] also showed that PEGylation decreases the apparent affinity of antibody fragment by approximately 5-fold. On the other hand, the negligible effect on hydrophobic interactions implies that CB materials should not affect the efficiency of biological processes driven by hydrophobic interactions. For example, CB materials can protect chymotrypsin without sacrificing its activity[8].

3.4 Conclusions

We studied the influences of CB and OEG moieties on hydrophobic interactions using molecular simulations. We investigated the PMFs of two nonpolar plates in CB, EG_4, EG_2, TMAO, urea solutions and water using well-tempered metadynamics simulations. The similar PMFs of CB and water indicate that CB moieties do not impact hydrophobic interactions. However, the PMFs of EG_4 and EG_2 moieties differ from the one in water in two aspects. First, the value of the minimum at 0.4 nm increases. This increase indicates that OEG moieties weaken the hydrophobic interactions between the two plates. Second, a new minimum occurs around 0.78 nm. This minimum represents an

indirect association state that the two plates are associated with OEG moieties in between them. This indirect association state can impede the formation of a direct association state because the two plates need to overcome the free energy of indirect association to approach closer. Simulation results showed that the distinct effects of CB and EG_4 moieties on hydrophobic interactions result from their influences on the local environment hydrophobic plates, i.e., hydrophilic in the CB solution and more hydrophobic in the OEG solution. The different influences of CB and OEG moieties on hydrophobic interactions are responsible for their different influence on biological systems.

Chapter 4. Different Hydration of Carboxybetaine and Sulfobetaine Moieties

This chapter presented a molecular simulation study on the different hydration of carboxybetaine (CB) and sulfobetaine (SB) moieties. The coordination number, spatial distribution, dipole orientation distribution, and residence time of water molecules around the cationic group ($N(CH_3)_3^+$) and anionic group (CO_2^- for CB and SO_3^- for SB) were investigated to compare the hydration of these two betaine molecules. The results showed that the anionic group of SB moieties has more water molecules around it than the one of CB moieties, while the water molecules around the anionic group of CB moietiy have a sharper spatial distribution, more preferential dipole orientation, and longer residence time. The behavior of water molecules around the cationic groups of CB and SB moieties are similar. For both SB and CB moieties, the cationic groups are surrounded by more water molecules than the anionic groups, whereas the water molecules around the anionic groups are more ordered than those around the cationic groups. The hydration free energy of CB and SB moieties are considerable lower than the one of oligo(ethylene glycol).

4.1 Introduction

Materials that resist non-specific protein adsorption receive considerable attention because of their importance in many relevant chemical and biological applications[5, 94-95]. Polyethylene glycol (PEG) derived materials are currently the most widely used materials for this purpose[96]. However, the oxidization susceptibility of PEG in biochemical media precludes its use for long-term applications[97-98]. Zwitterionic poly(carboxybetaine methacrylate) (polyCBMA) and poly(sulfobetaine methacrylate) (polySBMA) are two new types of materials attracting attention recently because they show advantages

compared to conventional PEG derived materials[11, 99-102]. Both of them are ultra low fouling and stable in complex biological media such as human blood serum[11, 102].

Hydration of materials plays a key role in their nonfouling performance. For instance, Zheng et al.[18] studied the interactions between a protein and a surface in water when the protein was positioned at various distances from oligo(ethylene glycol) (OEG) self-assembled monolayers (SAMs), hydroxyl terminated SAMs, and methyl terminated SAMs. They found that the protein experiences a strong repulsive force only when it is close to the OEG-SAM. Furthermore, they found this repulsive force mainly arises from the interactions between the protein and water molecules. He et al.[17, 103] further clarified that the water molecules near OEG-SAM surface generate this strong repulsive force. Their studies also showed that the non-fouling OEG-SAM surface has a stronger ability to hold water molecules compared to the low-fouling OH-SAM surface by measuring the residence time of water molecules near surfaces. Hower et al.[104] reported that the water molecules near surfaces play a key role in the protein resistance of methylated and hydroxyl sugar based SAMs.

A thorough understanding about hydration of materials is crucial to investigate their nonfouling mechanism at the molecular level. The hydration of materials depends on many factors. An important one is the hydration of the moieties. A recent simulation study of Hower et al.[105] investigated the relationship between the nonfouling performance of several materials and the hydration of their moieties. By quantifying the coordination numbers and the molecular volumes, they show a close relationship between the nonfouling properties of materials and the moiety hydration.

PolyCBMA and polySBMA have CB and SB moieties, respectively. These two moieties share a common cationic group: quaternary amine group, whereas they have different anionic groups. A CB moiety has a COO^- group, whereas a SB moiety has a SO_3^- group. This difference could cause distinctive hydration, and a careful comparison between their hydration can advance our understanding about the nonfouling mechanisms and offer insight into materials selection and design. In this work, we will investigate and compare the hydration of CB and SB moieties from structure, dynamics and free energy. Previous studies have shown that these properties are important to study hydration[103, 106-107].

4.2 Simulation Details

4.2.1 Potential Models

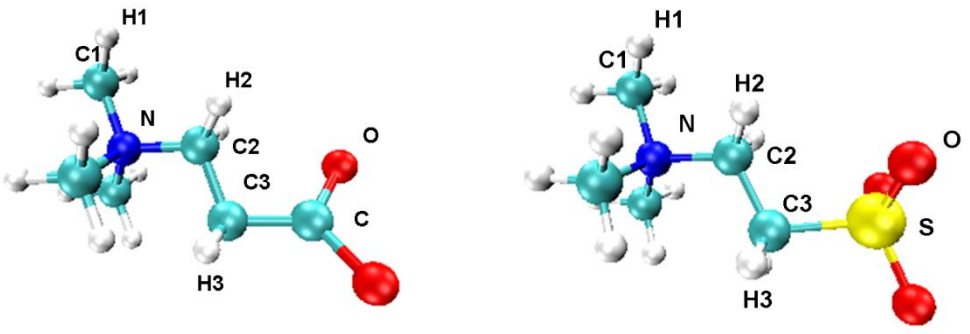

(a) (b)

Figure 4.1. Molecular structures of (a) a CB moiety and (b) a SB moiety

The structures of these two betaine molecules are shown in Figure 4.1. All atom models are used in this work. The SPC/E water model[49] was used because of its good representation of the structural and dynamic properties for water.

The potential energy of intermolecular interactions is calculated as a combination of a Lennard−Jones (L-J) 12−6 potential and a Coulombic potential, as shown in Equation 4.1.

$$U(r_{ij}) = 4\varepsilon_{ij}\left[\left(\frac{\sigma_{ij}}{r_{ij}}\right)^{12} - \left(\frac{\sigma_{ij}}{r_{ij}}\right)^{6}\right] + \frac{q_i q_j}{r_{ij}} \qquad (4.1)$$

where r_{ij} is the distance between atoms i and j, q_i is the partial charge assigned to atom i, and ε_{ij} and σ_{ij} are energy and size parameters obtained by Lorentz-Berthelot combining rules, where $\sigma_{ij} = (\sigma_i + \sigma_j)/2$ and $\varepsilon_{ij} = \sqrt{\varepsilon_i \varepsilon_j}$.

Table 4.1. The force field parameters of SB and CB moieties used in this work. Figure 4.1 shows the labels.

	σ (nm)	ε (kJ·mol^{-1})	q (e)		σ (nm)	ε (kJ·mol^{-1})	q (e)
SB				CB			
N	0.325	0.7113	0.3200	N	0.325	0.7113	0.3516
C1	0.350	0.2761	-0.2925	C1	0.350	0.2761	-0.3226
H1	0.250	0.06276	0.1470	H1	0.250	0.0628	0.1514
C2	0.350	0.2761	0.0186	C2	0.350	0.2761	0.0200
H2	0.250	0.06276	0.0848	H2	0.250	0.0628	0.0660
C3	0.350	0.2761	-0.2100	C3	0.350	0.2761	-0.1262
H3	0.250	0.1255	0.1010	H3	0.250	0.1255	0.0360
S	0.355	1.046	1.3193	C	0.375	0.4393	0.9070
O	0.296	0.7113	-0.755	O	0.296	0.8786	-0.8756

In simulations of zwitterionic moieties, the proper description of their partial charges is particularly important. To obtain the partial charges of the carboxybetaine and sulfobetaine, we carried out quantum calculations with DFT-B3LYP/6-31G** and CHELP with Gaussian 09[50]. The calculations were carried out using GridChem system[51]. The L-J parameters were obtained from the OPLS all atom force field[52] developed by Jorgensen group because of the force field's good representation of small organic

molecules. Table 1 lists the L-J parameters and partial charges used in this work. The bond interaction parameters were also derived from OPLS all atom force field.

4.2.2 Simulation Methodology

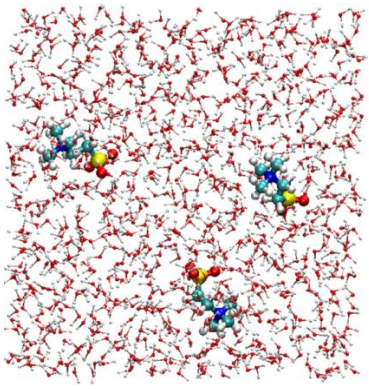

Figure 4.2 The schematic of the SB simulation system

The simulation system was a periodic water box (initial size: 3.1 × 3.1 × 3.1 nm) containing 966 water molecules and three zwitterionic moieties. The concentration of betaine moieties in this system is 0.19 M. The betaine moieties were solvated in the bulk water reservoir and it was ensured that the initial distance between each two betaine molecules is at least 1.2 nm to avoid initial solute pairing. Figure 4.2 shows the initial configuration for one simulation of SB, which was produced with the Visual Molecular Dynamics program (VMD)[53].

The molecular dynamics (MD) simulations were performed using Gromacs-4.05[54] in an isobaric-isothermal (NPT) ensemble. After energy minimization and a 1.0 ns MD run with an integral step of 1.0 fs for equilibrium, another 1.0 ns run was carried out with an integral step of 2.0 fs. The coordinates were saved every 0.2 ps. Long-range electrostatic interactions were computed with the particle mesh Ewald method with periodic boundary

conditions in all three dimensions[55]. The short-range van der Waals interactions were calculated with a cutoff distance of 1.1 nm. The system was maintained at 298 K (0.1 ps time constant) and 100.0 KPa with the Berendsen algorithm[56] (with a compressibility of 4.5 $\times 10^{-5}$ bar^{-1} and a 1 ps time constant). Intramolecular bonds of betaine molecules and water molecules were kept constrained with the LINCS algorithm[60]. For each type of betaine molecule, three independent simulations with different initial configurations were carried out. Furthermore, we selected one of the three simulations for each betaine molecule and extended it to 10.0 ns to ensure sufficient sampling.

4.2.3 Free Energy Perturbation

The hydration free energy of CB and SB moieties was calculated with the free energy perturbation (FEP) method. The perturbation process in this work mimics the reversible process of dehydration as described in literature[108-109]. The negative of the free energy change of this process is the hydration free energy. As shown in Equation 4.2, we change the interaction energy between the solute and water, including the van der Waals interaction energy and electrostatic interaction energy, from the normal values to zero gradually as λ changes from zero to 1.

$$U(\lambda) = 4\varepsilon_{ij}(1-\lambda)\left[\left(\frac{\sigma_{ij}}{r_{ij}}\right)^{12} - \left(\frac{\sigma_{ij}}{r_{ij}}\right)^{6}\right] + \frac{(1-\lambda)q_i q_j}{r_{ij}} \qquad (4.2)$$

This interaction change causes the potential energy of the system to vary gradually from $U_A(\lambda = 0)$ to $U_B(\lambda = 1)$. λ should decrease as small as possible in every step in order to preserve reversibility. Taking into consideration both the precision required in this work and the tolerance of computational cost, we divided λ into 50 intervals from zero to 1 evenly. For every λ_{n+1}, a 600 ps MD simulation was carried out with the initial structure

obtained from the final structure of MD simulation of λ_n. The potential energy is the average of the last 300 ps. The other simulation parameters were the same as the classical MD simulation described in section 4.2. Three independent FEP calculations with different initial structures were carried out for each betaine molecule. The FEP calculations in this work were carried out with Gromacs-4.05[54].

4.3 Results and Discussion

This work mainly focuses on the hydration of two charged groups of CB and SB moieties. A CB moiety possesses an anionic COO^- group and a SB moiety possesses an anionic SO_3^- group. Both of them have the same cationic group: $N(CH_3)_3^+$.

4.3.1 Spatial Distribution

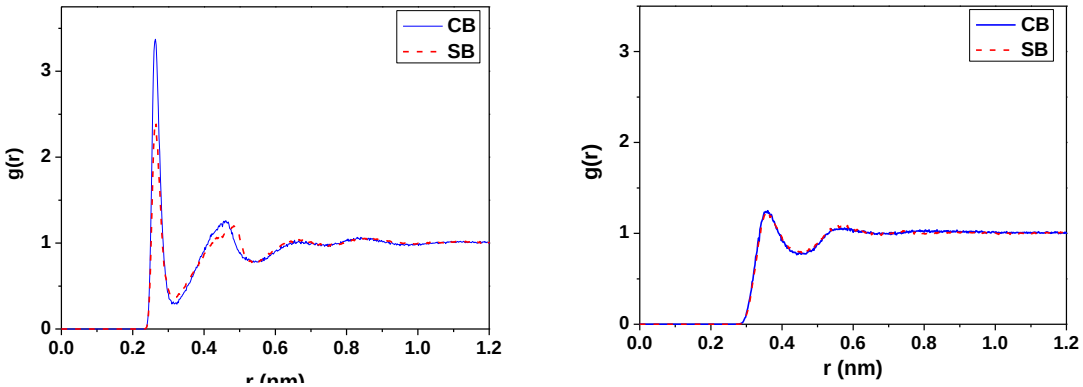

(a) (b)

Figure 4.3. Radial distribution functions between water molecules and atoms of CB and SB moieties. (a) The oxygen atoms of the betaine moieties (O-Ow); (b) the carbon atoms in the methyl groups linked to nitrogen atom of the betaine moieties (C1-Ow).

The anisotropic solute-water interactions cause the water molecules to spatially rearrange around the solute. One of the important spatial distributions is the water-solute distance distribution. This is most often represented with the radial distribution functions (RDFs). Figure 4.3 shows the RDFs of the oxygen atoms of water molecules and certain

atoms of the CB and SB moieties. This can be considered as the RDFs of water molecules and the selected atoms of the solute because the center of mass of water molecules is nearly identical to the oxygen atom position.

We find in Figure 4.3a that both the O-Ow RDF profiles of the two zwitterionic moieties have maxima around 0.23 nm and minima nearby around 0.32 nm. The significant maxima indicate the existence of a coordination shell around the anionic groups of the betaine moieties. The identical maximum and minimum positions of O-Ow RDFs for these two zwitterionic moieties imply that the first coordination shell radii of their anionic groups are nearly same. Since a SB moiety has three oxygen atoms and a CB moiety has just two oxygen atoms, the first coordination shell volume of the anionic group of SB is larger than that of CB. However, we can observe in Figure 4.3a that the first maximum value of O-Ow RDF of CB is higher than that of SB, indicating there are differing spatial distributions of water molecules in the first coordination shells.

Figure 4.3b shows the RDFs between the carbon atoms (C1) of the $N(CH_3)_3^+$ group and the oxygen atoms of water molecules. We can observe a maximum at 0.35 nm and a minimum at 0.44 nm. Similar to the observation of the anionic group, C1-Ow RDFs of CB and SB have nearly identical first maximum positions, indicating the similar shell size. Furthermore, we find the nearly identical maximum value of C1-Ow RDFs of these two zwitterionic moieties. This indicates that the water molecules in the first shells of these two betaine moieties have very similar water-solute distance distributions.

Table 4.2. Coordination numbers of the first coordination shells of the anionic and cationic groups of CB and SB moieties

		First shell	
CB		Size (nm)	Coor. No.
	Anionic	0.32	5.94±0.04
	Cationic	0.46	18.54±0.11
SB			
	Anionic	0.32	7.08±0.01
	Cationic	0.46	18.64±0.01

We calculated the coordination numbers (*N*) of the first coordination shell of the anionic and cationic groups of CB and SB based on the RDFs shown in Figure 4.3. The results are listed in Table 4.2. For both CB and SB moieties, *N* of the cationic group is larger than the one of the anionic group. However, as shown in Figure 4.3, the maximum value of C1-Ow RDF of either CB or SB moieties is much lower than that of the O-Ow RDF. The value of C1-Ow RDF is only around 1.3, whereas the O-Ow RDF of CB is 3.5 and that of SB is 2.5.

N of the cationic groups of CB and SB moieties are nearly the same, whereas those of their anionic groups are different. This agrees with the observation of RDFs in Figure 4.3. As listed in Table 4.2, the anionic group of a SB moiety has 1.54 more water molecules around it. However, the previous results show that the maximum value of O-Ow RDF of SB moiety is smaller than that of CB moiety. The larger *N* of the anionic group of SB molecule is due to its extra oxygen atom.

The water-solute RDF represents the *r* distribution. This is adequate for the hydration of inorganic ions because they are usually treated as a perfect sphere. However, it is inadequate to fully understand the spatial distribution of water molecules around the solute with aspherical structures. We also need to know the angle distribution of water

relative to the solvent in order have a complete description of the spatial distribution of water molecules near a solute.

Figure 4.4a shows the definitions of θ and ϕ for the water molecules around the positively charged group of CB. A plane was defined based on three atoms: the nitrogen atom (N), the carbon atom (C(COO^-)) of the COO^- group and the carbon atom (C1) of one methyl group attached to the nitrogen atom. Owp is the projection point of the oxygen atom of water molecule on this plane. ϕ is defined as the angle between the line C-Owp and N-C(COO^-). θ is defined as the angle between the line Ow-C(COO^-) and the plane. For water molecules around the negatively charged group of CB, the plane was established based on N, C(COO^-) and one oxygen atom (O) of the COO^- group. is defined as the angle between the line O-Owp and N-C, and θ is defined as the angle between the line Ow-O and the plane.

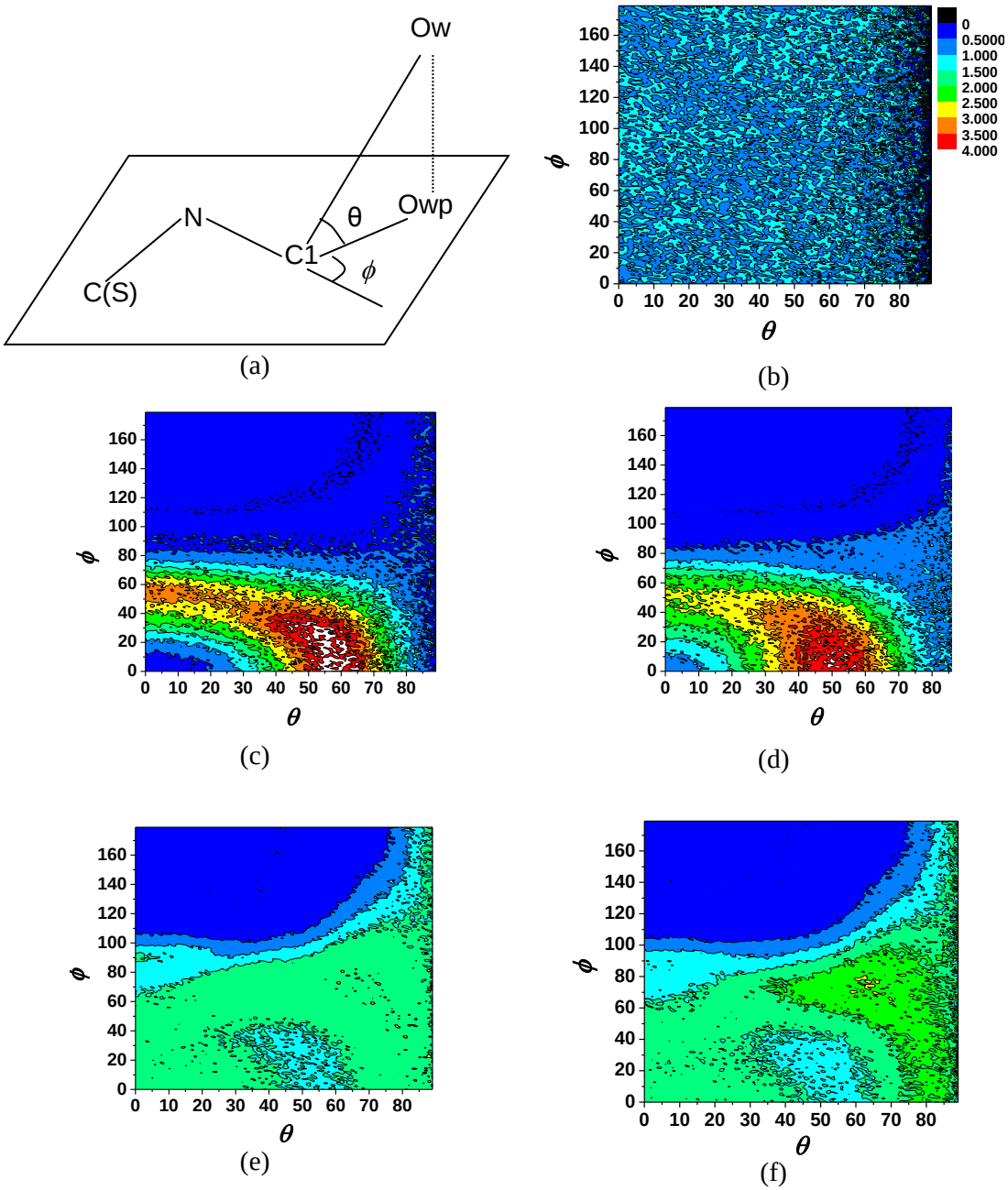

Figure 4.4. P_1 dependences as function of θ and ϕ. (a) the definitions of θ and ϕ for the water molecules around the cationic group of CB; P_1 as functions of θ and ϕ for water molecules in the first hydration shell of (b) Na^+, (c) the anionic group of CB moiety, (d) the anionic group of SB moiety, (e) the cationic group of CB moiety, and (f) the cationic group of CB moiety.

We define a parameter P_1, as shown in Equation 4.3, to represent the angle distributions of water molecules referring to certain atom of the solute.

$$P_1 = < N_1(\theta,\phi) > / \overline{N}(\theta,\phi) \qquad (4.3)$$

As shown in Equation 4.3, $N_1(\theta,\phi)$ is the ensemble-averaged number of water molecules to appear within a certain range with θ and ϕ. $\overline{N}(\theta,\phi)$ is the number for water molecules to appear in a certain range with θ and ϕ in assuming they distribute evenly as in the bulk phase. P_1 larger than 1 means that the water prefer to stay in this area, while P_1 less than 1.0 indicates that the possibility of water molecules appearing in this area is less than that in the bulk phase.

Figure 4.4b shows P1 as functions of θ and ϕ for water molecules in the first coordination shell of Na^+. We can observe that the distribution is quite random, indicating that there are no preferential orientation for water molecules around Na^+. This random distribution verifies that only a RDF is adequate for describing the spatial distribution of water molecules around Na^+.

However, we find that the water molecules around either the positively charged group or the negatively charged group of the betaine molecule have certain angle distribution, as shown in Figure 4.4 (c-f). Figure 4c and 4d shows P_1 as functions of θ and ϕ for water molecules in the first shells of the negatively charged groups of carboxybetaine and sulfobetaine. We can observe that the preferential distributions for the CB and SB moieties are quite similar. The majority of water molecules prefer to stay in the region with $0° < \theta < 80°$ and $0° < \phi < 80°$. This is probably due to the geometric effect of other atoms in the betaine molecules. Interestingly, in the region with $0° < \theta < 30°$ and $0° < \phi < 20°$,

which is the region in front of the line C(COO^-)-O or S(SO_3^-)-O, P_1 is less than 1. This indicates that the probability for water molecules to appear there is less than the average probability. This preferential distribution is probably caused by the geometric requirement of hydrogen bond formation between the water molecules and the solute.

We can observe from Figures 4.4e and 4.4f that there are still preferential distributions for the water molecules near the cationic groups of CB and SB moieties. This indicates that the water molecules in the first shell do not have random distributions as opposed to those around a single ion. However, the partial charge distribution of the cationic group is much more even than the anionic group. The P_1 distributions for the cationic groups are much broader than those near the anionic groups. Water molecules near the cationic group of CB moiety have a P_1 less than 1.0 in region with $0° \leq \theta < 80°$ and $100° \leq \phi < 180°$. This may also be attributed to the van der Waals repulsion from the atoms of the solute itself. The distribution of P_1 for the cationic group of SB moiety, as shown in Figure 4.4f, is similar to that of CB moiety shown in Figure 4.4e.

4.3.2 Dipole Orientation Distribution

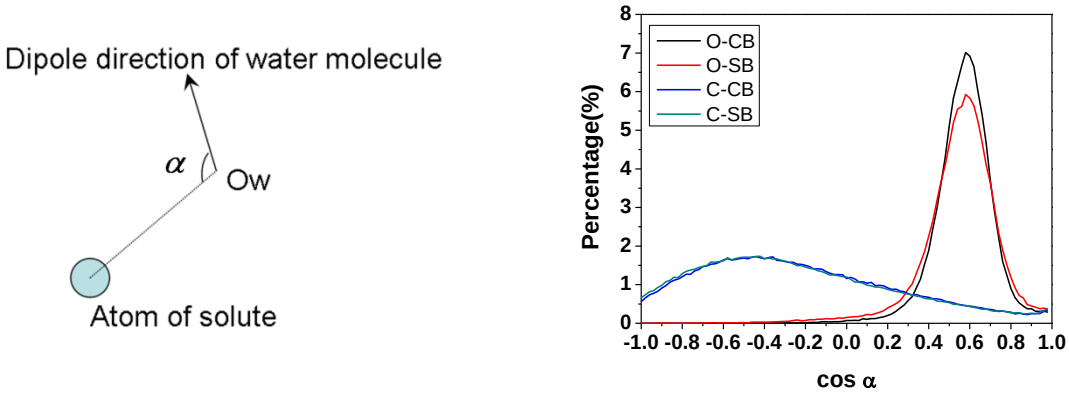

(a) (b)

Figure 4.5. Dipole orientation distributions of water molecules in the first coordination shells of certain atoms of the CB and SB moieties. (a) Definitions of α and (b) distributions of cos*α* for the water molecules in the first coordination shells of the carbon atom (C-CB) of methyl groups linked to the nitrogen atom and the oxygen atoms (O-CB) of CB moiety, and the carbon atom (C-SB) of methyl groups linked to the nitrogen atom and the oxygen atoms (O-SB) of SB moiety.

Another important effect of solute on water molecules is the orientation distribution. Several theoretical studies showed that the preferential orientation is very important to assess the hydration strength of solute[106-107, 110-111]. To evaluate the orientation distribution of water molecules around the solute, we define an angle α between the dipole moment of water molecule and a certain solute atom, as illustrated in Figure 4.5a. For CB molecule, we selected the carbon atom of methyl groups linked to the nitrogen atom and the oxygen atoms of COO^- group. For SB moiety, we selected the same carbon atom as for the CB moiety and the oxygen atoms of SO_3^- group. Figure 4.5b shows the distributions of cos*α* for these four types of atoms.

We can observe that the distribution profiles of cosα for O-CB and O-SB have maxima around 0.6, whereas those of C-CB and C-SB have maxima around -0.5. These

distributions are consistent with the dipole orientation distributions of water molecules around halogen anions and alkali metal cation as reported by previous molecular simulations[106, 110]. Furthermore, we can observe that the peak height for the O-CB and O-SB are much higher than the corresponding one of C. This observation indicates that the water molecules near the cationic groups of the betaine molecules orient much more randomly than those water molecules around the anionic groups. The anionic group interacts with individual water molecules significantly stronger than the cationic group.

Comparing the profiles shown in Figure 4.5b, we find that the profiles of C-CB and C-SB are nearly the same, whereas a difference is found between the O-CB and C-SB. The value of peak height for O-CB is 16.7% higher than that of O-SB. Previous studies of ionic hydration have suggested that the relationship between the sharpness of the orientation distribution and the strength of hydration[107, 110]. The higher maximum value observed for O-CB implies that the anionic group of CB moiety interact with individual water molecules stronger than the anionic group of SB moiety.

4.3.3 Residence Time

The hydration dynamics of the CB and SB moieties were analyzed using residence times of water molecules in the first coordination shells of the cationic and anionic groups. The residence function $C(t_1)$ is defined in Equation 4.4.

$$C(t_1) = \frac{\sum \delta_{i,t0,t_1}}{N_{t0}} \qquad (4.4)$$

N_{t0} is the amount of water molecules in the first shell at t_0, $\delta_{i,t0,t_1}$ equals 1 when the water molecules i is in the first shell at time t_0 and t otherwise 0. Figure 4.6a is an illustration of the definition of $\delta_{i,t0,t_1}$.

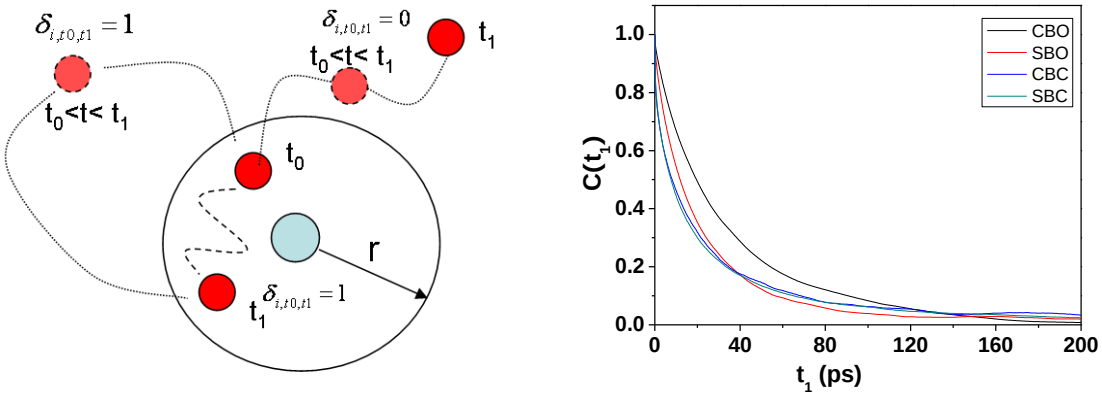

(a) (b)

Figure 4.6. Residence times of water molecules in the first coordination shells of solute. (a) illustration of definition of $\delta_{i,t0,t_1}$ and (b) the residence curve of water molecules in the first shell of negatively charged group of CB (CBO) and SB (SBO) and positively charged group of CB (CBC) and SB (SBC).

Figure 4.6b shows $C(t_1)$ curves of the anionic and cationic groups of CB and SB moieties. Comparing the corresponding curves of CB and SB moieties, we can see that the two curves for the cationic groups are quite similar, whereas the curve for the anionic group of CB moiety decreases slower than the corresponding curve of SB moiety. This observation demonstrates that the major difference between hydration dynamics also occurs around the anionic groups.

$$\tau = \int_0^{1ns} C(t_1)dt_1 \qquad (4.5)$$

To further analyze the residence property quantitatively, we calculated the residence time τ based on $C(t_1)$ curves shown in Figure 4.6b. It should be noticed that the curve does not decrease exponentially. The previous literature have reported several algorithm methods [112-113] on how to derive τ using single or multiple exponential functions fitting

with $C(t_1)$ curve, or the combination of numerical integration and fitting function[114]. The focus of this work is on the difference between the CB and SB moieties, thus we applied the numerical integration from 0 to 1 ns, as shown in Equation 4.5, to obtain τ. The results are listed in Table 4.3.

Table 4.3 Residence time τ of water molecules in the first shells of the negative and positively charged groups of CB and SB

		τ (ps)
CB		
	Anionic	35.64±0.51
	Cationic	25.85±0.53
SB		
	Anionic	25.64±0.93
	Cationic	24.34±0.58

Table 4.3 shows that τ of the anionic group of CB moiety is larger than the one of SB moiety. The water molecules tend to stay longer around the anionic group of CB moiety than around the anionic group of SB moiety. This also implies that the interaction between water molecules and COO^- group is stronger than that between the water molecules and SO_3^- group. This is consistent with the observations of the dipole orientation distribution. τ of the cationic groups of CB and SB moieties are found to be quite similar, indicating a similar tendency for water molecules to stay around them. When comparing τ of the cationic and anionic groups belonging to the same molecule, we can observe that, for CB moiety, τ of the anionic group is much larger than that of cationic group. For SB moiety, τ of the anionic and cationic groups is very similar. The different shell volumes and partial charge distributions are responsible for this.

4.3.4 Hydration Free Energy

Table 4.4. Hydration free energy of CB and SB. The hydration free energy of EG_4, Na^+, Water, F^-, Cl^- and Br^- were also listed for comparison

	This work(kJ mol^{-1})	Experiment(kJ mol^{-1})	Simulation(kJ mol^{-1})
CB	-404.0±9.9	---	---
SB	-519.0±9.8	---	---
OEG_4	-182	---	---
Na^+	-350	-365[42]	-398[43]
Water	-33	-26.38[44]	-24.79 [33]
F^-	-607	-465[42]	-580[43]
Cl^-	-362	-340[42]	-371[43]
Br^-	-311	-315[42]	-358[43]

Table 4.4 lists the hydration free energy of CB and SB moieties. The hydration free energy of water molecule, Na^+, F^-, Cl^- and Br^- were calculated with the same procedure and are also listed in Table 4.4. The aim of the extra free energy calculations is to verify the process and to provide a basis for comparison. The values of hydration free energy for water molecule, Na^+, F^-, Cl^- and Br^- calculated with the process in our work agree well with the experimental and theoretical results reported in literature[108, 115-117].

Table 4.4 shows that the hydration free energy of CB and SB moieties is lower than the general values of amino acids with normal forms, which are usually around -40 to -16 kJ mol^{-1} [108], and comparable to those of ions[116]. EG_4 ($HO(CH_2CH_2O)_4H$) has a hydration free energy of -182 kJ mol^{-1}, much higher than the ones of the zwitterionic molecules. Nonfouling material should have strong hydration[95]. Experiments have shown that polyCBMA and polySBMA have excellent nonfouling performance. Experimental results agree with simulation findings in this work that SB and CB moieties have low hydration free energy.

4.5 Conclusions

We investigated the hydration structures, dynamics and free energy of CB and SB moieties using quantum mechanics, MD simulations and free energy perturbation calculations. These two zwitterionic molecules represent the head groups of two ultra low fouling zwitterionic materials: polyCBMA and polySBMA. The main hydration difference was observed around the anionic groups, while the hydration of the cationic groups is very similar. The anionic group of SB moiety has more water molecules in its first coordination shell than that of CB moiety. However, the water molecules around the anionic group of CB moiety have sharper spatial distributions, more preferential dipole orientation and longer residence time. These simulation results show that the anionic group of CB moiety interacts with water molecules stronger than the anionic group of SB moiety, whereas the latter interacts with more water molecules. For either CB or SB moiety, the coordination number of the cationic group is larger than that of the anionic group. However, the water molecules around the anionic group are found to have higher structure order and lower mobility. Both CB and SB moieties have hydration free energy considerably lower than that of EG_4 moieties.

Chapter 5 Different Ionic Interactions of Carboxybetaine and Sulfobetaine Moieties

This chapter presented a simulation study on the associations between zwitterionic moieties (carboxybetaine and sulfobetaine) and four monovalent cations (Li^+, Na^+, K^+ and Cs^+) in aqueous solutions. We studied the number and lifetime of zwitterion-cation associations, and observed that carboxybetaine and sulfobetaine moieties have the same order of association number and lifetime: $Li^+ > Na^+ > K^+ > Cs^+$. Simulation results showed that the carboxybetaine-cation association varies differently from the sulfobetaine-cation association as a function of cation type. The effect of anion type on the order was also investigated by varying the anions from Cl^- to Br^- or F^-. In order to further investigate zwitterion-cation association, we simulated two types of systems: one has only type of zwitterionic moiety and two types of cations, and the other has both carboxybetaine and sulfobetaine moieties and one type of cations. These two systems allowed direct competition among the solutes and ions, and the observed association number and lifetime validated the order. Simulation results further demonstrated that carboxybetaine moieties associate stronger with Li^+ and Na^+, and sulfobetaine moieties associate stronger with K^+ and Cs^+.

5.1. Introduction

Biocompatible materials with high resistance to nonspecific protein adsorption are critical for many applications[94-95, 118]. Recently, zwitterionic materials such as poly (carboxybetaine methacrylate) (polyCBMA) and poly (sulfobetaine methacrylate) (polySBMA) are receiving considerable attention because they present excellent nonfouling properties even in undiluted blood serum[95]. Significant efforts have been

devoted to develop applications of these materials, such as drug delivery carriers, marine coatings, and medical devices[1, 6, 119-120].

The rational design and application of zwitterionic materials requires a fundamental understanding of interactions among zwitterions themselves and their interactions with the surroundings. Chapter 4 has shown that zwitterionic CB and SB moieties have different hydration, although they both present strong hydration[48]. Ions are ubiquitous in biological and industrial systems. For instance, ions such as Na^+ and K^+ exist in the cellular and extracellular environments. Similarly, marine environments have various ions. These ions can influence the properties of zwitterionic materials profoundly because zwitterionic materials possess highly charged groups[95]. For instance, zwitterionic polymers have antipolyelectrolyte property: adding more salts increases the solubility of zwitterionic polymers[121-123]. A thorough understanding of zwitterion-ion interactions is therefore crucial for the application of zwitterionic materials in complex media.

Effects of ions on properties of materials have been studied theoretically and experimentally for more than a century. Experimental observations led to the Hofmeister series[124], which ranks ions into a series according to their ability to salt out proteins. The classical view considers ions such as Li^+ and Na^+ as structure makers that enhance water structure. These ions are viewed as strong ions. Another type of ions, such as K^+ and Cs^+, is viewed as structure breakers that weaken water structure[125-127]. These ions are considered as weak ions. Collins[128] proposed a theory to explain the relationship between the strong and weak ions, which explains the preferential association between different types of inorganic monovalent ions quite well. In this theory, strong cations prefer to associate with strong anions and vice versa for weak ions. Using this “like-likes-like”

theory, Jungwirth and his colleagues[129] studied the associations between the organic anions such as CH_3COO^- and $CH_3SO_3^-$ with inorganic monovalent cations using molecular simulations. They suggested that CH_3COO^- prefers to associate with Na^+, whereas $CH_3SO_3^-$ favors association with K^+ based on their results of association free energy. Hess et al.[130] also found an order of increasing binding affinity with carboxylate ions from their molecular simulation study of specific ion binding to a protein. The order they found is $Li^+ > Na^+ > K^+$. These studies serve as a good starting point for the fundamental understanding of zwitterion-ion associations.

Zwitterionic moieties have their own features that make them distinguished from other molecules. One feature is in that they possess both cationic and anionic groups. For example, although a CB moiety has the anionic carboxylic group (COO^-) as an acetone group, it possesses a large cationic group (quaternary amine) that can influence the nearby charged groups. Association competition is another studied aspect. Zwitterionic moieties themselves are neutral. This means that there are at least one type of anion and one type of cation in solvent, which causes competitive association between the charged groups of zwitterionic molecules and ions.

Several recent researches suggested that ionic effects still have many unrevealed aspects[127, 131]. Lund et al.[132] showed that the weak anions such as I^- prefer to bind the hydrophobic surface groups of a protein instead of the cationic surface groups. The weak ions prefer to approach the air-liquid interface, not stay in the bulk solution as predicted by the classical theory of electrolyte solution[133-134]. Recent molecular simulations carried out by Zangi[135] implied that both strong and weak ions decrease water structure, instead of the conventional view that strong ions increase water structure and weak ions decrease

water structure. All these new findings provide strong justification for studying zwitterion-ion association at the molecular level.

This work conducted molecular dynamics simulations of zwitterionic CB and SB moieties in various electrolyte solutions. The goals of these simulations are to characterize zwitterion-ion associations and rank association strengths. We selected four cations (Li^+, Na^+, K^+ and Cs^+) in this study. The former two (Li^+ and Na^+) are strong ions and the latter two (K^+ and Cs^+) are weak ones. Since our study[48] has shown the hydration difference of CB and SB moieties, it is interesting to explore if they also have any difference in ionic association, especially for the competitive association.

5.2 Simulation Details

Each simulation system is a periodic box (initial size: 3.58 × 3.58 × 3.58 nm) containing 10 zwitterionic molecules, 50 cations, 50 anions and 1300 water molecules. The simulation system was created in the following steps: at the first step, the zwitterionic molecules were placed randomly in the simulation box using packmol[136]. Next, the ten zwitterionic molecules were solvated in a water box containing 1400 water molecules. Finally, 100 water molecules were selected randomly in the simulation system and replaced by 50 cations and 50 anions. The final simulation system contains 10 zwitterion molecules, 50 cations, 50 anions and 1300 water molecules.

The potential energy of intermolecular interactions is calculated as a combination of Lennard-Jones (L-J) 12-6 potential and Coulombic potential, as shown in Equation 5.1.

$$U(r_{ij}) = 4\varepsilon_{ij}\left[\left(\frac{\sigma_{ij}}{r_{ij}}\right)^{12} - \left(\frac{\sigma_{ij}}{r_{ij}}\right)^{6}\right] + \frac{q_i q_j}{r_{ij}} \qquad (5.1)$$

where r_{ij} is the distance between atoms i and j, q_i is the partial charge assigned to atom i, and ε_{ij} and σ_{ij} are energy and size parameters obtained by Lorentz-Berthelot combining rules, where $\sigma_{ij} = (\sigma_i + \sigma_j)/2$ and $\varepsilon_{ij} = \sqrt{\varepsilon_i \varepsilon_j}$. The force field parameters for zwitterions were the same as those in Chapter 4. The ion was treated as a single Lennard-Jones site and the force field parameters from the work of Aqvist were used[137]. The SPC/E water model[49] was used because of its good replication of the dipole moment, dielectric constant and diffusion properties of water molecules. Table 5.1 lists the force field parameters for all the ions in this study.

Table 5.1 The force field parameters of ions

	σ (nm)	ε (kJ·mol^{-1})	q (e)
Ions			
Li^+	0.213	0.0765	1.0
Na^+	0.333	0.0116	1.0
K^+	0.493	0.00137	1.0
Cs^+	0.672	0.000339	1.0
F^-	0.273	3.01	-1.0
Cl^-	0.440	0.470	-1.0
Br^-	0.462	0.377	-1.0

Molecular dynamics (MD) simulations were performed using Gromacs-4.5.3[54] in an isobaric-isothermal (NPT) ensemble. After energy minimization and a 1.0 ns MD run with an integral step of 1.0 fs for equilibrium, another 5.0 ns run was carried out with the integral step of 1.0 fs for data collection. The coordinates were saved every 0.1 ps. Long-range electrostatic interactions were computed with the particle mesh Ewald method[55] with periodic boundary conditions in all three dimensions. The short-range van der Waals (VDW) interactions were calculated with a cutoff distance of 1.1 nm. The system was maintained at 298 K (0.1 ps time constant) and 100.0 kPa with the Berendsen algorithm[56] (with a compressibility of 4.5×10^{-5} bar^{-1} and a 1 ps time constant). Intramolecular bonds

of zwitterionic molecules and water molecules were kept constrained with the LINCS algorithm[60].

5.3. Results and Discussion

5.3.1 Radial Distribution Functions

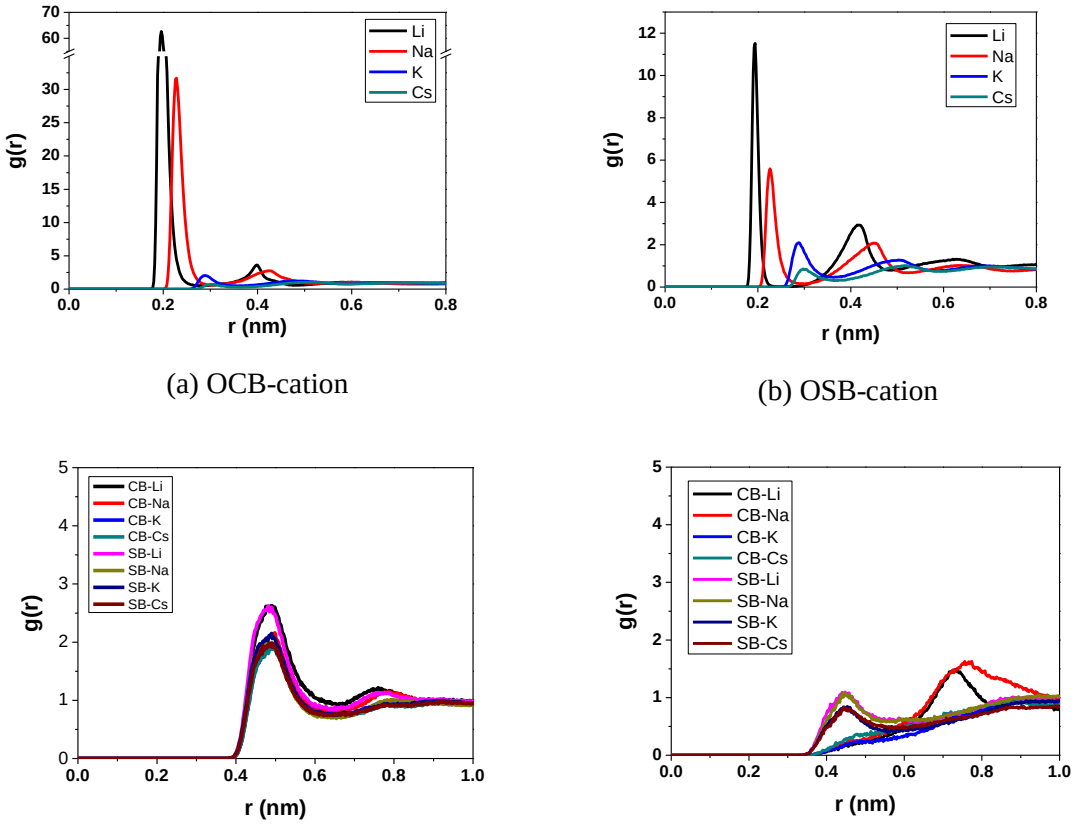

(a) OCB-cation

(b) OSB-cation

(c) N-Cl^-

(d) N-O

Figure 5.1. Radial distribution functions (RDFs) of zwitterions and ions. (a) The RDFs between the oxygen atoms of CB and cations (OCB-cation), (b) the RDFs between the oxygen atoms of SB and cations (OSB-cation), (c) the RDFs between the nitrogen atoms of zwitterions and Cl^- (N-Cl^-) and (d) the RDFs between the nitrogen and oxygen atoms of zwitterions (N-O)

We first studied the radial distribution functions (RDFs) between zwitterionic moieties and ions, and between zwitterionic moieties. We investigated three types of RDFs: (a)

between the oxygen atoms of zwitterionic moieties and the cations; (b) between the nitrogen atoms of zwitterionic moieties and the anions; and (c) between the oxygen atoms and the nitrogen atoms belonging to different zwitterionic moieties. The purpose is to explore the association among zwitterions, cations, and anions in the three-component systems and the possible self-associations of zwitterionic moieties themselves. Figure 5.1 shows the RDFs and Figure 5.2 shows the representative snapshots of CB-Na^+ and SB-Na^+ associations.

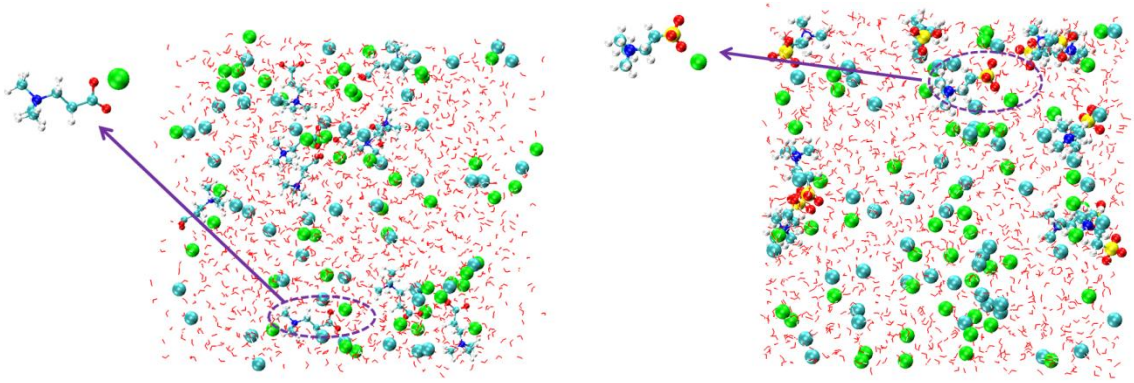

(a) (b)

Figure 5.2 Snapshots for the representative associations between zwitterion and cations (a) CB-Na^+ associations and (b) SB-Na^+ associations. The green ones are Na^+, Cyan ones are Cl^-. Red ones are oxygen atoms of zwitterions.

Previous simulations have shown that hydration of the quaternary ammine groups of both CB and SB are nearly identical[48]. From Figure 5.1c, we can observe that the peak locations of the RDFs of N-Cl^- are identical. Figure 5.1d shows that there is no significant peak for O-N RDFs, indicating that there is no stable association between the zwitterion themselves in electrolyte solutions. The main difference occurs around the anionic groups. As shown in Figure 5.1a and 5.1b, the peak locations for Li^+, Na^+, K^+ and Cs^+ are 0.20,

0.23, 0.30 and 0.3 nm, respectively. For CB moieties, the peak height decreases following the order: $Li^+ > Na^+ > K^+ > Cs^+$. This observation is consistent with those simulation results of Hess *et al.*[130] that the cation affinity to carboxylate anion follows the order: $Li^+ > Na^+ > K^+$. The same order was also observed for SB moieties, as shown in Figure 5.1b. This order correlated well with the decreasing order of the ion VDW radius size. Our previous simulation study has shown that the oxygen atoms of these two zwitterionic moieties have highly partial charge[8]. The ion with smaller size has higher charge density and probably causes stronger zwitterion-cation association.

5.3.2 Association Numbers

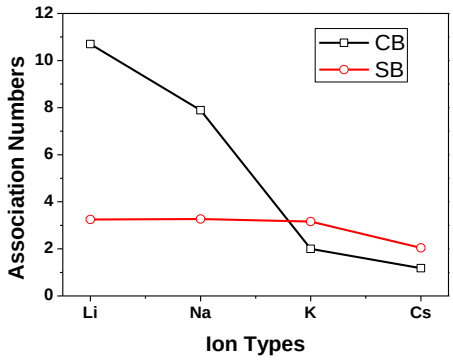

Figure 5.3. Zwitterion-cation association numbers (ANs) for various cations with Cl^- ions.

In order to investigate the zwitterion-cation association more in details, we obtained the association numbers (ANs) by counting the number of cations whose distances from the oxygen atoms of zwitterionic molecules are less than the first minimum of the corresponding RDFs. Figure 5.3 shows the results of ANs for CB and SB moieties as a function of cation type. The ANs of CB moieties are 10.70 (Li^+), 7.89 (Na^+), 2.00 (K^+), and 1.18 (Cs^+), decreasing in the order: $Li^+ > Na^+ > K^+ > Cs^+$, in a very good agreement

with the observations of RDFs. The ANs of SB moieties with various cations vary much less significant. As shown in Figure 5.3, the ANs of SB moieties with various cations are quite similar. Even for Cs^+ case in which we observed the most reduction, the decrease is only 37% relative to the SB-Li^+ AN. This is insignificant comparing to the dramatic decrease of AN from CB-Li^+ to CB-Cs^+ case, a nearly 90% drop.

The different variations of ANs of CB and SB moieties result in a crossover point. As shown in Figure 5.3, for Li^+ and Na^+, the ANs of CB moieties are larger than the ones of SB moieties. For K^+ and Cs^+, the ANs of SB moieties are larger than the ones of CB moieties. In other words, CB moieties can associate more with two strong cations (Li^+ and Na^+), whereas SB moieties can associate more with two weak cations (K^+ and Cs^+).

5.3.3 Association Lifetime

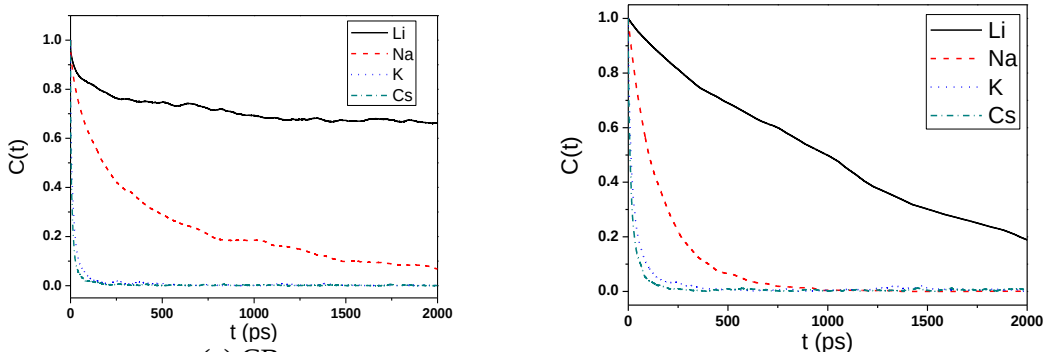

(a) CB (b) SB

Figure 5.4. Residence curves of zwitterions-cation associations for (a) CB and (b) SB.

Besides the AN, we studied the association lifetime. A longer lifetime indicates a more stable association. The association curve is defined as $C(t) = \frac{\sum \delta_{i,t0,t_1}}{N_{t0}}$, where N_{t0} is the amount of association exists at t_0, and $\delta_{i,t0,t}$ is equal to 1 when the association i exists at t_0 and t, otherwise 0, regardless whether the association forms or not during t_0 to t. Figure

5.4 shows the $C(t)$ curves of CB and SB moieties with various cations. For both CB and SB moieties, the decrease of $C(t)$ curve follows the order: $Li^+ < Na^+ < K^+ < Cs^+$. This indicates that the association stability for both CB and SB moieties with cations also obeys the same order that we found for ANs. Hence, for both CB and SB moieties, their associations with cations follow the order: $Li^+ > Na^+ > K^+ > Cs^+$.

To further quantitatively analyze the association lifetime between zwitterionic molecules with various cations, we fitted the curve with $C(t) = e^{-\frac{t}{\tau}}$ and obtained the association lifetime τ. The integration is only done to Na^+, K^+ and Cs^+, not to Li^+ because tail of the Li^+ curve still has a very high value even after a 5 ns MD simulation. Table 5.2 lists τ of CB and SB moieties with Na^+, K^+ and Cs^+.

Table 5.2. The association lifetime τ for Na^+, K^+ and Cs^+ with CB and SB with Cl^-, Br^- and F^- as the anions

	τ (ps)		
	Na^+	K^+	Cs^+
CB-Cl^-	432.6	13.9	7.8
CB-F^-	468.5	13.6	6.9
CB-Br^-	473.1	13.0	6.3
SB-Cl^-	163.8	27.8	17.4
SB-F^-	208.5	28.0	18.8
SB-Br^-	67.5	26.7	15.9

As listed in Table 5.2, with Cl^- as the anions, τ of CB-Na^+ association is larger than SB-Na^+ one, whereas τ of CB-K^+ and CB-Cs^+ associations are less than ones of SB moieties. From Figure 5.3 we can observe that CB-Li^+ curve decreases significantly slower than the SB-Li^+ one. In the previous section, we have shown a crossover point for ANs of CB and SB moieties. In this section we observed the same phenomenon for the association lifetime τ. Thus both the AN and lifetime τ show that CB moieties associate more as well as stronger to the two strong cations (Li^+ and Na^+). SB moieties associate more as well as

stronger to the two weak cations (K^+ and Cs^+). In our previous simulations, we have shown the different hydration behavior of CB and SB moieties[48]. The observation here indicates that these two zwitterionic moieties also have different interactions with various salts, especially with Na^+ and K^+.

5.3.4 Effect of Anion

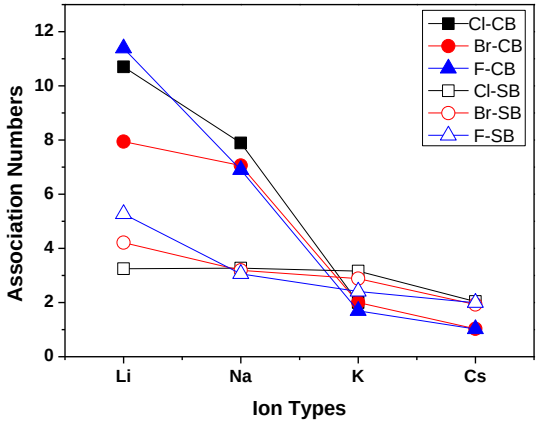

Figure 5.5. ANs of zwitterion-cation associations with various anions.

In order to study the effect of anions, in addition to the anion above, Cl^-, we studied two more anions, Br^- and F^-. The simulation systems and simulation procedures were the same as those with Cl^-. Figure 5.5 shows the ANs of CB and SB moieties with the four cations studied along with the three different anions. It can be seen that with variation of the anion, the ANs for zwitterion-cation association change quantitatively. However, the order of ANs is the same: $Li^+ > Na^+ > K^+ > Cs^+$. We similarly observed that the identity of the anion preserved the preferential association of CB with Li^+ and Na^+ and SB with K^+ and Cs^+.

Table 5.2 shows the lifetime τ for the association of Na^+, K^+ and Cs^+ with CB and SB when Br^- or F^- are present as the anion. We can observe in Table 5.2 that the change of

anion types from Cl^- to Br^- or F^- changes the lifetime quantitatively. However, this variation does not change the order $Li^+ > Na^+ > K^+ > Cs^+$. We can also observe that, with Br^- and F^- as the anions, the CB associates longer with Li^+ and Na^+, while the SB associates longer with K^+ and Cs^+. This is the same as the observations with Cl^-. Anions therefore do not influence the zwitterion-cation association qualitatively, although they can change the association properties quantitatively.

5.3.5 Competitive Associations

To further verify the phenomena observed for the zwitterion-cation association, we studied two types of competitive scenarios. One is with one type of zwitterionic moieties and two types of cations (i.e., *Competition of different cations)*. The other is with one type of cation and both CB and SB moieties (i.e., *Competition of different zwitterions).* The investigation of these two types of competitions will help to understand the preferential association between zwitterionic moieties and cations in a more direct way. Because the anion type does not affect the association order qualitatively, we chose Cl^- as the anions.

Competition of Different Cations

To investigate the preferential association order found based on single ion in a more direct way, we selected three cases: Li^+/Na^+, Na^+/K^+ and K^+/Cs^+. These cases enable to directly elucidate which cation preferentially associates with zwitterionic molecules. The used simulation systems are similar to what we described in section 5.2. The major difference is that instead of having 50 same-type cations, we have two types of cations with 25 each. All the other simulation details are the same as that described in section 5.2.

Table 5.3 The ANs and association lifetime τ for CB and SB with various cations in the system with one type of zwitterion and two types of cations (Cl^- as the anions)

	AN				τ (ps)			
	Li^+	Na^+	K^+	Cs^+	Li^+	Na^+	K^+	Cs^+
CB-Li^+/Na^+	6.06	2.67				495.2		
CB-Na^+/K^+		3.15	0.91			347.8	17.8	
CB-K^+/Cs^+			1.15	0.52			12.7	6.1
SB-Li^+/Na^+	2.27	1.99				292.7		
SB-Na^+/K^+		2.39	1.37			237.9	28.2	
SB-K^+/Cs^+			1.76	0.89		-	34.1	15.6

Table 5.3 shows the ANs and association lifetime τ of various cations when they are competing with other cations. Figure 5.6 shows residence curves of the association of Li^+ and Na^+ with respective zwitterionic molecules in the zwitterion-Li^+/Na^+ solutions. For both CB and SB molecules, the order for both AN and τ is still the same as we found in the previous section. Valchy et al.[129] investigated the associations of different cations with organic solutes, and they considered SO_3^- as weak ion because their results showed that the association of a single K^+ to SO_3^- is favored over that of single Na^+ to SO_3^-. However, our simulations show that both CB and SB molecules prefer to associate more with Na^+ than K^+. This observation indicates that if we rank the zwitterions, both of these two zwitterions are probably considered as strong ones according to the "like-likes-like" theory[16], although CB molecules are stronger than SB molecules. However, a recent simulations carried out by Zangi showed that there is no disruption or sudden change in the observed properties as we might think of the strong and weak ions[135]. This means more effort will be needed to have an insightful view of the effects of ions and their ranking.

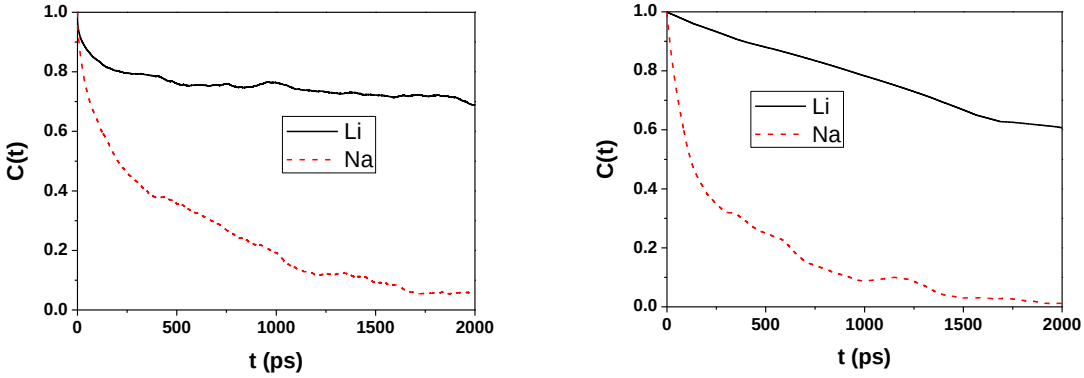

(a) (b)

Figure 5.6. Residence curves of zwitterion-cation associations for (a) in the CB-Li^+/Na^+ solvent and (b) SB- Li^+/Na^+ solvent.

Competition of different zwitterions

In the previous section, we have shown that Li^+ and Na^+ associate with the CB stronger than with the SB, while K^+ and Cs^+ seems to associate preferentially with SB. To verify this phenomenon in more detail, we simulated the system with the same type of cation and both CB and SB presented. A typical simulation system used for this purpose has five CB and SB moieties distributed randomly in the simulation box. All the other simulation details are exactly the same as described in section 5.2.

Table 5.4. The ANs and association lifetime τ for CB and SB in the system with one type of cation and both CB and SB presented (Cl^- as the anion)

	AN		τ(ps)	
	CB	SB	CB	SB
Li^+	8.16	3.06	-	-
Na^+	3.58	1.89	517.67	268.3
K^+	1.05	1.57	14.41	26.0
Cs^+	0.64	0.79	8.32	14.8

Table 5.4 lists the ANs and the lifetime of each type of cation with CB and SB moieties. We can observe directly that, for Li^+ and Na^+, the ANs of CB moieties are significantly larger than the ones of SB moieties. As to K^+ and Cs^+, the ANs of SB moieties are larger than the ones of CB moieties. The same is observed for τ. This observation demonstrates directly what we found in previous sections, namely that the Li^+ and Na^+ associate with the CB moieties stronger than with SB moieties, while K^+ and Cs^+ associate preferentially with SB moieties.

5.4 Conclusions

This chapter presented a molecular simulation study to investigate the associations of two zwitterionic moieties, CB and SB, with four cations (Li^+, Na^+, K^+ and Cs^+). We studied the radial distribution functions between the zwitterionic molecules and the ions, the association number per zwitterionic moiety and the association lifetimes. Simulation results show that, for both CB and SB moieties, the association number and lifetime follow the order: $Li^+ > Na^+ > K^+ > Cs^+$. This order is verified by simulations of competitive association of single type of zwitterionic molecules with two types of cations and simulations of varying anion types. CB moieties prefer to associates with strong cations significantly than weak ones while SB moieties has the similar trend, but in much less degree. This demonstrates that CB moieties are stronger than SB moieties. Consequently, the two strong cations (Li^+, Na^+) associate with CB moieties stronger than with SB moieties, while the two weak cations (K^+, Cs^+) associate stronger with SB moieties.

Chapter 6 Different Stimulus-Responses of Sulfobetaine and Carboxybetaine Polymers

Zwitterionic materials play important roles in biological applications. The associations among zwitterionic moieties dictate properties of zwitterionic materials. However, the underlying interactions that determine their associations and properties are still not known. This work compared thermal and salt responsive behaviors of sulfobetaine polymers and carboxybetaine polymers by examining their rheological properties as a function of temperature and their hydrodynamic sizes as a function of salt concentration. Results showed that carboxybetaine polymers do not have stimuli-responses as predicted from the classical theory about zwitterionic polymers such as sulfobetaine polymers. We further performed molecular simulations to study the associations among zwitterionic moieties in these two zwitterionic polymers at the molecular level. Simulation results provide a fundamental understanding of underlying interactions among cationic and anionic group within zwitterionic moieties, which are responsible for different associations and responsive properties of carboxybetaine and sulfobetaine polymers.

6.1 Introduction

Zwitterionic materials have many unique properties: they resist biofouling in complex environments[10]; they protect enzymes from denaturation without sacrificing bioactivity[8]; and they prevent capsule formation *in vivo*[12]. Zwitterionic moieties are common in nature such as cell membranes, proteins or osmolytes. These observations position zwitterionic materials as an excellent candidate for many biological applications.

Zwitterionic moieties are believed to form associations among themselves, which make zwitterionic polymers stimuli responsive. Schultz et al.[138] showed that adding salts

could decrease the upper critical solution temperature of zwitterionic sulfobetaine (SB) polymers. They also observed an inverted lower critical solution temperature for SB polymers. They proposed that such behaviors are due to the variation of the associations between the sulfonate and trimethyl ammonium groups of SB moieties. Zwitterionic polymers are suggested to possess antipolyelectrolyte effects: adding salts can enhance the solubility of zwitterionic polymers. Recent studies further showed that the swelling[139], mechanical and other properties of SB polymers[140-141] vary with salt concentration and temperature.

However, it is still unclear what underlying interactions of zwitterionic moieties determine the associations among them and the responsive properties of zwitterionic polymers. To address this question, we compared thermal and salt responses of two types of zwitterionic polymers: SB and carboxybetaine (CB) polymers. The zwitterionic moiety of SB polymers has a cationic trimethyl ammonium group and an anionic sulfonate group. The zwitterionic moiety of CB polymers shares the same cationic group as the one of SB polymers, but has an anionic carboxylic group, which has stronger charge strength than the sulfonate group. We also performed atomistic simulations to analyze the associations of cationic and anionic groups of zwitterionic moieties in these two types of zwitterionic polymers at the molecular level. Our results showed that the associations are dictated by matching the charge strength of cationic and anionic groups.

6.2 Experiment Details

6.2.1 Polymer Preparation

In a typical radical polymerization reaction of sulfobetaine or carboxybetaine polymer synthesis, 2 g monomer and 20 mg initiator (2,2'-azobis[2-(2-imidazolin-2-

yl)propane]dihydrochloride, VA-044) were dissolved into 20 ml solvent (water for CB polymers; 0.5M NaCl solution for SB polymers). The solution was subsequently deoxygenated on an ice bath by bubbling filtered nitrogen through for 1 hour. Following the deoxygenation, the reaction solution was heated to 40 ^{o}C and stirred vigorously for 18 h. After 18h, the reaction was stopped by exposure to air. The polymer solutions were subsequently purified via dialysis and followed by lyophilization, resulting a white power for both PCBMA and PSBMA. The polymers were then used without further purification. Figure 6.1 shows the molecular structures of PCBMA and PSBMA.

(a) (b)

Figure 6.1. Molecular structure of (a) SB and (b) CB polymers

6.2.2 Rheology Measurement

The dynamic viscoelasticity was measured with a Kinexus Pro rheometer (Malvern Instruments Ltd.) using parallel plates of 40-mm diameter and plate-to-plate distance of 900 μm. The temperature dependence of the storage modulus (G') and loss modulus (G") was determined by oscillatory shear deformation with the temperature range from 10 ℃ to 40 ℃. The frequency was fixed at 10 Hz and the strain was fixed at 1%. The concentrations of polymer solution were 50 g/L.

6.2.3 Dynamic Lighting Scattering Measurement

Dynamic light scattering (DLS) measurements were performed at room temperature by using a Zetasizer NanoZS Instrument (ZEM4228, Malvern Instruments, UK) equipped with a 4 mW He-Ne laser (λ_0 = 633 nm) and with noninvasive backscattering (NIBS) detection at a scattering angle of 173 °. The autocorrelation function was converted in a volume-weighted particle size distribution with Dispersion Technology Software 5.06 from Malvern Instruments. Each measurement was repeated at least three times.

6.3 Simulation Details

6.3.1 Force Field Parameters

Water molecules in this work were represented with the SPCE model[80]. We used the force filed parameters[82] developed in our previous work to describe zwitterionic moieties. The other atoms of polymers were described by the OPLSAA force field[52].

A combination of a Lennard-Jones (L-J) 12-6 potential and a Coulomb potential (Equation 6.1) was used to calculate the non-bonded potential energy.

$$U(r_{ij}) = 4\varepsilon_{ij}\left[\left(\frac{\sigma_{ij}}{r_{ij}}\right)^{12} - \left(\frac{\sigma_{ij}}{r_{ij}}\right)^{6}\right] + \frac{q_i q_j}{r_{ij}} \qquad (6.1)$$

where r_{ij} is the distance between atoms i and j, q_i is the partial charge assigned to atom i, and ε_{ij} and σ_{ij} are energy and size parameters obtained by Jorgensen combining rules.

6.3.2 Molecular Dynamics Simulations of Polymer Solutions

The systems used for molecular dynamics simulations of polymer solutions contain 10 SB or CB polymer chains and varying numbers of water molecules. Each polymer chain has 30 monomers. The initial configurations of the polymer chains in the simulation

systems were generated by packmol[136]. Figure 6.2 shows the initial configuration of the SB polymer system. Table 6.1 lists the numbers of molecules in the simulation systems.

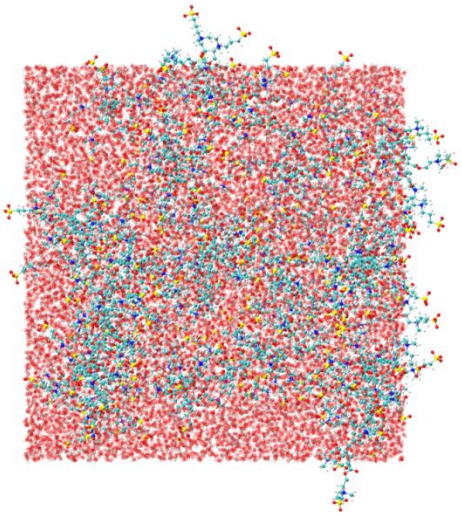

Figure 6.2 Initial configuration of SB polymer system

Table 6.1. Details of the simulation systems

	Number of monomers per chain	Number of polymer chains	Number of water molecules	Concentration of zwitterionic moieties
SB polymer	30	10	11279	1.5 M
CB polymer	30	10	11201	1.5 M

For simulation systems at 298 K, after energy minimization, a 40 ns MD simulation was run with an integral step of 1.0 fs in NPT ensemble for equilibrium. After this, another 10 ns MD simulation was carried out with temperatures coupling to 298 K, 320 K, 340 K, 360 K, 340 K, 320 K, 340 K, 360 K, 330 K and 298 K for every nanosecond to relax the system. After this, another 40 ns MD run was carried out with integral step of a 2.0 fs in NPT ensemble and the last 20 ns was used to collect the coordinate data with a frequency of 2 ps.

Long-range electrostatic interactions were computed with the particle mesh Ewald method with periodic boundary conditions in all three dimensions.[55] The short-range van der Waals interactions were calculated with a cutoff distance of 1.0 nm.

During the first 40 ns MD simulation for equilibrium, the temperature and pressure were coupled using the Berendsen algorithm[56] (with a compressibility of 4.5 × 10-5 bar-1 and a 1 ps time constant). During the 10 ns MD simulation, the temperature was coupled with the Berendsen algorithm[56], During the 40 ns MD simulation after the temperature annealing, the temperature was maintained with Nose-Hoover algorithm[57-58] and pressure was maintained with Parrinello-Rahman algorithm. Intramolecular bonds involving hydrogen atoms were kept constrained with the LINCS algorithm.[60] The MD simulations were performed using Gromacs-4.5.5[83].

6.3.3 Molecular Dynamics Simulations of Small Zwitterionic Molecules

The simulation systems for 2.0 M solution have 50 zwitterionic molecules and 1400 water molecules, and the systems at 4.0 M solution have 100 zwitterionic molecules and 1400 water molecules. For each simulation system, after an energy minimization, a 5.0 ns MD simulation in an NPT ensemble (T=298 K, P=100 KPa) was carried out for equilibrium. The system was maintained at temperature and pressure with the Berendsen algorithm[56] (with a compressibility of 4.5×10^{-5} bar^{-1} and a 1 ps time constant). Another 5.0 ns MD simulation in an NVT ensemble was carried out for data collection. The temperature was maintained with Nose-Hoover algorithm[57-58]. The other details were the same as the MD simulations of zwitterionic polymer solutions in S.6.3.2.

6.4 Results and Discussion

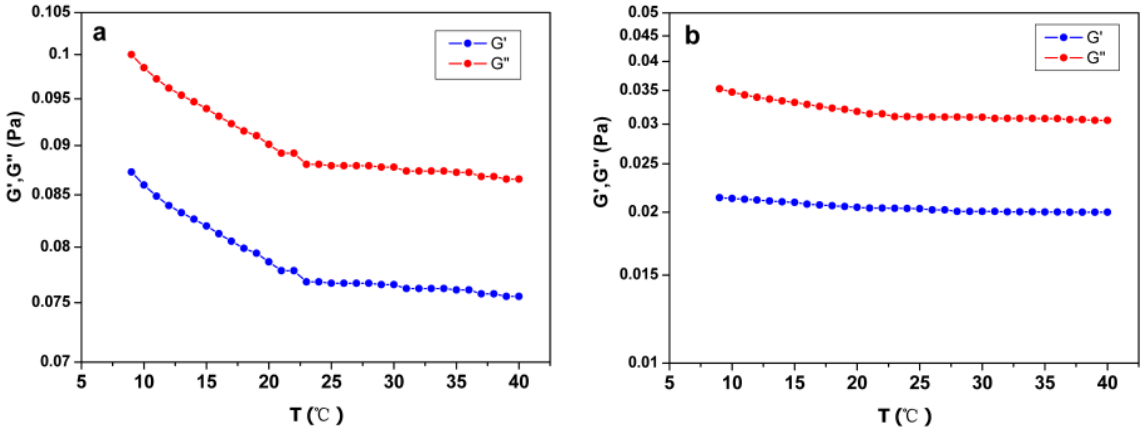

Figure 6.3. Rheology properties of (a) SB polymers and (b) CB polymers as a function of temperature (T). G' is the storage modulus and G" is the loss modulus.

We first compared the thermal responses of SB and CB polymers by analyzing the storage (G') and loss (G") moduli of 50 g/L polymer solutions as a function of temperature. Figure 6.3 shows G' and G" of SB and CB polymer solutions from 10 to 40 ℃. In this temperature range, the SB polymer solution shows larger moduli than the CB polymer solution, indicating that SB polymers possess more associations among their zwitterionic moieties. Furthermore, increasing temperature results in a significant reduction in G' and G" of SB polymers. This reduction is due to the dissociations caused by temperature increase, consistent with what is observed for SB hydrogels[122] and SB polymer solids[142]. However, G' and G" of CB polymers do not show such reduction as temperature increases, indicating that CB polymers may have few inter-polymer associations.

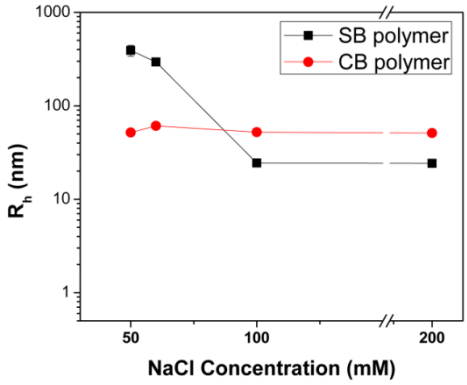

Figure 6.4. Hydrodynamic sizes (R_h) of SB and CB polymer solutions as a function of NaCl concentration.

We further studied the hydrodynamic sizes (R_h) of SB and CB polymer solutions as a function of NaCl concentration using dynamic lighting scattering. Zwitterionic polymers are well known to show the antipolyelectrolyte effect[14]. Thus, we can expect that the R_h of the zwitterionic polymers will decrease with salts addition. Figure 6.4 shows R_h of 2 g/L SB and CB polymer solutions with NaCl concentrations from 50 to 200 mM. In this NaCl concentration range, both SB and CB polymers dissolved well. As shown in Figure 6.4, R_h of SB polymers decreases as NaCl concentration increases, consistent with what is expected from the classical theory of zwitterionic polymers[123]. However, R_h of CB polymers is nearly unchanged as NaCl concentration increases. Our previous study[143] has shown that zwitterionic CB moieties interact with Na^+ stronger than zwitterionic SB moieties, excluding the possibility that NaCl has less influences on associations among CB moieties than on those among SB moieties. Hence, CB polymers may have few zwitterionic associations, different from what is commonly known about zwitterionic polymers.

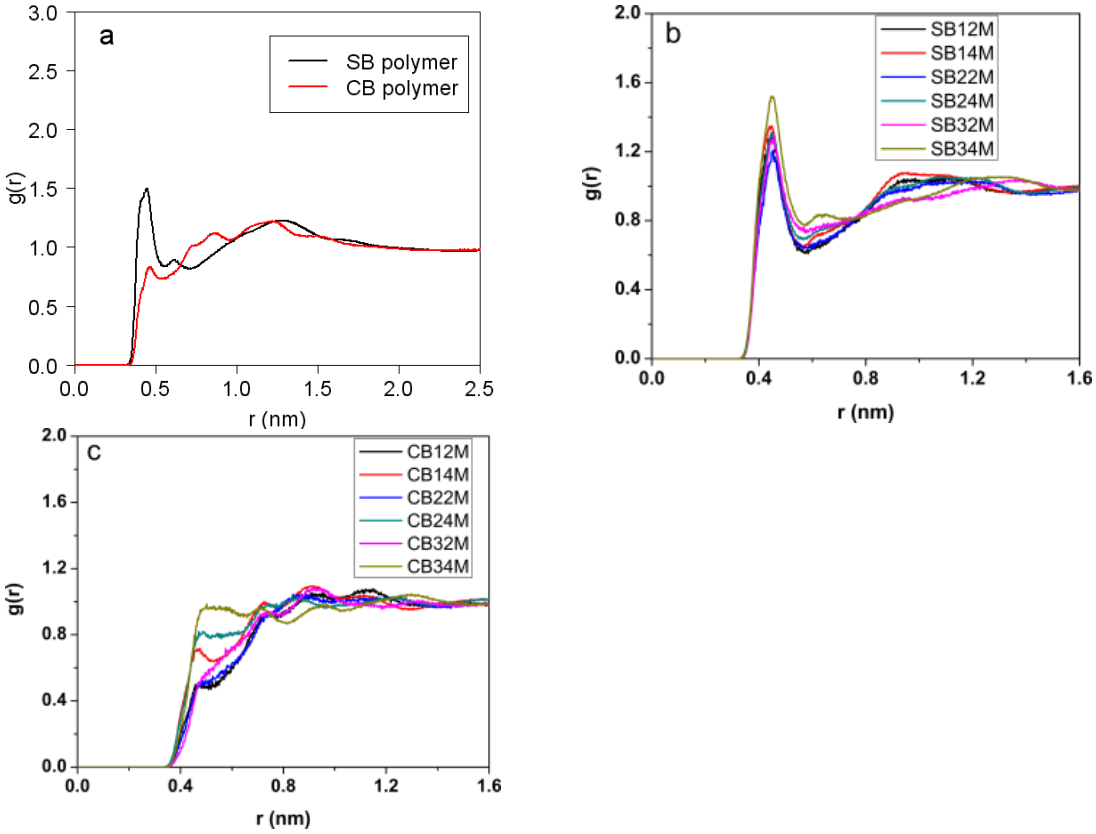

Figure 6.5. Radial distribution functions of the nitrogen atoms of cationic groups and the oxygen atoms of anionic groups for (a) PSBMA (N-O-SB RDF) and PCBMA (N-O-CB RDF), (b) small SB molecules with various carbon spacer lengths, and (c) small CB molecules with various carbon spacer lengths.

To investigate the origin of different behaviors of SB and CB polymers, we performed molecular dynamics simulations to study how cationic and anionic groups of zwitterionic moieties interact in these two zwitterionic polymers. Figure 6.5a shows the radial distribution functions (RDFs) of the nitrogen atoms in cationic groups and the oxygen atoms in anionic groups of SB polymers (N-O-SB) and CB polymers (N-O-CB) in 3 g/L solutions. As shown in Figure 6.5a, the N-O-SB RDF has a peak with a height of 1.5 at 0.5 nm, and the N-O-CB RDF does not have any significant peaks higher than 1. This

indicates that the zwitterionic SB moieties of SB polymers prefer to form associations among themselves, while the zwitterionic CB moieties of CB polymers do not.

The CB moieties of CB polymers have two methylene groups between the cationic and anionic groups, and the SB moieties of SB polymers have three methylene groups. To study if the carbon spacer length plays a role in the different associations of SB and CB moieties, we performed molecular dynamics simulations to study the associations among cationic and anionic groups of small SB and CB molecules with carbon spacers from one to three methylene groups. The molar concentrations of zwitterionic molecules were 2 and 4 mol/L, higher than the ones of zwitterionic moieties in the polymer solutions (~1.5 mol/L). Figures 6.5b and 6.5c showed that the three N-O RDFs of SB molecules all have a peak, which is not observed in CB molecules. This observation excluded the effect of carbon spacer length and confirmed that zwitterionic associations result from interactions of cationic and anionic groups.

Table 6.2 N-O pair numbers and lifetimes of SB and CB polymers

	Number	Elapsed time (ps)
PSBMA	373	323
PCBMA	163	115

We further studied the zwitterionic associations of SB and CB polymers by analyzing the numbers and dynamics of nitrogen atom-oxygen atom (N-O) pairs at 298 K and 100 kPa. The distance threshold to define an N-O pair of SB polymers is set to be 0.56 nm, *r* of the first minimum of the N-O-SB RDF. The elapsed time (τ) for the N-O pairs at certain time to decay to 1/e portion was used to characterize the pair dynamics. We also analyzed the N-O pair number and lifetime of CB polymers using the same method. As shown in Table 6.2, the N-O pairs of SB polymers have several folds the number and

elapsed time of CB-polymer N-O pairs, confirming that SB polymers have more and stronger zwitterionic associations than CB polymers.

Collins[125] proposed that cations and anions with similar hydration preferentially associate. Fennell et al.[144] showed that the relative affinity of ions in solution depends on the matching of cation and anion sizes. The observations here indicate that zwitterionic associations follow the same principle: cationic and anionic groups with similar charge strength preferentially form associations. SB polymers possess cationic and anionic groups that match well in charge strength, leading to zwitterionic associations and stimuli- responses. CB polymers possess charged groups that do not match in charge strength. Therefore, CB has few zwitterionic associations, and its does not have stimuli-responses, which are generally expected for zwitterionic polymers.

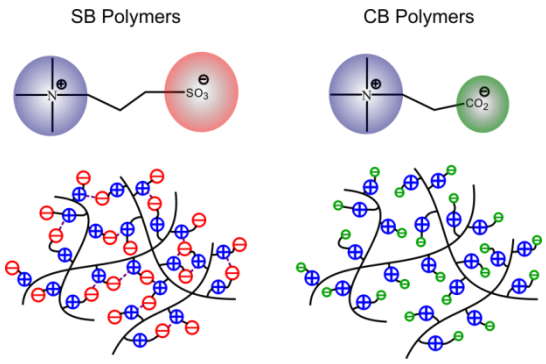

Schematic 6.1. Charge-strength matching determines associations among zwitterionic moieties in zwitterionic polymers.

6.5 Conclusions

We investigated the relationship between the thermal and salt responses of SB and CB polymers, and the structure and dynamics of associations among cationic and anionic groups in these two zwitterionic polymers. The results showed that matching in the

charge strength of cationic and anionic groups of zwitterionic moieties determines associations among moieties: better matching results in more and stronger associations. These different interaction behaviors lead to diversified properties of zwitterionic materials.

Zwitterionic CB moieties have cationic and anionic groups that do not match in charge strength, leading to fewer associations. This can allow zwitterionic moieties in CB materials to be fully hydrated and make CB materials have stronger hydration. In addition, the few associations make CB materials inert to external stimuli, different from the classical theory of conventional zwitterionic materials. At the same time, zwitterionic SB moieties have cationic and anionic groups that match well, and the formed associations make SB polymers stimuli responsive. Following this principle, zwitterionic phosphorylcholine (PC) moieties have cationic and anionic groups that match even better, and they can associate more and stronger than SB moieties. This could be the reason why zwitterionic PC groups are chosen by nature for cell membranes and why zwitterionic PC head groups can form highly ordered self-assembled monolayers[145].

Chapter 7 Carbon-Spacer-Length Effects on Hydration and Ionic Interactions of Carboxybetaine Moieties

Zwitterionic carboxybetaines (CBs) are ubiquitous in nature and considered promising materials for biological and chemical applications. A thorough understanding of the effect of carbon spacer length (CSL) on molecular properties is important. This chapter presented a study on the effects of CSL on the properties of CB moieties using molecular dynamics simulations, quantum mechanics and well-tempered metadynamics simulations. The hydration number, structure, and dynamics of carboxylic and trimethyl ammonium groups were investigated and found to present different behaviors in regards to the variation of CSL. The simulation results with partial charges developed from quantum mechanical calculations were compared with those with partial charges from the OPLS all atom (OPLSAA) force field. The hydration free energy of CB moieties and CB−Na^+ association was also studied as a function of CSL.

7.1. Introduction

Zwitterionic carboxybetaines (CBs) have received increasing attraction because of their importance in nature and their chemical and biological applications. In nature, glycine betaine and β–alanine betaine act as naturally occurring osmolytes and protein protectants[25, 146]. Recent experiments have shown CB-derived materials to be excellent candidates for applications such as drug delivery[6], gene delivery[147], and protein conjugation[8] because of their excellent resistance to nonspecific protein adsorption, biocompatibility and versatility[95]. A thorough illustration of the structure-property relationship is critically important for not only understanding the role of CB molecules in nature but also develop the applications of CB materials. A CB moiety possesses a

cationic trimethyl ammonium group and an anionic carboxylic group that are linked by methylene groups. The two charged groups are considered to be important for the properties of CB moieties, and their distance can be altered by varying the number of methylene groups, which is called carbon spacer length (CSL).

The effect of CSL on zwitterionic molecules has been studied[148-149] in several experiments. Zhang et al.[150] investigated the protein adsorption of CB-derived materials with CSLs of one, two, three and five methylene groups. Experiments showed that the CB materials with various CSLs can all resist nonspecific protein adsorption but have different applicable pH scales. Vaisocherova et al.[151] further showed that only materials derived from CBs with CSLs of one and two methylene groups are able to resist nonspecific protein adsorption from 100% blood serum, while CBs with CSLs of three or more methylene groups cannot resist protein adsorption from this complex medium. More recently, Mi et al.[152] showed different binding behaviors of divalent cations for CB materials with different CSLs, leading to different interactions with polysaccharides outside bacteria. The effect of CSL on the other properties of materials has also been studied, including adsorbed protein conformation[153], mobility of ionic group[154], thermal stability of the material[155], adsorption at the air-water interface[156] and electroosmotic flow[157]. These observations offer solid proofs about the important roles of CSL.

Weers et al.[148] have studied how the solution properties of betaine surfactant varies with CSL and their research showed the relationship between several properties of CB moieties and CSL. For instance, they showed that the pKa of the molecule increases as the CSL increases. They also showed that the molecular dipole increases monotonically with the increase in CSL and suggested that there is probably no intramolecular

association for charged groups. The critical micelle concentration was also found to be affected by the CSL.

However, the effect of CSL on the properties of CB moieties is poorly understood. One is its effect on hydration. Hydration is recognized to play an important role for applications in an aqueous environment[6, 158-159]. It is well known from studies of surfactants and lipids that the variation of alkyl chain length can change the ratio of hydrophobicity/hydrophilicity of molecule[160-161] and thus the hydration. However, the variation of CSL brings more effects on the CB moiety than just alternating its hydrophobicity/hydrophilicity ratio. It could change the interplay of charged groups and the overlap of their coordination shells. The variation of these two factors can affect basic molecular hydration. Therefore, a thorough study of how the hydration of a CB moiety varies as a function of CSL can not only offer insight in the hydration-structure relationship for a zwitterionic molecule but also guide the rational design of CB materials. Another critical effect of CSL regards the ionic association of the CB moiety. Previous studies have shown the important role of ionic association to the performance of zwitterionic materials[143, 162-163]. Since the charges of charged groups are expected to vary with the variation of CSL, this may cause the variation of ionic association, which has not been thoroughly studied yet.

To address these issues, we will study the effect of CSL on the properties of CB moiety, focusing on hydration and ionic association. We will investigate hydration and ionic association from structural, dynamic and energy aspects. The electron density distributions of CB moieties with various CSLs will also be investigated. The

corresponding properties of CB molecules with different CSLs will be compared in the aim to explore the effect of CSL.

7.2 Simulation Details

7.2.1 Quantum Chemical Calculations

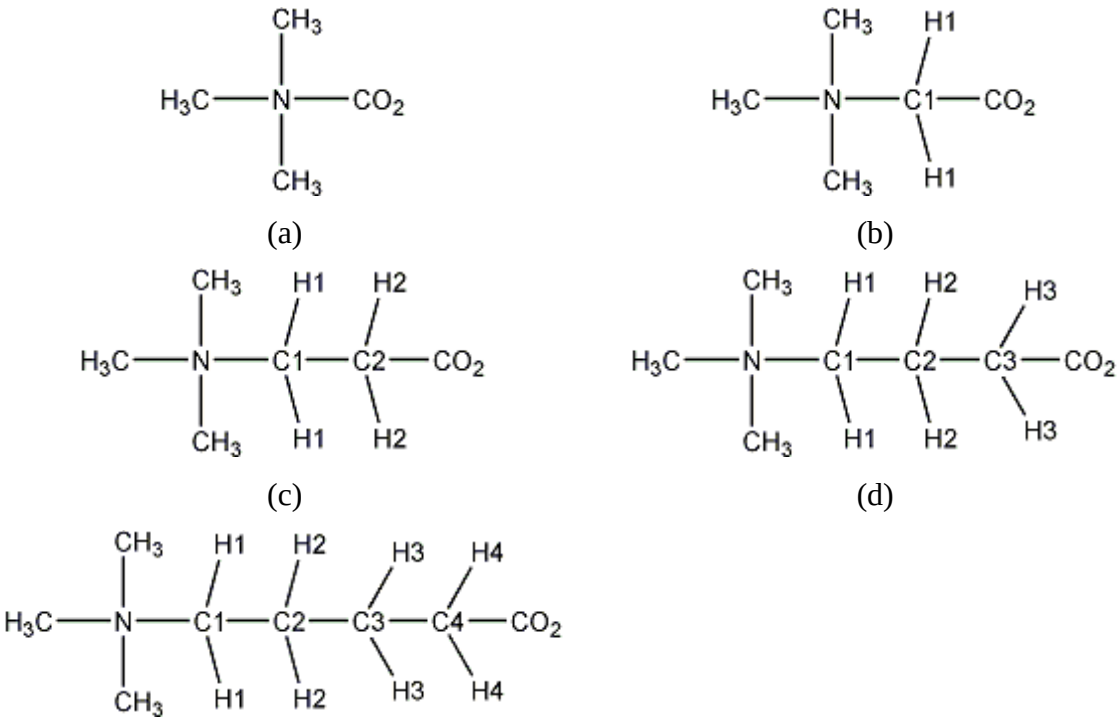

Figure 7.1 Schematic of the five CB moieties (a) CB0, (b) CB1, (c) CB2, (d) CB3 and (e) CB4.

Quantum mechanical calculations were carried out using the Gaussian 2009[50]. For each CB moiety, we rotated the dihedral angles C(N)-N-C-C and C-C-C-O to generate the input conformations for quantum mechanical calculations. All of the conformations were first minimized with a classical UFF force field[164] and then further optimized in an implicit water solvent at the B3LYP/6-311++G (d, p) level. The polarizable continuum model was used to describe the implicit water solvent.[165] The optimized conformations

were used for the calculation of partial charge and analysis of electrostatic potential surface and the electron density. For each CB moiety, the conformation with the lowest potential energy was chosen for single pointe calculation for the analysis of electrostatic potential surface.

In this work, a new set of partial charges were calculated for each CB moiety with quantum mechanical calculation. The atomistic charges of CB moieties were calculated with the CHELP algorithm[166], which fits the atomic charges to the electrostatic potential of the molecule. For each CB moiety, the partial charges used in MD simulations were obtained by averaging in two steps. The first is the average among the same type of atoms in one single conformation. For one CB moiety, the same type of atoms means all the atoms in the same geometrical and chemical positions, such as the nine hydrogen atoms of the three methyl groups bonding to the nitrogen atom. The second is the average among various conformations weighted by the Boltzmann factor. The L-J parameters were obtained from the OPLS all atom (OPLSAA) force field[52] developed by the Jorgensen group because of its good representation of small organic molecules. The force field parameters of all five CB moieties were listed in Tables 7.1-7.4.

Table 7.1. Nonbond interaction parameters of atoms of the five CB moieties. See the labels in Figure 6.1

	q (e)					σ (nm)	ε(kJ mol^{-1})
	CB0	CB1	CB2	CB3	CB4		
Trimethyl ammonium group							
N	0.3080	0.3838	0.3516	0.2849	0.3382	0.325	0.7113
C	-0.2740	-0.3224	-0.3226	-0.2955	-0.3082	0.350	0.2761
H	0.1120	0.1519	0.1514	0.1506	0.1517	0.250	0.0628
Carboxylic group							
C	0.8100	0.9414	0.9070	0.9586	0.9741	0.375	0.4393
O	-0.6520	-0.8584	-0.8756	-0.9122	-0.9211	0.296	0.8786
Carbon Spacer Length							
C1		-0.1833	0.0200	-0.1153	-0.1024	0.350	0.2761
H1		0.0875	0.0660	0.1013	0.0947	0.250	0.0628
C2			-0.1262	0.1422	-0.0028	0.350	0.2761
H2			0.0360	-0.0025	0.0248	0.250	0.1255
C3				-0.1441	0.1336	0.350	0.2761
H3				0.0158	-0.0267	0.250	0.1255
C4					-0.1414	0.350	0.2761
H4					0.0083	0.250	0.1255

Table 7.2. Bond parameters of the five CB moieties

	k_b(kJ mol^{-1} nm^{-2})	b(nm)
N-C	307105	0.147
C-H	284512	0.109
C-O	548940.8	0.125
C-C	224262.4	0.153

$$V_b(r) = \frac{1}{2} k_b (r - b)^2$$

Table 7.3. Angles parameters of the five CB moieties

	k_θ (kJ mol^{-1} rad^{-2})	θ_0(degree)
C-N-C	418.40	113.0
N-C-O	418.40	109.5
C-C-O	585.76	117.0
H-C-H	276.144	107.8
H-C-C	292.88	109.5
C-C-C	488.273	112.7
H-C-N	292.880	109.5

$$V_a(\theta) = \frac{1}{2} k_\theta (\theta - \theta_0)^2$$

Table 7.4. Torsion parameters of the five CB moieties (*Ci*: kJ mol^{-1} rad^{-i})

	C_0	C_1	C_2	C_3	C_4	C_5
H-C-N-C	0.63179	1.89535	0.00000	-2.52714	0.00000	0.00000
C-N-C-C	3.04176	-1.35144	0.51881	-2.20915	0.00000	0.00000
N-C-C-C	5.77183	-2.67148	0.95814	-4.05848	0.00000	0.00000
N-C-C-H	0.80333	2.40999	0.00000	-3.21331	0.00000	0.00000
C-C-C-C	2.92880	-1.46440	0.20920	-1.67360	0.00000	0.00000
H-C-C-C	0.62760	1.88280	0.00000	-2.51040	0.00000	0.00000
H-C-C-H	0.62760	1.88280	0.00000	-2.51040	0.00000	0.00000
C-C-C-O	3.43088	0.00000	-3.43088	0.00000	0.00000	0.00000
H-C-C-O	0.00000	0.00000	0.00000	0.00000	0.00000	0.00000
N-C-C-O	3.43088	0.00000	-3.43088	0.00000	0.00000	0.00000
C-N-C-O	0.00000	0.00000	0.00000	0.00000	0.00000	0.00000

$$V_{rb}(\varphi) = \sum_{n=0}^{5} C_n \left(cos(\varphi - 180^o)\right)^n$$

7.2.2 Molecular Dynamics Simulations

The schematics of the five CB molecules are shown in Figure 7.1. All atom models are used in this work. The SPC/E water model[49] was used because of its good representation of the dipole moment, dielectric constant and diffusion properties of water molecules. The potential energy of intermolecular interactions is calculated as a combination of a Lennard-Jones (L-J) 12-6 potential and a Coulomb potential, as shown in Equation 7.1.

$$U(r_{ij}) = 4\varepsilon_{ij}\left[\left(\frac{\sigma_{ij}}{r_{ij}}\right)^{12} - \left(\frac{\sigma_{ij}}{r_{ij}}\right)^{6}\right] + \frac{q_i q_j}{r_{ij}} \qquad (7.1)$$

where r_{ij} is the distance between atoms i and j, q_i is the partial charge assigned to atom i, and ε_{ij} and σ_{ij} are energy and size parameters obtained by Jorgensen combining rules.

The simulation system for the investigation of hydration was a periodic water box containing water molecules and one CB moiety. The molecular dynamics (MD) simulations were performed using Gromacs (version 4.5.4) [54] in an isobaric-isothermal ensemble (NPT). For all the five CB cases, after energy minimization and a 1.0 ns MD run with an integral step of 1.0 fs for equilibrium, another 1.0 ns run was carried out with an integral step of 2.0 fs. The coordinates were saved every 0.2 ps. Long-range electrostatic interactions were computed with the particle mesh Ewald method with periodic boundary conditions in all three dimensions.[55] The short-range van der Waals interactions were calculated with a cutoff distance of 1.1 nm. During the first 1.0 ns MD run for equilibrium, the system was maintained at 298 K (0.1 ps time constant) and 100.0 kPa with the Berendsen algorithm[56] (with a compressibility of 4.5×10^{-5} bar^{-1} and a 1 ps time constant). During the second 1.0 ns MD simulation for data collection, the system was maintained at 298 K with the Nose-Hoover algorithm[57-58] and 100 kPa with the

Parrinello-Rahman algorithm.[59] Intramolecular bonds of betaine molecules and water molecules were kept constrained with the LINCS algorithm.[60] MD simulations with the developed partial charges and the original ones from the OPLSAA force field were performed and compared.

In order to compare the force fields with partial charges developed in this work and from the OPLSAA force field, we also calculated the interaction energy *E* of the CB moiety and one water molecule from QC calculations and with these two sets of force fields, as listed in Table 7.5. The initial conformations of the five CB-water systems were shown in Figure 7.5. The result of CB0 with partial charges developed in this work is much closer to that from QC calculations than that with partial charges from the OPLSAA force field is. In addition, *E* values for the CB moieties with longer CSL are lower than those for the CB moieties with shorter CSL. This indicates the variation of the partial charges of those CB moieties with CSL and the necessity to recalculate their partial charges, especially to those with shorter CSL in which charge transfer occurs.

For the five CB-Na^+ simulation cases, a 10.0 ns MD simulation was carried out for data collection after energy minimization and a 10.0 ns MD run for equilibrium. The simulation system was the same as that used in our previous work.[143] The other details were the same as in the CB cases.

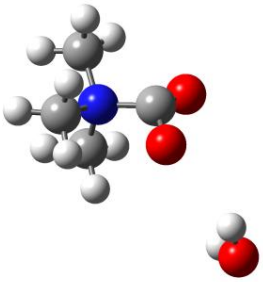

(a) CB0-Water

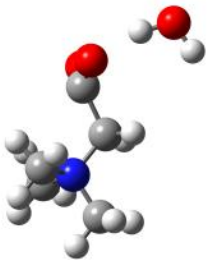

(b) CB1-Water

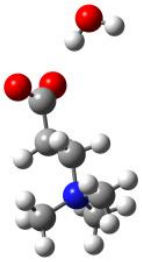

(c) CB2-Water

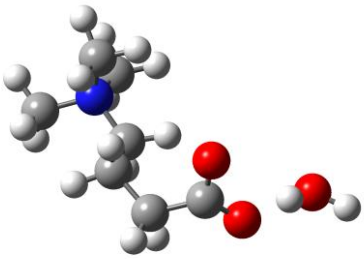

(d) CB3-Water

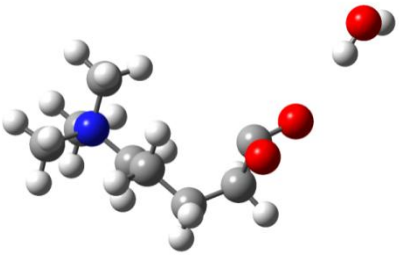

(e) CB4-Water

Figure 7.2. Conformations of CB-water systems

Table 7.5 Interaction energy *E* calculated with quantum chemical calculations and classical force fields

	B3LYP (kJ mol^{-1})	this work(kJ mol^{-1})	OPLSAA (kJ mol^{-1})
CB0	-45.4	-41.9	-65.4
CB1	-42.2	-41.6	-42.7
CB2	-59.0	-48.8	-49.8
CB3	-86.5	-80.5	-75.6
CB4	-86.3	-82.2	-84.9

7.2.3 Metadynamics Calculations for Na^+ Association Free Energy

The metadynamics algorithm developed by Laio et al.[85] was used to evaluate the association free energy of Na^+ and CB moieties. We applied a well-tempered metadynamics simulation[84] since it rescales the Gaussian weight factor and guarantees the convergence of simulation. The two selected collective variables were the distances between Na^+ and the two oxygen atoms of CB moiety. The initial Gaussian weight factor was set to be 1.5 kJ mol^{-1} and the deposition rate of the Gaussian bias terms was set to be 250 fs with a bias factor of 10. The standard deviation for the Gaussian bias term was set to be 0.05. The whole simulation time is 100 ns and the output frequency is 250 fs. All the metadynamics simulations were carried out in a NVT ensemble with v-rescale algorithm [86] to control the temperature around 298 K using Plumed-1.3.0[87] implemented gromacs-4.5.5.

7.3. Results and Discussions

7.3.1 Electrostatic Potential Surfaces of CB Moieties

Partial charges of the two charged groups are critical to the hydration and ionic association of a zwitterion. Variation of the CSL changes their distance and affects the charges. Figure 7.3 shows the electrostatic potential surfaces (EPSs) of the most optimized structure of the five CB moieties in implicit water solvent. It can be seen that the EPS color of carboxylic groups of CB0 and CB1 is considerably lighter than the others. The same phenomenon is observed in the color depths of EPS around trimethyl ammonium groups. This observation indicates that the two charged groups in CB0 and CB1 are both less charged than their counterparts in CB moieties with longer CSLs, due to the strong interplay between them.

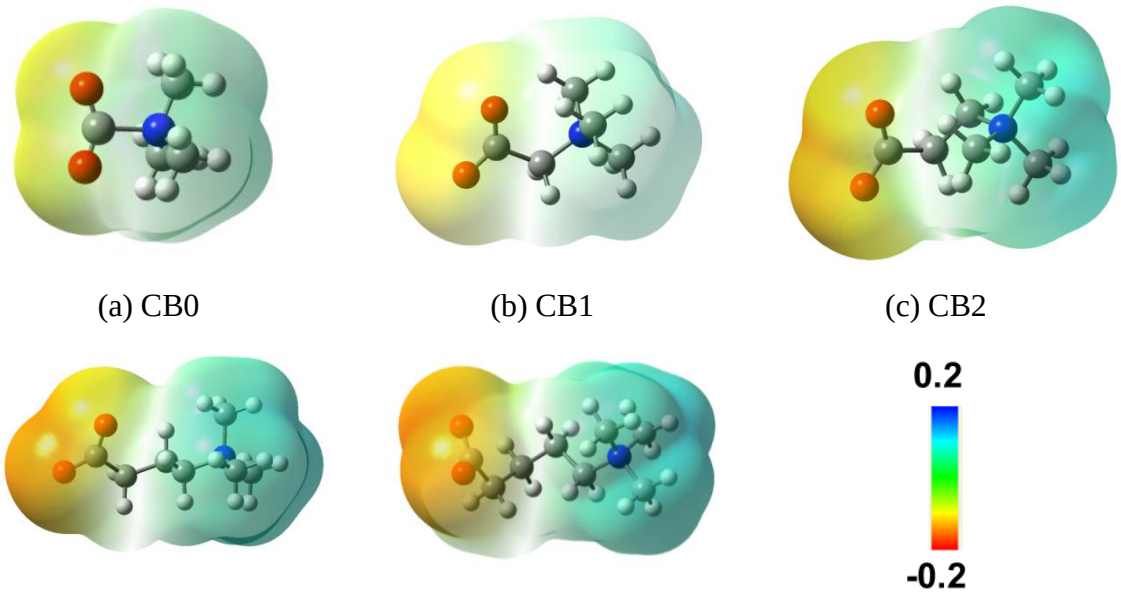

(a) CB0 (b) CB1 (c) CB2

(d) CB3 (e) CB4

Figure 7.3 EPSs of (a) CB0, (b) CB1, (c) CB2, (d) CB3 and (e) CB4.

In CB moieties with longer CSLs, the interplay between charged groups decreases sharply. As shown in Figure 7.3, the color depths of corresponding EPSs around charged groups are similar in CB3 and CB4. This similarity indicates that variation of the CSL cannot affect the interplay between charged groups as significantly as in CB molecules with shorter CSLs. This is expected because the two charged groups must be very close to interplay with each other. The distance increase induced by growing CS weakens this interplay sharply. It has been reported[148] that the pKa of a CB1 surfactant is around 2, lower than that of CB2 surfactant (around 3.2), which is consistent with the sharp decrease in interplay observed in this work. Thus, we may expect that when the CSL < 3, the variation of CSL may affect the hydration and ionic association significantly. When CSL ≥ 3, the variation of CSL may just tune the number of methylene groups in the

molecule and molecular flexibility, but hardly change the partial charges of two charged groups.

We further analyzed the electron distributions around the carboxylic groups of the five conformations shown in Figure 7.3 using Bader analysis[167-168]. Different from CHELP algorithm, Bader analysis calculates the atomic charge based on the number of electrons near the atom. In Bader analysis, the whole space of electrons is divided into Bader regions by the zero flux surfaces. A zero flux is a 2-D surface on which the electron density is at a minimum perpendicular to the surface. The aim of this analysis is to observe whether the partial charges obtained from electron densities and calculated from the CHELP algorithm have similar tendency as CSL varies. As shown in Table 7.6, the partial charges calculated with these two methods showed the same trend with the variation of CSL, though their values are different. The carboxylic group in CB0 is much less negatively charged as compared to those in the CB moieties with longer CSL. Increasing CSL results in the enhancement of the negative charges of the carboxylic group, but this effect decreases as the CSL increases. The carboxylic groups in CB3 and CB4 have similar partial charges.

Table 7.6. Partial charges of the carboxylic groups of the five CB moieties obtained with Bader's analysis and CHELP algorithm

	CB0	CB1	CB2	CB3	CB4
Bader(e)	-0.388	-0.822	-0.917	-0.964	-0.938
CHELP(e)	-0.494	-0.775	-0.844	-0.866	-0.868

7.3.2 Radial Distribution Functions between Water and CB Moieties

Hydration is recognized to be critically important to assess a zwitterion thoroughly.[6] To evaluate the hydration of a CB moiety properly, we first analyzed the radial distribution functions (RDFs) of water molecules and selected atoms of the CB moiety. We selected the oxygen atoms of the carboxylic group, carbon atoms of the trimethyl ammonium group and carbon atoms in the CS part as the feature atoms of these three parts. Figure 7.4 shows the RDFs of these atoms and oxygen atoms of the water molecules for MD simulations with the partial charges developed in this work and from the OPLSAA force field.

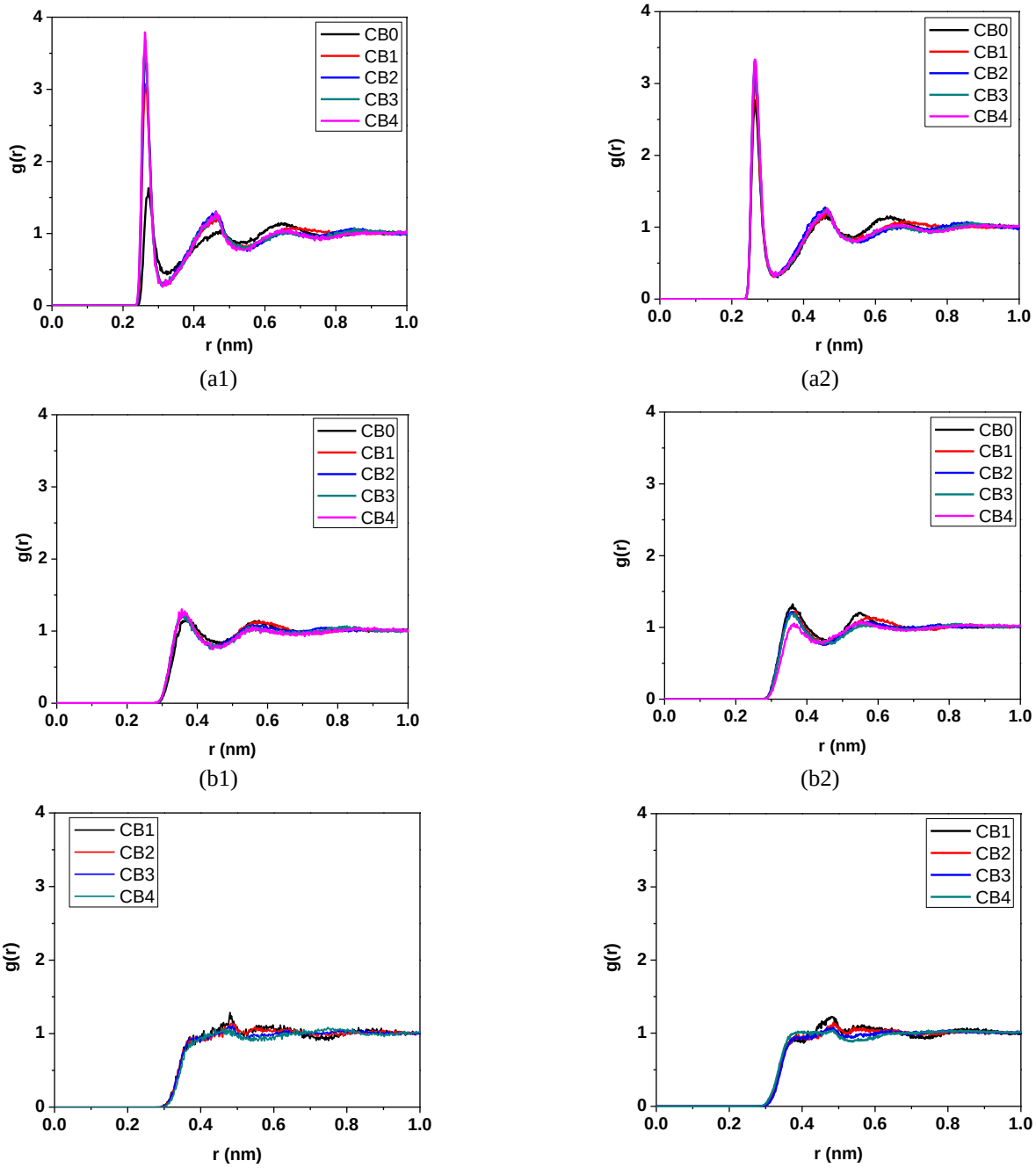

Figure 7.4. RDFs of atoms of CB moieties and oxygen atoms of water molecules in simulations with partial charges developed in this work or from the OPLSAA force field. (a1) O-Ow (this work), (a2) O-Ow (OPLSAA), (b1) C(N)-Ow (this work), (b2) C(N)-Ow (OPLSAA), (c1) C(C)-Ow (this work) and (c2) C(C)-Ow (OPLSAA).

A peak in a RDF profile indicates the existence of a coordination shell and its position defines the geometric radius of the coordination shell. As shown in Figure 7.4, both the RDFs with partial charges in this work and those from the OPLSAA force field show that only the O-Ow RDFs have obvious peaks, whereas no significant peaks can be observed for the other two RDFs. This difference in RDFs indicates the difference in the hydration of the carboxylic group and other parts of the molecule and these two sets of force field parameters give consistent results. To O-Ow RDFs, we observe that their peaks in Figure 7.4a1 and Figure 7.4a2 are at same positions. These two sets of force field parameters give the same results on the size of the coordination shell of the carboxylic group.

With the partial charges in this work, the peaks of O-Ow RDFs show a variation as a function of CSL similar to that observed for EPS color depth. As shown in Figure 7.4a1, the peak height for CB0 is 1.5 and increases to 3.0 for CB1. The peak heights for CB3 and CB4 are higher than the ones of CB1 and CB0, and very similar to each other. This indicates that the hydration of the carboxylic group may show variation in CB moieties with shorter CSLs and be similar in those with CSL ≥ 3. For the other parts of molecule, we can observe that C(N)-Ow and C(C)-Ow RDFs merely change as the CSL varies, indicating that their hydration may not show a significant change as the CSL varies. In the OPLSAA force field, the carboxylic groups in five CB moieties are set to have same partial charges, and there is not significant variation in peak height, as shown in Figure 7.4a2.

7.3.3 Coordination Numbers

A previous study has shown that water molecules in the coordination shells of trimethyl ammonium and carboxylic groups have significantly different structures and dynamics.[48]

When close enough, the two coordination shells may overlap geometrically and affect the behavior of water molecules in the shells. We investigated the overlap phenomenon by analyzing the numbers of water molecules in the overlap region of the coordination shells of the two charged groups and only in the shells of the charged groups. The coordination shells of these two charged groups are defined in the same way as in our previous work[48] based on the RDFs shown in Figure 7.4. Table 7.7 lists the numbers of water molecules in the overlap (in the shells of both carboxylic and trimethyl ammonium groups), negative (only in the shell of carboxylic group), positive (only in the shell of trimethyl ammonium group) and CS (only in the shell of CS part) regions, as well as the number of water molecules in these regions obtained from MD simulations with partial charges developed in this work and from the OPLSAA force field.

Table 7.7 Number of water molecules in positive, negative, CS and overlap regions and their sum

		Positive	Negative	CS	Overlap	Total No.
CB0	This work	17.10	2.91	0.00	2.26	22.27
	OPLSAA	17.70	4.46	0.00	2.58	24.74
CB1	This work	17.35	5.56	2.63	1.61	27.15
	OPLSAA	17.67	6.21	2.96	1.39	28.23
CB2	This work	18.06	6.62	4.31	0.76	29.75
	OPLSAA	17.4	5.21	3.86	1.34	27.81
CB3	This work	17.85	6.25	7.34	0.98	32.42
	OPLSAA	20.23	4.83	6.03	1.26	32.35
CB4	This work	18.60	6.76	9.44	0.50	35.30
	OPLSAA	16.09	6.62	11.86	0.74	35.31

As listed in Table 7.7, the numbers of water molecules in the four regions from MD simulations with partial charges developed in this work are similar to those from simulations with partial charges from the OPLSAA force field. Therefore, the effect of CSL will be analyzed only based on the simulation results with partial charges developed in this work. For CB0, the numbers of water molecules in the negative and overlap regions are 2.91 and 2.26, respectively, which means that around 44% of water molecules in the coordination shell of the carboxylic group are also considered in the shell of the trimethyl ammonium group. This significant overlap indicates the water molecules in the coordination shell of the carboxylic group of CB0 have structure and dynamics differently from those CB moieties with longer CSs. This overlap decreases rapidly as the CSL increases. For instance, for CB1, the numbers for the overlap and negative regions are 1.61 and 5.56. This means that the percentage decreases from 44% to only 23%. For CB moieties with a CSL ≥ 2, the number for the overlap region decreases to less than one, indicating that the overlap may be not even a stable phenomenon.

To the water molecules in the coordination shell of trimethyl ammonium groups, the effect of overlap may be weaker since the coordination number for the trimethyl ammonium group is definitively larger than the corresponding number for the carboxylic group. As listed in Table 7.7, the water molecules in the overlap region only count for at most 12% of all the water molecules in the coordination shell of the trimethyl ammonium group. However, since the effect of the carboxylic group on a water molecule is profoundly stronger than the that of the trimethyl ammonium group,[48] it is not clear up to now about how the water molecules in the coordination shell of the positively charged

group would vary because of this overlap. Further investigation of the hydration structure and dynamics is necessary to offer a clear view.

The number for the CS region increases monotonically with the growing CSL, as listed in Table 7.7. The previous RDFs in Figures 7.4c1 and 7.4c2 have indicated that the water molecules of this region behave like those near a nonpolar substance. Thus, this increase implies that there is more hydrophobic part in the hydration of molecule.

7.3.4 Hydration Structures and Dynamics of CB Moieties

Besides the number of water molecules, their structure[48, 107] and dynamics[48] are also critically important to evaluate the molecular hydration thoroughly. The hydration structure and dynamics of carboxylic and trimethyl ammonium groups were investigated by analyzing the distributions of dipole orientation θ and residence curve $C(t)$ of water molecules in the respective coordination shells of charged groups, as defined in our previous study.[48] The water molecules in the overlap region are considered to be in the coordination shells of both charged groups. Figure 4 shows the distributions of $\cos\theta$ of the coordination shells of the two charged groups with partial charges developed in this work (Figure 7.5a and 7.5b) and from the OPLSAA force field (Figure 7.5c and 7.5d). Figure 5 shows $C(t)$ of the coordination shells of the two charged groups with partial charges developed in this work (Figure 7.6a and 7.6b) and from the OPLSAA force field (Figure 7.6c and 7.6d).

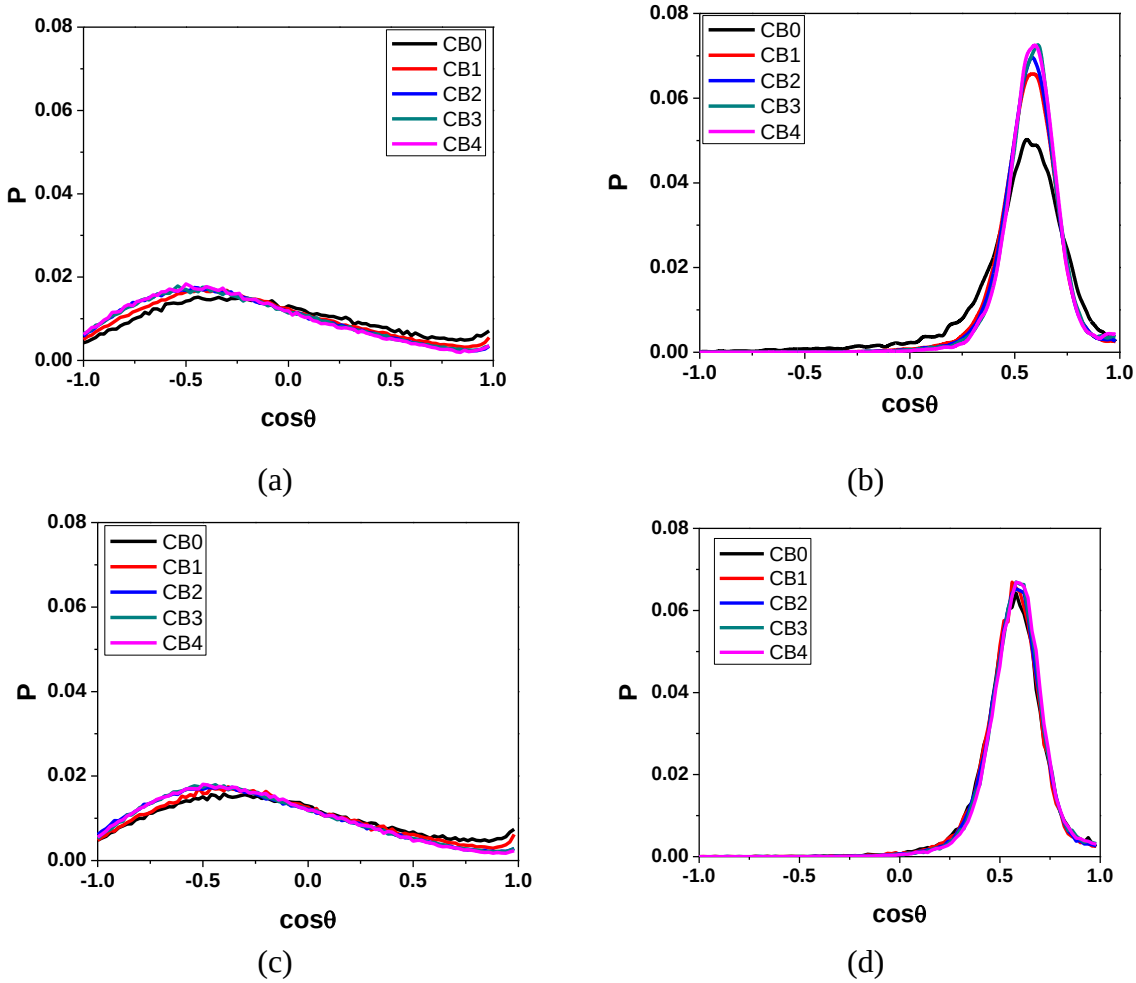

Figure 7.5. Distributions of cosθ for the dipole moment of water molecules in the coordination shells of trimethyl ammonium and carboxylic groups with partial charges developed in this work and from the OPLSAA force field. (a) trimethyl ammonium and (b) carboxylic groups with partial charges from this work, (c) trimethyl ammonium and (d) carboxylic groups with partial charges from the OPLSAA force field.

As shown in Figure 7.5, the distributions of cosθ for the carboxylic group from simulations with partial charges developed in this work and from the OPLSAA force field present different variations as to the variation in the CSL. The distribution with partial charges developed in this work has its peak height increase when the CSL increases. The peak height remains identical when the CSL $\geq$ 3. This indicates that the

hydration structure of the carboxylic group increases as the CSL increases, and reaches a steady state when CSL ≥ 3. The distribution from simulations with partial charges from the OPLSAA force field does not present the similar variation. Instead, the distributions for all five CB molecules are nearly identical, as shown in Figure 7.5d. This indicates that the hydration structures of the carboxylic groups of all five CB molecules are similar. The simulation results with both of these two sets of partial charges show that the distribution of $\cos\theta$ for the trimethyl ammonium group does not have a significant variation as the CSL varies.

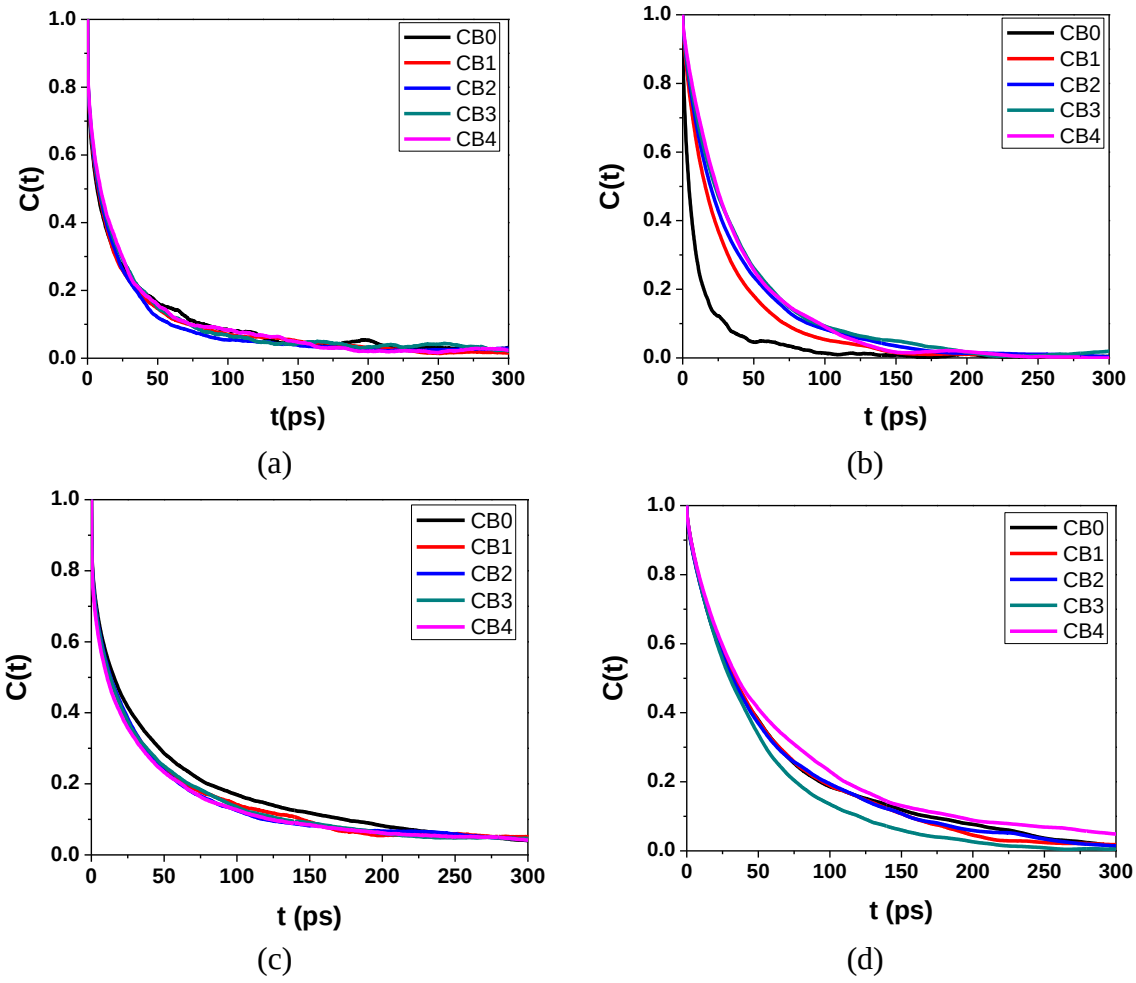

Figure 7.6. Residence time curves *C*(*t*) of water molecules in the coordination shells of trimethyl ammonium and carboxylic groups with partial charges developed in this work and from the OPLSAA force field. (a) trimethyl ammonium and (b) carboxylic groups with partial charges from this work, (c) trimethyl ammonium and (d) carboxylic groups with partial charges from the OPLSAA force field.

The analysis of *C*(*t*) reveals the tendency for water molecules to stay near the carboxylic group. The respective residence times τ for the five curves in Figure 7.7b, calculated with the same method as in our previous paper,[48] are 8.64 ps (CB0), 27.06 ps (CB1), 33.54 ps (CB2), 37.28 ps (CB3) and 37.01 ps (CB4). The increment ratios are 213% (CB0-CB1), 24% (CB1-CB2), 11% (CB2-CB3) and -1% (CB3-CB4). This indicates that

water molecules stay in the coordination shell of the carboxylic group longer as the CSL increases and this increase only occurs when the CSL < 3. When the CSL ≥ 3, the CSL variation will not change the residence time of water molecules near the carboxylic group. τ for the five curves in Figure 7.6d are 56.58 ps (CB0), 55.92 ps (CB1), 55.69 ps (CB2), 46.83 ps (CB3) and 65.00 ps (CB4). This indicates that, with partial charges from the OPLSAA force field, there is no CSL dependence for τ.

Experiments have shown that the CB moiety with a shorter CSL has a lower pKa. The lower pKa indicates that the carboxylic group in a CB molecule with a shorter CSL has a weaker ability to attract hydrogen atoms. Therefore, the interaction between the carboxylic group and water molecules should be weaker for a CB moiety with a shorter CSL. The results from MD simulations with partial charges developed in this work show a CSL dependence consistent with that trend in pKa measurements, while the simulations with partial charges from the OPLSAA force field does not show such variation.

As the CSL increases, the carboxylic group is becoming more highly charged and the overlap with the coordination shell of the trimethyl ammonium group is decreasing. The interaction between water molecules and the carboxylic group is growing stronger and the behavior of water molecules is more determined by the carboxylic group only. Consequently, the hydration structure and dynamics increases. When CSL ≥ 3, variation of the CSL cannot cause significant variation of partial charges in the carboxylic group and the overlap. Thus the cosθ distribution and $C(t)$ are nearly identical.

7.3.5 Hydration Free Energy of CB Moieties

Hydration free energy ΔG is used in the aim to describe the hydration of the whole molecule as a function of CSL. The hydration free energy was calculated using the

perturbation method as in our previous study[48]. We only studied Δ*G* with partial charges developed in this work because the results with them are consistent with the observations from experimental pKa measurements. In addition to the five CB moieties with CSLs ranging from one to four, we added three more CB moieties with CSLs of six, eight and ten methylene groups to investigate the effect of the CSL on hydration free energy on a larger scale. For the three newly added CB moieties, the partial charges of atoms in their charged groups are the same as the ones of the CB4 moiety and the additional methylene groups are parameterized with the OPLSAA force field. Figure 7.7 shows the relative hydration free energy (ΔΔ*G*) of these eight CB molecules as a function of CSL with the average hydration free energy of CB3 taken as a reference.

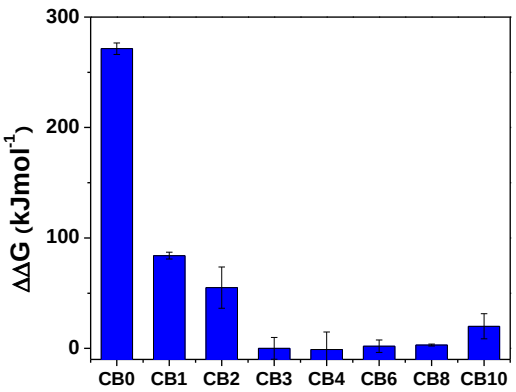

Figure 7.7 Relative hydration free energy (ΔΔ*G*) of CB molecules as a function of CSL.

The hydration free energy of CB0 is the highest among these eight CB molecules. For CB molecules with CSL < 3, the increase of CSL results in a decrease of ΔΔ*G*. This is attributed to the charge increase of the two charged groups. However, the reduction rate decreases as CSL increases. For instance, the hydration free energy of CB1 is nearly 170 kJ mol^{-1} lower than that of CB0, while the hydration free energy of CB2 is only around

30 kJ mol^{-1} lower than that of CB1. The hydration free energy is related to the hydration structure and dynamics around the overall molecule. For CB molecules with shorter CSLs, the main contributor to the variation of hydration free energy is the hydration of the two charged groups. As shown in the previous analysis, from CB0 to CB1, the hydration structure and dynamics around the carboxylic group exhibits the most significant change. With the increase in the CSL, the variation rate of the hydration structure and dynamics in regards to the CSL decreases. Consequently, the variation rate of the hydration free energy decreases.

We cannot observe significant variation of the hydration free energy for those CB molecules with CSL $\geq$ 3. As we have shown in previous sections, the trimethyl ammonium and carboxylic groups in these molecules have similar hydration structure and dynamics. Thus the main contributor to the variation of hydration free energy for these CB molecules may come from the CS part itself. The methylene group is hydrophobic and supposed to increase the hydration free energy. However, the change of hydration free energy brought by the methylene group is small. For instance, the hydration free energy of ethane is 11.0 kJ mol^{-1}, while the value for propane is 12.1 kJ mol^{-1},[169] indicating that the addition of one methylene group may just add around 1.1 kJ mol^{-1} to the hydration free energy; this is not very noticeable compared to that caused by the charge variation of the two charged groups.

7.3.6 Association of Na^+ with CB Moieties

Na^+ is ubiquitous in nature and associates with the carboxylic group of CB moieties. The association can vary with CSL since the variation of CSL results in the change of electron density for the carboxylic group. In this work, Na^+-CB associations were

analyzed from structure, dynamics and energy aspects. The association is also only studied with partial charges developed in this work because these results are consistent with the observations from experimental pKa measurements. The association structure was investigated with RDF between Na^+ and oxygen atoms of the CB moiety, as shown in Figure 7.8a. All five profiles present a significant peak at a position of around 0.25 nm, demonstrating that Na^+ can form a stable and direct association with the oxygen atoms of all of them. The peak height varies significantly with the CSL. As shown in Figure 7.8a, the peak height follows the sequence: CB0 < CB1 < CB2 < CB3 ≈ CB4. The peak heights of CB3 and CB4 are nearly five times as that of CB0. Such considerable difference indicates that CB moieties with longer CSLs may have a much higher preference to associate with Na^+, due to the higher partial charges of their carboxylic group. This tendency is further confirmed by the analysis of association dynamics. As shown in Figure 7.8b, the association residence curve for the CB moiety with a long CSL decays slower than the ones of short CSL, indicating a stronger and more stable association.

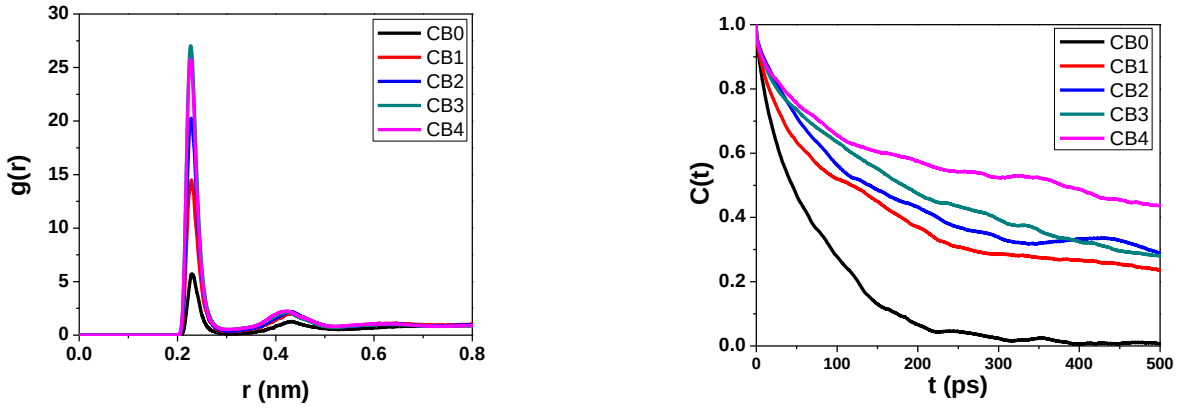

(a) (b)

Figure 7.8 Na^+-CB associations: (a) RDFs and (b) residence curves of association of Na^+ and oxygen atoms of CB moieties.

Figure 7.9 shows the free energy contour plots as a function of distances between Na^+ and two oxygen atoms of CB moieties r_1 and r_2. For every contour plot, we can observe three minimum regions labeled as A, B, and C in each figure. These three minimum regions correspond to two types of associations between Na^+ and CB moieties. As shown in Figure 7.9, region A has both r_1 and r_2 in the scale from 0.23 to 0.27 nm, close to the peak position (0.25 nm) observed in the RDFs. This represents the situation that Na^+ associates with both oxygen atoms. Regions B and C has either r_1 or r_2 close to 0.25 nm, and the other collect variables in the scale from 0.35 to 0.45 nm. These two regions represent the situation that Na^+ only associates with one oxygen atom.

The formation of a direct association needs to overcome an energy barrier sourced from the depletion and rearrangement of a certain part of coordination shells of both solutes. As shown in Figure 7.9, for every CB moieties, we can observe a plateau that represents the energy barrier. We can find that the maximum energy barriers for CB0 and CB1 are higher than 15 $kJ \cdot mol^{-1}$, whereas the corresponding values for CB2, CB3 and CB4 are all less than 15 $kJ \cdot mol^{-1}$. In addition, we can observe that the barrier region with an energy higher than 10 $kJ \cdot mol^{-1}$ decreases with an increasing CSL. These two observations also indicate that the CB moieties with long CSLs more easily form associations with Na^+.

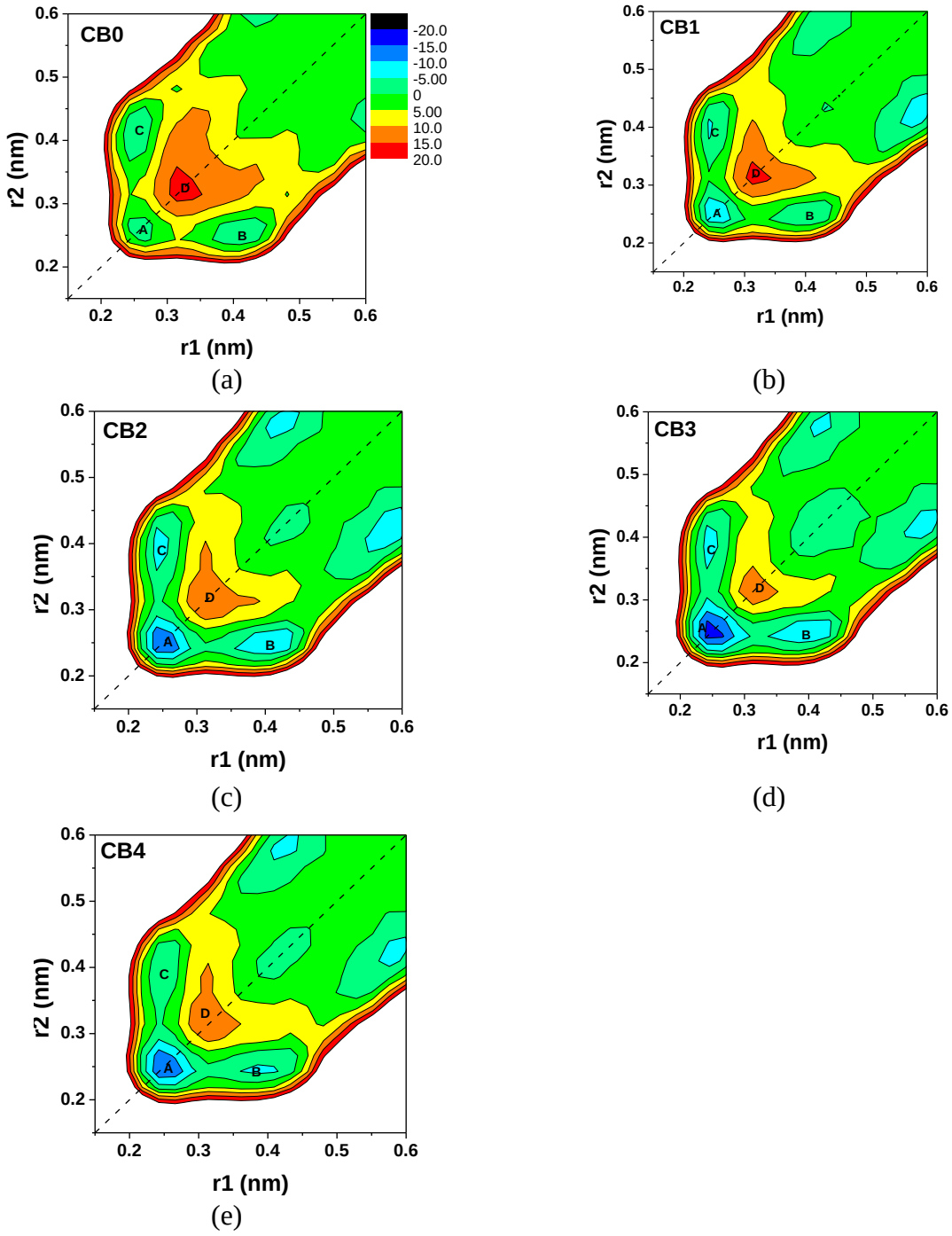

Figure 7.9. Association free energy of five CB moieties with Na^+ (a) CB0-Na^+, (b) CB1-Na^+, (c) CB2-Na^+, (d) CB3-Na^+ and (e) CB4-Na^+. r1 and r2 are the distances between Na^+ and the two oxygen atoms of CB moieties.

7.5. Conclusions

This work studied the effect of CSL on the properties of CB moieties using molecular simulations, quantum mechanical calculations and well-tempered metadynamics simulations. Five CB moieties with CSLs from zero to four were used. The EPS analysis showed that the charged groups in CB moieties with a short CSL are less charged and that their charges depends on the CSL, while the charged groups in the CB moieties with a CSL $\geq$ 3 have nearly identical charges. Hydration of the five CB moieties was studied using MD simulations with partial charges developed in this work and from the OPLSAA force field. Simulations with both force field sets show that the overlap of coordination shells of the trimethyl ammonium and carboxylic groups only occurs in the CB0 and CB1 moieties. However, these two force field sets show different results for hydration structure and dynamics of charged groups. Results with the OPLSAA force field did not show a significant dependence on CSL because the partial charges of the charged groups for all the five CB moieties are set to be identical. However, simulation results with partial charges developed in this work showed the determining effect of CSL, consistent with the experimental observation of pKa. Simulation results with partial charges in this work showed that hydration of trimethyl ammonium and carboxylic groups have different behaviors with the CSL variation. The hydration of the former does not vary, while the hydration of the latter becomes stronger as the CSL increases and become steady when CSL $\geq$ 3. The hydration free energy of CB moieties with a CSL < 3 also depends strongly on the CSL, while those of CB moieties with a CSL $\geq$ 3 do not show significant variation. The analysis of the RDF, lifetime and free energy of CB-Na^+ association also shows a strong dependence on the CSL, affirming its importance.

Chapter 8 Nonfouling Zwitterionic Moieties beyond Carboxybetaine and Sulfobetaine: a Molecular Simulation Study

This chapter presents a computational simulation study on investigating protein-resistant zwitterionic moieties beyond conventional carboxybetaine and sulfobetaine. Zwitterionic carboxybetaine and sulfobetaine materials have shown their excellent ability of resisting nonspecific protein adsorption. It is desirable to have a better understanding of zwitterionic materials from their molecular structures. This work aims to understand the roles of charged groups in zwitterionic moieties and to design new protein-resistant zwitterionic moieties beyond carboxybetaine and sulfobetaine. We conducted molecular simulations to study the hydration, self-associations and protein interactions of 12 zwitterionic moieties derived from three anionic groups (carboxylic, sulfonate, and sulfate) and four cationic groups (quaternary ammonium, tertiary ammonium, secondary ammonium, and primary ammonium). The force field parameters of these moieties were developed using quantum mechanical calculations. The hydration was studied through the hydration free energy of moieties, and the hydration structure and dynamics of the charged groups. All zwitterionic moieties have strong hydration, but their hydration structural and dynamic properties depend on the types of the cationic and anionic groups involved. The self-associations and protein interactions also show relationships with charged groups. The simulation results indicate the good protein-resistant capability of several zwitterionic moieties, one of which has been shown by recent experiments.

8.1. Introduction

Zwitterionic carboxybetaine and sulfobetaine materials excel in many biological and chemical applications[10]. They resist nonspecific protein adsorption in complex media[11,

[101], protect enzymes against denaturing effects of urea and high temperature[8], and prevent the capsule formation *in vivo* for at least three months[12].

The excellence of zwitterionic materials urges a thorough understanding of zwitterionic materials from their molecular structures. The performance of zwitterionic materials depends strongly on the properties of zwitterionic moieties that possess cationic and anionic groups. Our previous studies have demonstrated the distinguishable effects of zwitterionic carboxybetaine from non-ionic molecules[68, 170], the differences between carboxybetaine and sulfobetaine[48, 143], and the differences between carboxybetaines with various distances between charged groups[82]. Considering the vast numbers of cationic and anionic groups, zwitterionic moieties can have many molecular structures beyond conventional carboxybetaine and sulfobetaine. This provides a rich pool for understanding the roles of charged groups in properties of zwitterionic moieties.

Charged groups of zwitterionic moieties behave somewhat similar to ions. Many studies have been conducted to rank ions based on their charges, sizes, hydration, and other properties. One well-known correlation is the Hofmeister series. The Hofmeister series was originally used to rank the ability of salts to precipitate proteins, and has been employed to explain the influence of ions on other substances[126, 171-173]. Collins et al[14] and Fennell et al.[17] showed that the similarity in hydration and size determines the ion-ion interactions. Vlachy et al.[129] found that the interactions between organic ions and inorganic ions can be ranked in the same way as those between inorganic ions are. Our previous study[143] showed that zwitterion-ion interactions obey similar rules as ion-ion interactions. The hydration of zwitterionic moieties is also suggested to be dominated by electrostatic interactions, similar to the hydration of ions[17]. However, the charged groups

of zwitterionic moieties interfere with each other permanently if close enough[82]. This interference depends on the charge densities of the cationic and anionic groups, and can reversely influence the charge densities. Varying the cationic group may influence the properties of anionic group in the same zwitterionic moiety, and vice versa. Therefore, we may develop the design principles of zwitterionic materials based on the knowledge of ion-ion interactions with a consideration of unique features of zwitterionic moieties.

We selected three anionic groups: carboxylic (CO2), sulfonate (SO3), and sulfate (OSO3). These three anionic groups all have a net charge as -1, and their molecular volumes follow the order: CO2<SO3<OSO3. As a result, their charge densities follow the order: CO2>SO3>OSO3. We selected four cationic groups: quaternary ammonium (NC4), tertiary ammonium (NC3), secondary ammonium (NC2), and primary ammonium (NC1). These four cationic groups all have a net charge as +1 and their molecular volumes follow the order: NC1<NC2<NC3<NC4. Consequentially, their charge densities follow the order: NC4<NC3<NC2<NC1. These seven charged groups have been observed in many natural molecules. 12 zwitterionic moieties have been derived from these charged groups, as shown in Figure 1. The chemical groups between the charged groups were fixed to one methylene group because a long carbon spacer length compromises the capability of resisting nonspecific protein adsorption.

The protein-resistant capability of zwitterionic moieties can be assessed from three properties. The first is the hydration of zwitterionic moieties. Strong hydration is believed to be the main source of resisting protein adsorption[18]. The second is the self-associations among zwitterionic moieties. Too many associations may weaken the hydrophilicity of the zwitterionic moieties[47] and result in a hydrophobic material[174]. The third is the

interactions between zwitterionic moieties and proteins. The specific zwitterion-protein interactions will compromise the protein-resistant capability of zwitterionic moieties.

This work will study the hydration, self-associations, and protein interactions of the 12 zwitterionic moieties shown in Figure 8.1. We focus on the relationships between variations in charged groups and three properties mentioned above. At the same time, we are interested in exploring new protein-resistant zwitterionic moieties beyond conventional carboxybetaine and sulfobetaine.

8.2 Details of Molecular Simulations

8.2.1 Partial Charge Calculation

Our previous studies[48, 82] showed that the partial charges of the current force fields cannot represent zwitterionic moieties well. We calculated the partial charges of atoms for the 12 zwitterionic moieties using quantum mechanical calculations. The quantum mechanical calculations were carried out at HF/6-31G* level using Gaussian 09[50]. For each zwitterionic moiety, 8-12 conformations were generated by rotating the N-C-C-O, N-C-S-O or N-C-O-S dihedral angles. These conformations were optimized in vacuum and then the atomistic charges of individual conformations were obtained with single point calculation using the CHELP algorithm. Two steps of averages were conducted to obtain the final values. The first is the average among various conformations weighted by the Boltzmann factor. The second is the average among the atoms that should be equal based on consideration of their chemical and physical environments. Table 8.1 lists the partial charges of atoms of these 12 zwitterionic moieties. The individual zwitterionic moieties were labeled by the cationic and anionic groups they possess. For instance, a

zwitterionic moiety possessing ammonium group (NC1) and a carboxylic group (CO2) was labeled as NC1-CO2.

Table 8.1 Partial charges of atoms of 12 zwitterionic moieties

	(e)		(e)		(e)
NC1-CO2		NC1-SO3		NC1-OSO3	
N	-0.495	N	-0.318	N	-0.618
H(N)	0.330	H(N)	0.314	H(N)	0.373
H(CH2)	0.061	H(CH2)	0.144	H(CH2)	0.036
C(CH2)	0.007	C(CH2)	-0.224	C(CH2)	0.480
C	0.870	S	1.346	S	1.458
O	-0.747	O	-0.678	O1	-0.564
				O2	-0.649
NC2-CO2		NC2-SO3		NC2-OSO3	
N	-0.059	N	0.108	N	-0.224
H(N)	0.251	H(N)	0.238	H(N)	0.304
H(CH3)	0.108	H(CH3)	0.106	H(CH3)	0.098
C(CH3)	-0.151	C(CH3)	-0.151	C(CH3)	-0.076
H(CH2)	0.101	H(CH2)	0.172	H(CH2)	0.065
C(CH2)	-0.212	C(CH2)	-0.406	C(CH2)	0.309
C	0.878	S	1.369	S	1.450
O	-0.742	O	-0.686	O1	-0.517
				O2	-0.658
NC3-CO2		NC3-SO3		NC3-OSO3	
N	0.251	N	0.205	N	0.009
H(N)	0.229	H(N)	0.275	H(N)	0.342
H(CH3)	0.116	H(CH3)	0.135	H(CH3)	0.125
C(CH3)	-0.249	C(CH3)	-0.262	C(CH3)	-0.231
H(CH2)	0.102	H(CH2)	0.190	H(CH2)	0.06
C(CH2)	-0.262	C(CH2)	-0.472	C(CH2)	0.299
C	0.878	S	1.414	S	1.472
O	-0.749	O	-0.696	O1	-0.547
				O2	-0.661
NC4-CO2		NC4-SO3		NC4-OSO3	
N	0.253	N	0.352	N	0.232
H(CH3)	0.142	H(CH3)	0.154	H(CH3)	0.147
C(CH3)	-0.288	C(CH3)	-0.312	C(CH3)	-0.294
H(CH2)	0.082	H(CH2)	0.221	H(CH2)	0.060
C(CH2)	-0.188	C(CH2)	-0.584	C(CH2)	0.147
C	0.937	S	1.425	S	1.464
O	-0.790	O	-0.695	O1	-0.533
				O2	-0.667

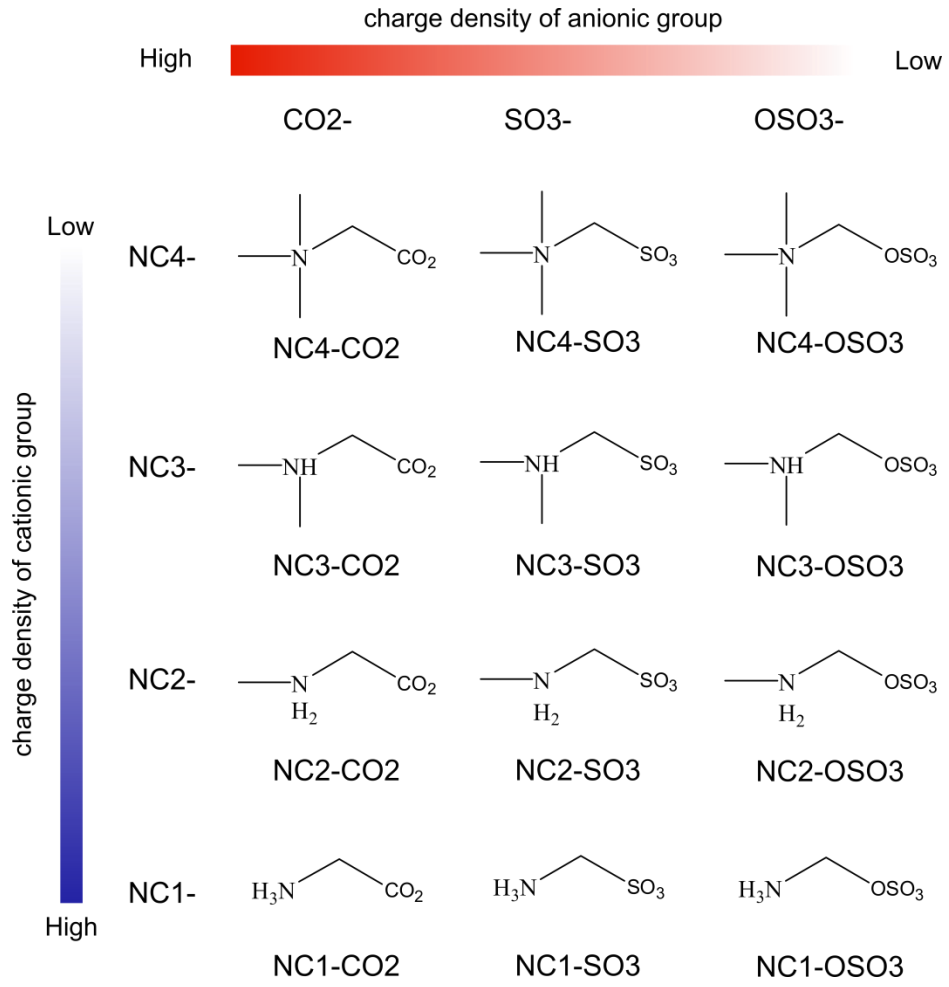

Figure 8.1. Molecular structures of 12 zwitterionic moieties.

8.2.2 Force Field Parameters

Water molecules were described by the Tip4p model[175]. We applied the OPLSAA force field[52] to describe the bond and non-bond interactions between molecules. The potential energy of intermolecular interactions is calculated as a combination of a Lennard−Jones (L-J) 12−6 potential and a Coulombic potential, as shown in Equation 1.

$$U(r_{ij}) = 4\varepsilon_{ij}\left[\left(\frac{\sigma_{ij}}{r_{ij}}\right)^{12} - \left(\frac{\sigma_{ij}}{r_{ij}}\right)^{6}\right] + \frac{q_i q_j}{r_{ij}} \qquad (8.1)$$

where r_{ij} is the distance between atoms i and j, q_i is the partial charge assigned to atom i, and ε_{ij} and σ_{ij} are energy and size parameters obtained by Jorgensen combining rules.

8.2.3 Molecular Dynamics Simulations

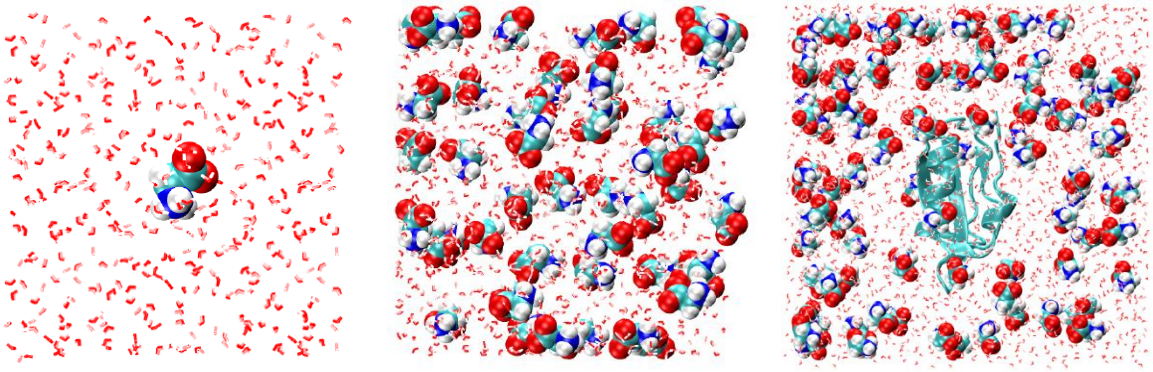

(a) (b) (c)

Figure 8.2. Snapshots of simulation systems for (a) hydration, (b) self-associations among zwitterionic moieties and (c) zwitterion-protein interactions.

Hydration

The simulation system was a cubic box containing a zwitterionic moiety and 566 water molecules. After energy minimization and a 5 ns MD simulation with a step of 1fs in an isobaric-isothermal (NPT) ensemble for energy equilibrium, another 10 ns MD simulation with a step of 2 fs in a canonical (NVT) ensemble was performed for data collection at a frequency of 1ps. Figure 2a shows a snapshot of the simulation system. Long-range electrostatic interactions were computed with the particle mesh Ewald method with periodic boundary conditions in all three dimensions.[55] The short-range van der Waals interactions were calculated with a cutoff distance of 1.0 nm. During the first 5ns MD simulation, the system was maintained at 298 K (0.1 ps time constant) and 100.0 kPa with the Berendsen algorithm[56] (with a compressibility of 4.5×10^{-5} bar^{-1} and a 1 ps time constant). During the 10 ns MD simulation for data collection, the system was

maintained at 298 K with the Nose-Hoover algorithm[57-58]. Intramolecular bonds with hydrogen atoms were kept constrained with the LINCS algorithm[60]. The MD simulations were performed using Gromacs-4.5.4[54]. For each zwitterionic moiety, we carried out three independent MD simulations using different initial configurations.

Self-associations among zwitterionic moieties

The simulation system was a cubic box containing 50 zwitterionic moieties and 1400 water molecules. After an energy minimization and a 5 ns MD simulation with a step of 1 fs in an NPT ensemble for energy equilibrium, another 20 ns MD simulation with a step of 2 fs in an NVT ensemble was performed for data collection at a frequency of 1ps. Figure 2b shows a snapshot of the simulation system. During first 5 ns MD simulation, the system was maintained at 298 K (0.1 ps time constant) and 100.0 kPa with the Berendsen algorithm[56] (with a compressibility of 4.5×10^{-5} bar^{-1} and a 1 ps time constant). During the 20 ns MD simulation for data collection, the system was maintained at 298 K with the Nose-Hoover algorithm[57-58]. The MD simulations were performed using Gromacs-4.5.4[54]. The other simulation details were the same as the hydration study.

Zwitterion-protein interactions

The simulation system for studying zwitterion-protein interactions was a cubic box containing 100 zwitterionic molecules, 5500 water molecules and one chymostrypsin inhibitor 2(CI2, PDB ID: 1YPC). After an energy minimization and a 50 ns MD simulation with a step of 1 fs in an NPT ensemble for energy equilibrium, another 50 ns MD simulation with a step of 2 fs in an NVT ensemble was performed for data collection at a frequency of 10 ps. The other simulation details are the same as for hydration study.

The MD simulations were performed using Gromacs-4.5.4[54]. Figure 2c shows a snapshot of the simulation system.

8.2.4 Free Energy Perturbation

The hydration free energy of individual zwitterionic moieties was calculated using the free energy perturbation (FEP) method. The perturbation process in this work mimics the reversible process of dehydration as described elsewhere[108-109]. The negative of the free energy change of this process is the hydration free energy. As shown in Equation 2, we change the interaction energy between the moiety and water, including the van der Waals interaction energy and electrostatic interaction energy, from the normal values to zero gradually as λ changes from zero to 1.

$$U(\lambda) = 4\varepsilon_{ij}(1-\lambda)\left[\left(\frac{\sigma_{ij}}{r_{ij}}\right)^{12} - \left(\frac{\sigma_{ij}}{r_{ij}}\right)^{6}\right] + \frac{(1-\lambda)q_i q_j}{r_{ij}} \qquad (8.2)$$

This interaction change causes the potential energy of the system to vary gradually from $U_A(\lambda = 0)$ to $U_B(\lambda = 1)$. λ should decrease as small as possible in every step in order to preserve reversibility. Taking into consideration both the precision required in this work and the tolerance of computational cost, we divided λ into 20 intervals from zero to 1. For every λ_{n+1}, a 1 ns MD simulation was carried out with the initial structure obtained from the final structure of MD simulation of λ_n. The potential energy is the average of the last 500 ps. The other simulation details were the same as the hydration study. Five independent FEP calculations with different initial structures were carried out for each zwitterionic molecule. The FEP calculations in this work were carried out with Gromacs-4.5.4[54].

8.3 Results and Discussion

8.3.1 Hydration of Zwitterionic Moieties

Table 8.2 Hydration free energy of 12 zwitterionic moieties (kJ/mol^{-1})

	Cationic group			
Anionic group	NC4	NC3	NC2	NC1
CO2	-261±12	-224±12	-230±25	-216±6
SO3	-251±17	-259±3	-249±9	-240±6
OSO3	-238±14	-303±11	-290±4	-296±8

As listed in Table 8.2, the hydration free energy of the 12 zwitterionic moieties is lower than that of the (ethylene glycol)$_4$ (EG$_4$) moiety (-180 kJmol^{-1})[48]. A surface covered with EG$_4$ moieties can resist nonspecific protein adsorption well[18]. The low hydration free energy indicates that these zwitterionic moieties should have strong hydration. From the hydration aspect, these zwitterionic moieties should all have good capability of resisting nonspecific protein adsorption.

Hydration free energy of zwitterionic moieties depends on the charge densities of the charged groups, which are tuned by the influence between the cationic and anionic groups. The charged groups with higher charge densities can influence others stronger and are also susceptible to the influence. NC3-OSO3, NC2-OSO3, and NC1-OSO3 have hydration free energy lower than other zwitterionic moieties. These three zwitterionic moieties possess an OSO3 group and a cationic group with one or more hydrogen atoms attached to the nitrogen atom, and the influences between the charged groups may be less compared to the others.

We further studied the local hydration of the charged groups of zwitterionic moieties by analyzing the numbers and residence times of water molecules in the first coordination

shells of certain atoms of charged groups. The radius of the first coordination shell was set as the first-minimum position of the corresponding radial distribution function (RDF) shown in Figures 8.3-8.5. The residence time τ of water molecules is calculated through a numerical integration of the residence curve from zero to 1 ns.

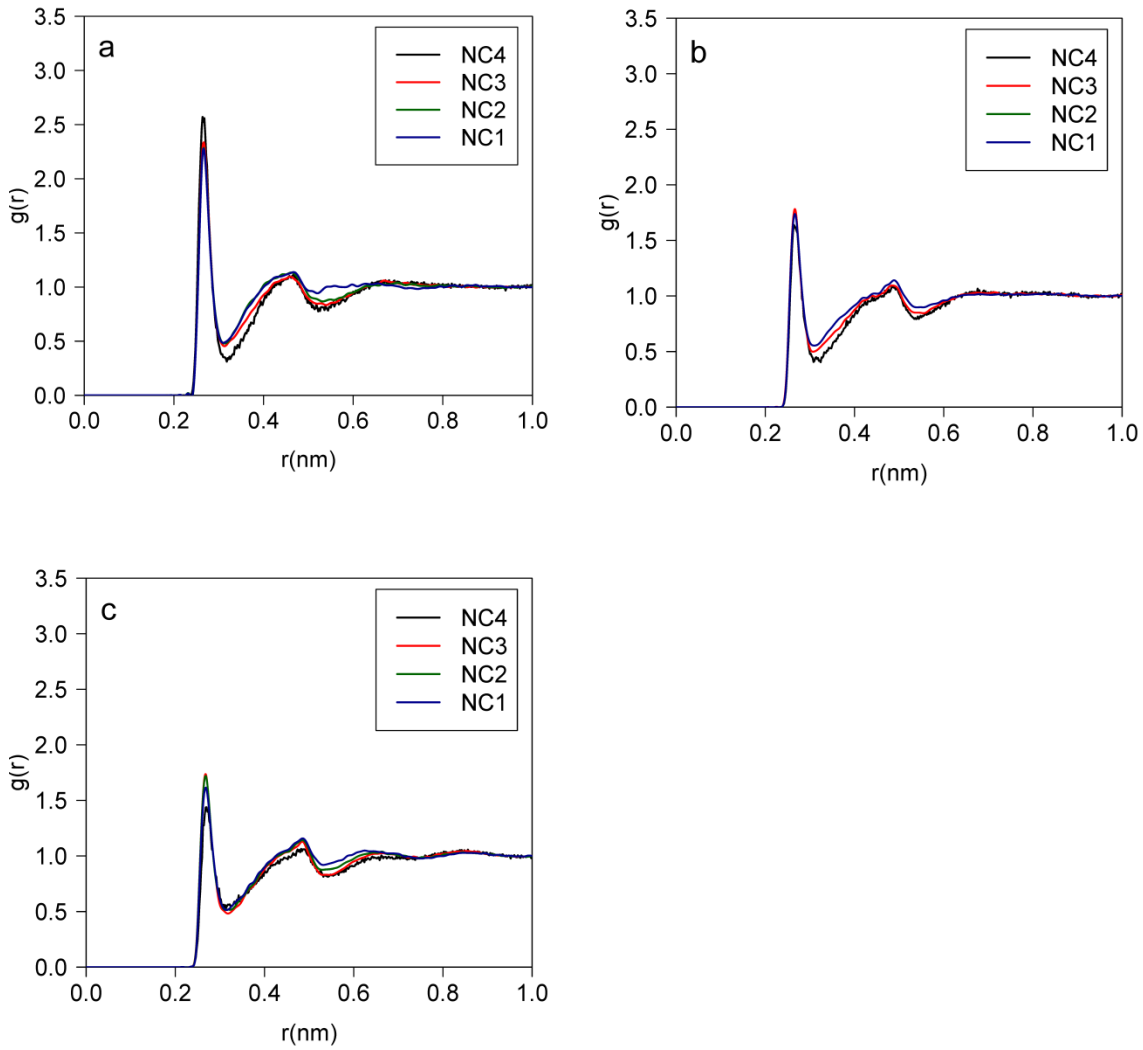

Figure 8.3. Radial distribution functions of oxygen atoms of zwitterionic moieties with the oxygen atoms of water molecules. (a) Carboxylic groups, (b) sulfonate groups and (c) sulfate groups.

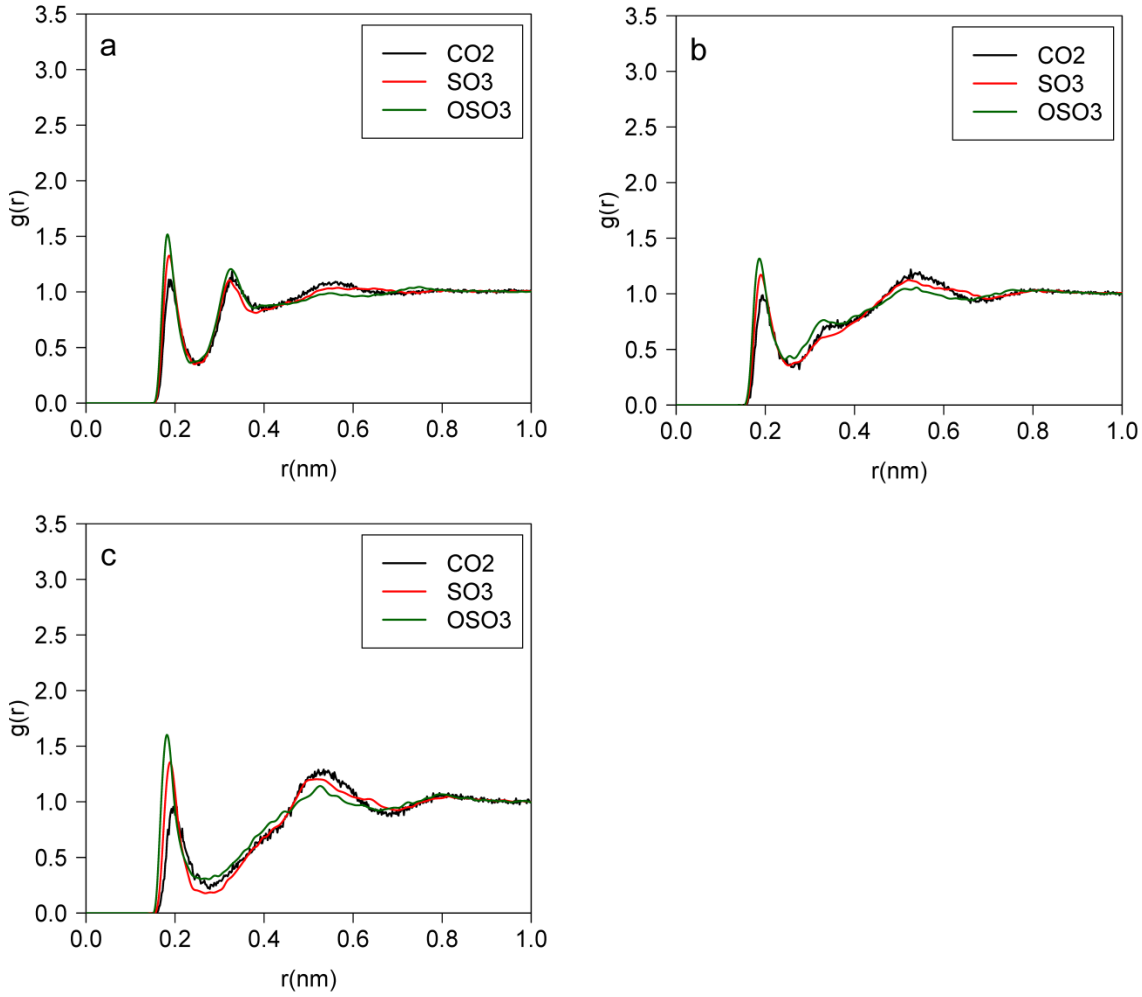

Figure 8.4. Radial distribution functions of hydrogen atoms attached to the nitrogen atoms of zwitterionic moieties with the oxygen atoms of water molecules. (a) NC1, (b) NC2 and (c) NC3 groups.

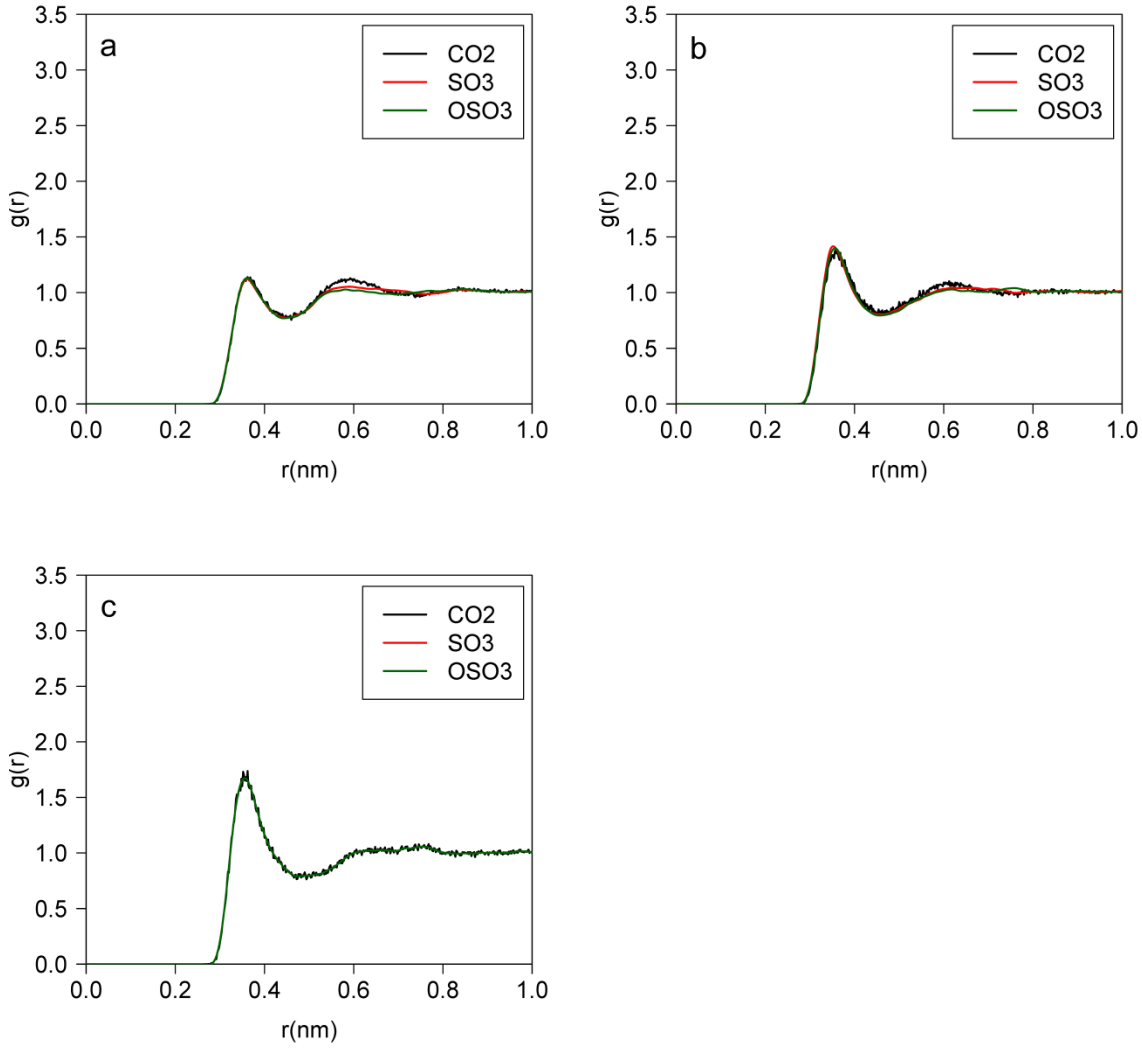

Figure 8.5 Radial distribution functions of carbon atoms attached to the nitrogen atom of zwitterionic moieties with the oxygen atoms of water molecules. (a) NC2, (b) NC3 and (c) NC4 groups.

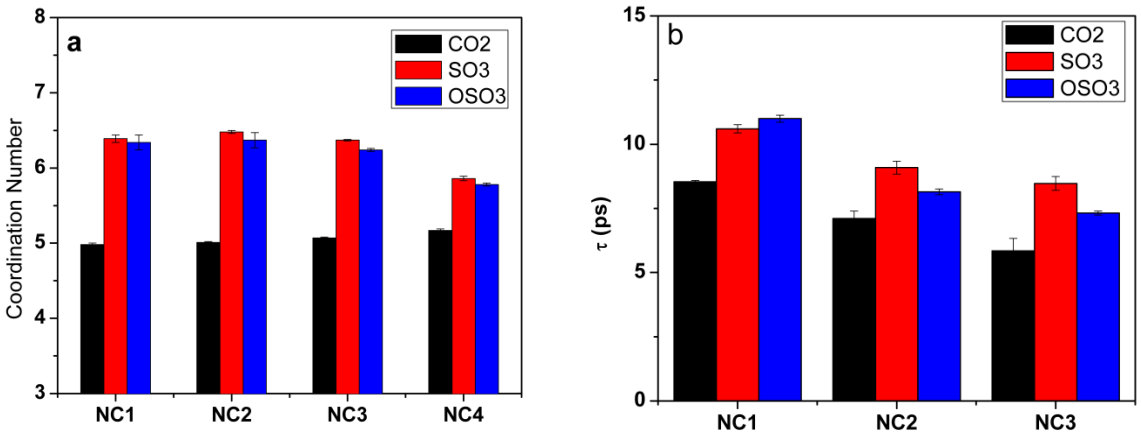

Figure 8.6 Structural and dynamic properties of water molecules in the first coordination shells of the oxygen atoms of the anionic groups of zwitterionic moieties. (a) Coordination number N, and (b) residence time τ.

Figure 8.6 shows the number N and residence time τ of water molecules in the first coordination shells of the oxygen atoms of the CO2, SO3, and OSO3 groups as a function of the type of the cationic group. the values of N of the CO2 group are always less than those of the SO3 and OSO3 groups, consistent with our previous observation[48] that the anionic group of a carboxybetaine moiety has N less than the anionic group of a sulfobetaine moiety does. The variation in the cationic group does not influence the number of water molecules near the anionic group.

However, the variation in the cationic group influences the dynamic properties of water molecules near the anionic group. As shown in Figure 8.6b, when the NC4 group is the cationic group, τ for the CO2 group is much higher than those for the SO3 and OSO3 groups, consistent with our previous observations[48] of carboxybetaine and sulfobetaine moieties. However, when the cationic group is the NC1, NC2 or NC3 group, the values of τ for the three anionic groups are quite similar, indicating the similarity in their

attractions to individual water molecules. The interference from cationic groups makes the charge densities of the carboxylic group lower, and weakens its attractions with individual water molecules.

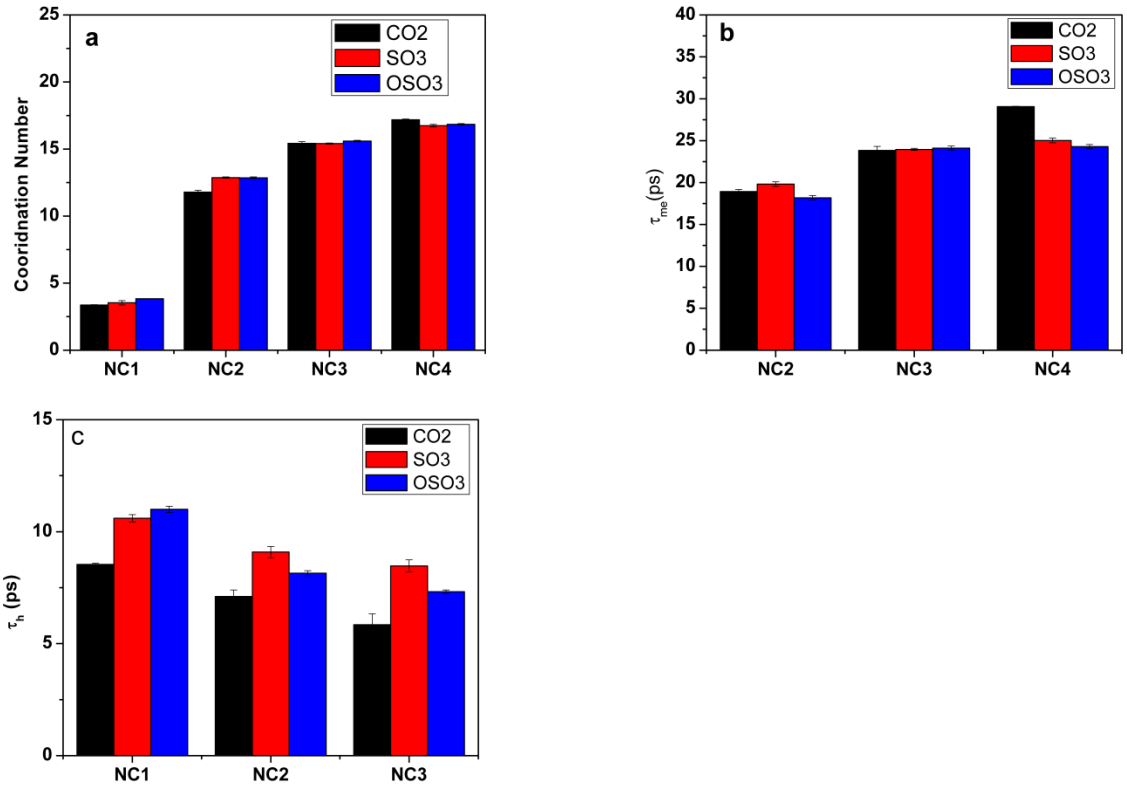

Figure 8.7 Structural and dynamic properties of water molecules near the cationic group of zwitterionic moieties. (a) Coordination number of water molecules in the first coordination shells of carbon atoms or hydrogen atoms attached to the nitrogen atoms, (b) residence time τ_{me} of water molecules in the first coordination shells of carbon atoms of cationic groups and (c) residence time τ_h of water molecules in the first coordination shells of carbon atoms of cationic groups

The structural and dynamic properties of water molecules near the cationic groups do not show significant variations as a function of the anionic group. Figure 8.7a shows the total numbers of water molecules in the first coordination shells of the carbon atoms and

hydrogen atoms attached to the nitrogen atoms of the cationic groups. For each type of cationic group, the coordination number is nearly unchanged, and increases as the size of the coordination shell increases. Figures 8.7b and 8.7c show the residence times, τ_{me} and τ_h, of water molecules in the first coordination shells of carbon atoms and hydrogen atoms attached to the nitrogen atom. For each cationic group, τ_{me} and τ_h do not show significant variation with the type of the anionic groups. The properties of the cationic group are less influenced by the anionic groups, probably due to the weak hydration of cationic groups[47-48].

8.3.2 Self-associations among zwitterionic moieties

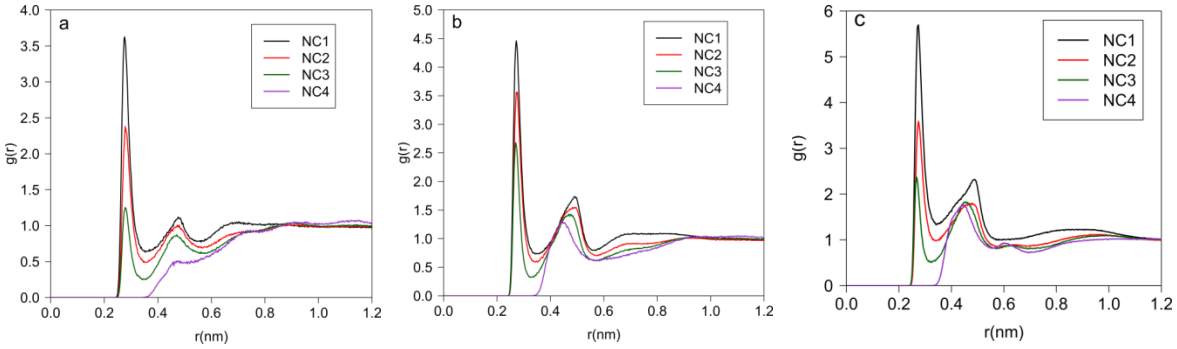

Figure 8.8 Radial distribution functions between the oxygen atoms of the anionic groups and the nitrogen atoms of the cationic groups for 12 zwitterionic moieties (N-O RDFs). (a) Zwitterionic moieties possessing a CO2 group, (b) zwitterionic moieties possessing a SO3 group, and (c) zwitterionic moieties possessing an OSO3 group

The above analysis has shown that the 12 zwitterionic moieties have strong hydration. But the strong hydration is not a guarantee of their good capability of resisting protein adsorption. Another critical property is self-associations among zwitterionic moieties. Self-associations among these moieties can bring interesting properties to materials such as antipolyelectrolyte effect[123] or thermal responses[138]. But too many self-associations

may change the chemical features of the materials[174] and influence their performance. To study the self-associations of these 12 zwitterionic moieties, we investigated the RDFs between the oxygen atoms of anionic groups and the nitrogen atom of cationic groups (N-O RDF), as shown in Figure 8.8.

The N-O RDFs in Figure 8.8 imply that, the zwitterionic moieties possessing a NC4 group have few or moderate self-associations. The materials with these zwitterionic moieties are well-known for their good ability of resisting nonspecific protein adsorption[10]. Therefore, we would like to explore some zwitterionic moieties that have few to moderate self-associations. The N-O RDFs of NC3-CO2, NC3-SO3, and NC3-SO4 have two peaks because their cationic groups have two methyl groups and one hydrogen atom attached to the nitrogen atom. As shown in Figure 8.8, N-O RDFs of NC3-CO2, NC3-SO3, and NC3-SO4 have a peak at 0.25 nm with a height of 1.0, 2.5, and 2.0, respectively. These zwitterionic moieties may still have moderate self-associations. The N-O RDF of NC2-CO2 also has a peak at 0.25 nm with a height of 2.5, indicating that the this type of zwitterionic moieties may also have moderate self-associations. Therefore, the zwitterionic moieties with a NC3 group and the NC2-CO2 may still be able to resist protein adsorption.

The N-O RDFs of other zwitterionic moieties all present peaks higher than 3.5, implying that these zwitterionic moieties may form many self-associations. White et al.[47] also found that the NC1-CO2 forms many self-associations at high concentration. The materials with the zwitterionic moieties that have strong self-associations may still be able to resist the adsorption of a single type of protein in a buffer solution, but their capability may be easily affected by the environments.

8.3.3 Protein interactions

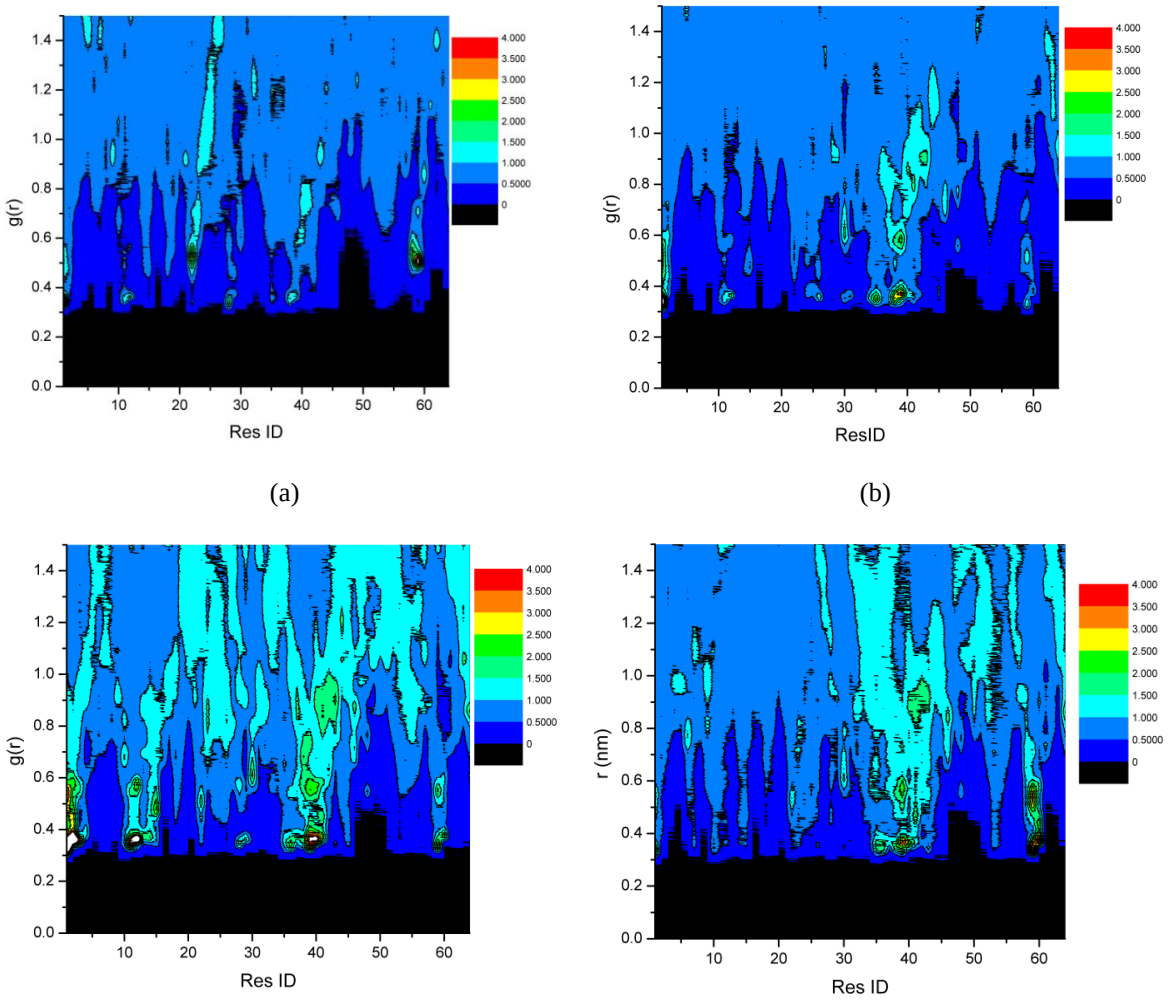

Figure 8.9 Radial distribution functions of the oxygen atoms of anionic groups of (a) NC3-CO2, (b) NC3-SO3 and (c) NC3-OSO3 and (d) NC2-CO2 and the Cα atom of each residue of the CI2.

The above analysis about the hydration and the self-associations has suggested that four zwitterionic moieties (NC3-CO2, NC3-SO3, NC3-OSO3, and NC2-CO2) beyond carboxybetaine and sulfobetaine may exhibit good capability of resisting nonspecific protein adsorption. However, strong specific interactions between moieties and proteins may compromise the capability. Our previous study[68] showed that carboxybetaine and

oligo(ethylene glycol) moieties do not accumulate near proteins. To study the potentials of these four zwitterionic moieties, we studied their interactions with a model protein: CI2. Figure 8.9 shows the RDFs between the oxygen atoms of the anionic groups of zwitterionic moieties (NC3-CO2, NC3-SO3, NC3-OSO3, and NC2-CO2) and the Cα atoms of 64 residues of the CI2. As shown in Figure 6, the RDFs of NC3-CO2, NC3-SO3 and NC2-CO2 have few peaks higher than one, indicating that these zwitterionic moieties should not interact with the CI2 specifically. These three zwitterionic moieties may have good protein-resistant capability. NC3-OSO3 shows some peaks higher than four in its RDFs, indicating that this type of moiety may specifically interact with some residues of the protein. Such specific interactions may influence its protein-resistant capability.

8.4 Conclusions

Using molecular simulations, we studied hydration, self-associations among zwitterionic moieties and protein interactions of 12 zwitterionic moieties derived from four cationic groups (NC1, NC2, NC3, and NC4) and three anionic groups (CO2, SO3, and OSO3), with the aim of understanding the roles of charged group in zwitterionic moieties and assessing their capability of resisting nonspecific protein adsorption. All 12 zwitterionic moieties have strong hydration, though the hydration structure and dynamics is related to the type of charged groups. The zwitterionic moieties possessing a NC4 group are already proven to resist nonspecific protein adsorption and they form few to moderate self-associations. The zwitterionic moieties with a NC3 group and the NC2-CO2 also show few to moderate self-associations, implying their capability of resisting nonspecific protein adsorption. The further analysis of the RDFs between the oxygen atoms of these zwitterionic moieties and the Cα atoms of the protein CI2 showed that the

zwitterionic moieties NC3-CO2, NC3-SO3, and NC2-CO2 do not specifically interact with the protein, further indicating that they may have good capability of resisting nonspecific protein adsorption. NC3-OSO3 specifically interacts with some residues, which may influence its capability of resisting nonspecific protein adsorption. Recently, our group successfully synthesized the zwitterionic materials with NC3-CO2 and tested their ability to resist nonspecific protein adsorption[176]. The experimental results showed that the NC3-CO2 materials can also resist protein adsorption well, agreeing well with the prediction of computational simulations in this work.

Among the 12 zwitterionic moieties, NC4-CO2 and NC3-CO2 have been shown to strongly resist nonspecific protein adsorption. They both have a high charge-density anionic group and a low charge-density cationic group with no or just one hydrogen atom attached to the nitrogen atom. This combination fits well the three criteria to assess the protein-resistant capability of zwitterionic moieties. Strong hydration is necessary for materials that resist nonspecific protein adsorption and all zwitterionic moieties studied have high hydration. The cationic group of a zwitterionic moiety that resists nonspecific protein adsorption needs to have as few hydrogen atoms attached to the nitrogen atom as possible to prevent possible self-associations among zwitterionic moieties. Another important factor is the specific interactions between a zwitterionic moiety and proteins. Proteins possess many amide groups that may interact with high charge-density cationic groups and low charge-density anionic groups. To avoid specific interactions with proteins, a zwitterionic moiety needs to possess a low charge-density cationic group and a high charge-density anionic group.

Chapter 9 Summary

This work conducted computational simulations and experiments to study the differences between zwitterionic and non-ionic moieties and differences among zwitterionic moieties, and design new protein-resistant zwitterionic moieties beyond the carboxybetaine and sulfobetaine. The work suggested three key properties for the protein-resistant materials: strong hydration, few or moderate self-associations, and few specific interactions with proteins.

To understand the differences between zwitterionic and non-ionic materials, the influences of zwitterionic CB and OEG moieties on protein structure and hydrophobic interactions were studied using molecular simulations. MD simulations were conducted to analyze the RMSD, hydrogen bonding and SASA of a CI2 in water, and the CB and OEG solutions. The results showed that, though the protein keeps its folded structure in both the CB and OEG solutions, it is more rigid and has more hydrophobic surface area covered in the OEG solution. The structure of the protein in the CB solution is similar to that in water. The influences of CB and OEG moieties on the hydrophobic interactions of two nonpolar plates were studied using well-tempered metadynamics simulations. Three reference systems were used: water, and TMAO and urea solutions. TMAO molecules do not change the hydrophobic interactions, and urea molecules weaken hydrophobic interactions. The PMFs showed that CB moieties have slight effect on hydrophobic interactions. In contrast, OEG moieties weaken the direct hydrophobic associations of the plates and result in an indirect association state that can impede the direct association. The analysis of density distributions from MD simulations revealed that the different effects of CB and OEG moieties are due to their ability to change the local environment

of the hydrophobic plates: the plate environment in the CB solution remains the same as in water, but in the OEG solutions becomes more hydrophobic. Zwitterionic CB moieties present themselves as a good replacement of water molecules, while OEG moieties present hydrophobic feature in water. Consequently, OEG moieties can influence the bioactivity more. The different influences of zwitterionic CB and non-ionic OEG moieties on protein structures and hydrophobic interactions well explained the different performance of zwitterionic and PEG materials. Zwitterionic materials can be a good candidate for the protein conjugation technique, and deserve further engineering effort to develop some real pharmaceutical applications.

To study the difference among zwitterionic materials, molecular simulations were first performed to study the differences between CB and SB moieties in the hydration, ionic interactions and associations among zwitterionic moieties. These two zwitterionic moieties share the same cationic group: trimethyl ammonium. A CB moiety possesses a carboxylic group and a SB moiety possesses a sulfonate group. Carboxylic groups have stronger charge strengthen than sulfonate groups. The studies showed that CB moieties attract individual water molecules stronger, interact with kosmotropic cations stronger, and have few associations among themselves. SB moieties attract more water molecules, interact with chaotropic cations stronger, and have moderate associations among themselves. Therefore CB materials can present strong hydration, resist non-specific protein adsorption even in complex media, and can be nearly inert to environmental factors such as temperature and salt concentration. SB materials can have decent hydration, resist non-specific protein adsorption well in buffer solution, and have stimuli-responsive properties. Molecular simulations were second performed to study the

influence of carbon spacer length on hydration and ionic interactions of CB moieties. Only in CB moieties with zero or one methylene group, the cationic group strongly interferes with the anionic group. In a CB moiety with two methylene groups, the interference is already moderate. In CB moieties with more than three methylene groups, the cationic and anionic groups have little interference between them. CB materials with different carbon spacer lengths present different antifouling performance in complex media. A careful examination of the simulation results of hydration and the experimental observations of protein resistance in whole blood serum implies that stronger hydration does not necessarily lead to better non-specific protein resistance. This challenges the development of a relationship between the hydration of materials and their biological applications, and the design of antifouling materials.

At last, to design new protein-resistant zwitterionic moieties, molecular simulations were conducted to study 12 zwitterionic moieties derived from four cationic and three anionic groups that have various charge densities. The studied properties include the hydration, associations among zwitterionic moieties and zwitterion-protein interactions. All 12 zwitterionic moieties have strong hydration, though the hydration structure and dynamics of charged groups has a relationship with the type of charged groups. The analysis of self-associations and protein interactions implies that the zwitterionic moieties NC3-CO2, NC3-SO3 and NC2-CO2 may have good protein-resistant capability.

Zwitterionic materials have paved a new avenue to develop desired materials by carefully selecting cationic and anionic groups and design molecular structure based on them. Zwitterionic molecules widely spread in nature and play important roles in biological processes. It would be interesting to study the mechanisms for the functions of

these naturally occurring zwitterionic molecules, in the aim to develop new functional zwitterionic materials.

Reference:

1. Yang, W.; Xue, H.; Carr, L. R.; Wang, J.; Jiang, S. Y., Zwitterionic poly(carboxybetaine) hydrogels for glucose biosensors in complex media. *Biosensors & Bioelectronics* **2011,** *26*, 2454-2459.
2. Zhao, C.; Li, L. Y.; Guo, M. M.; Zheng, J., Functional polymer thin films designed for antifouling materials and biosensors. *Chemical Papers* **2012,** *66*, 323-339.
3. Place, E. S.; Evans, N. D.; Stevens, M. M., Complexity in biomaterials for tissue engineering. *Nat Mater* **2009,** *8*, 457-470.
4. Banerjee, I.; Pangule, R. C.; Kane, R. S., Antifouling Coatings: Recent Developments in the Design of Surfaces That Prevent Fouling by Proteins, Bacteria, and Marine Organisms. *Advanced Materials* **2011,** *23*, 690-718.
5. Langer, R., Drug delivery and targeting. *Nature* **1998,** *392*, 5-10.
6. Cao, Z. Q.; Yu, Q. M.; Xue, H.; Cheng, G.; Jiang, S. Y., Nanoparticles for Drug Delivery Prepared from Amphiphilic PLGA Zwitterionic Block Copolymers with Sharp Contrast in Polarity between Two Blocks. *Angewandte Chemie-International Edition* **2010,** *49*, 3771-3776.
7. Tanzi, M. C.; Bozzini, S.; Candiani, G.; Cigada, A.; De Nardo, L.; Fare, S.; Ganazzoli, F.; Gastaldi, D.; Levi, M.; Metrangolo, P.; Migliavacca, F.; Osellame, R.; Petrini, P.; Raffaini, G.; Resnati, G.; Vena, P.; Vesentini, S.; Zunino, P., Trends in biomedical engineering: focus on Smart Bio-Materials and Drug Delivery. *Journal of Applied Biomaterials & Biomechanics* **2011,** *9*, 87-97.
8. Keefe, A. J.; Jiang, S. Y., Poly(zwitterionic)protein conjugates offer increased stability without sacrificing binding affinity or bioactivity. *Nature Chemistry* **2012,** *4*, 60-64.
9. Blaszykowski, C.; Sheikh, S.; Thompson, M., Surface chemistry to minimize fouling from blood-based fluids. *Chemical Society Reviews* **2012,** *41*, 5599-5612.
10. Chen, S.; Jiang, S., An New Avenue to Nonfouling Materials. *Advanced Materials* **2008,** *20*, 335-338.
11. Yang, W.; Zhang, L.; Wang, S. L.; White, A. D.; Jiang, S. Y., Functionalizable and ultra stable nanoparticles coated with zwitterionic poly(carboxybetaine) in undiluted blood serum. *Biomaterials* **2009,** *30*, 5617-5621.
12. Zhang, L.; Cao, Z. Q.; Bai, T.; Carr, L.; Ella-Menye, J. R.; Irvin, C.; Ratner, B. D.; Jiang, S. Y., Zwitterionic hydrogels implanted in mice resist the foreign-body reaction. *Nature Biotechnology* **2013,** *31*, 553-+.
13. Alfrey, T.; Morawetz, H.; Fitzgerald, E. B.; Fuoss, R. M., Synthetic Electrical Analog of Proteins. *Journal of the American Chemical Society* **1950,** *72*, 1864-1864.
14. Lowe, A. B.; McCormick, C. L., Synthesis and Solution Properties of Zwitterionic Polymers. *Chemical Reviews* **2002,** *102*, 4177-4190.
15. Ishihara, K.; Fukumoto, K.; Iwasaki, Y.; Nakabayashi, N., Modification of polysulfone with phospholipid polymer for improvement of the blood compatibility. Part 1. Surface characterization. *Biomaterials* **1999,** *20*, 1545-1551.
16. Chen, S.; Zheng, J.; Li, L.; Jiang, S., Strong Resistance of Phosphorylcholine Self-Assembled Monolayers to Protein Adsorption: Insights into Nonfouling Properties of Zwitterionic Materials. *Journal of the American Chemical Society* **2005,** *127*, 14473-14478.
17. He, Y.; Hower, J.; Chen, S. F.; Bernards, M. T.; Chang, Y.; Jiang, S. Y., Molecular simulation studies of protein interactions with zwitterionic phosphorylcholine self-assembled monolayers in the presence of water. *Langmuir* **2008,** *24*, 10358-10364.
18. Zheng, J.; Li, L. Y.; Tsao, H. K.; Sheng, Y. J.; Chen, S. F.; Jiang, S. Y., Strong repulsive forces between protein and oligo (ethylene glycol) self-assembled monolayers: A molecular simulation study. *Biophysical Journal* **2005,** *89*, 158-166.

19. Zhang, Z.; Chen, S.; Chang, Y.; Jiang, S., Surface Grafted Sulfobetaine Polymers via Atom Transfer Radical Polymerization as Superlow Fouling Coatings. *The Journal of Physical Chemistry B* **2006,** *110*, 10799-10804.
20. Zhang, Z.; Chao, T.; Chen, S.; Jiang, S., Superlow Fouling Sulfobetaine and Carboxybetaine Polymers on Glass Slides. *Langmuir* **2006,** *22*, 10072-10077.
21. Zhang, Z.; Chao, T.; Jiang, S., Physical, Chemical, and Chemical−Physical Double Network of Zwitterionic Hydrogels. *The Journal of Physical Chemistry B* **2008,** *112*, 5327-5332.
22. Cheng, G.; Xue, H.; Zhang, Z.; Chen, S.; Jiang, S., A Switchable Biocompatible Polymer Surface with Self-Sterilizing and Nonfouling Capabilities. *Angewandte Chemie* **2008,** *120*, 8963-8966.
23. Serge N, T., Control of Protein Stability and Reactions by Weakly Interacting Cosolvents: The Simplicity of the Complicated. In *Advances in Protein Chemistry*, Frederic M. Richards, D. S. E.; Peter, S. K., Eds. Academic Press: 1998; Vol. Volume 51, pp 355-432.
24. Timasheff, S. N., Protein-solvent preferential interactions, protein hydration, and the modulation of biochemical reactions by solvent components. *Proceedings of the National Academy of Sciences* **2002,** *99*, 9721-9726.
25. Yancey, P. H., Organic osmolytes as compatible, metabolic and counteracting cytoprotectants in high osmolarity and other stresses. *Journal of Experimental Biology* **2005,** *208*, 2819-2830.
26. Wiggers, H. J.; Cheleski, J.; Zottis, A.; Oliva, G.; Andricopulo, A. D.; Montanari, C. A., Effects of organic solvents on the enzyme activity of Trypanosoma cruzi glyceraldehyde-3-phosphate dehydrogenase in calorimetric assays. *Analytical Biochemistry* **2007,** *370*, 107-114.
27. Gangadhara; Kumar, P. R.; Prakash, V., The Stabilizing Effects of Polyols and Sugars on Porcine Pancreatic Lipase. *Journal of the American Oil Chemists Society* **2009,** *86*, 773-781.
28. Attri, P.; Venkatesu, P.; Lee, M. J., Influence of Osmolytes and Denaturants on the Structure and Enzyme Activity of alpha-Chymotrypsin. *Journal of Physical Chemistry B* **2010,** *114*, 1471-1478.
29. Chen, L. X.; Gao, Y. Q.; Russell, D. H., How Alkali Metal Ion Binding Alters the Conformation Preferences of Gramicidin A: A Molecular Dynamics and Ion Mobility Study. *Journal of Physical Chemistry A* **2012,** *116*, 689-696.
30. Shukla, D.; Schneider, C. P.; Trout, B. L., Complex Interactions between Molecular Ions in Solution and Their Effect on Protein Stability. *Journal of the American Chemical Society* **2011,** *133*, 18713-18718.
31. Livingstone, J. R.; Spolar, R. S.; Record, M. T., Contribution to The Thermodynamics of Protein Folding From The Reduction in Water-accessible Nonpolar Surface-area. *Biochemistry* **1991,** *30*, 4237-4244.
32. Capp, M. W.; Pegram, L. M.; Saecker, R. M.; Kratz, M.; Riccardi, D.; Wendorff, T.; Cannon, J. G.; Record, M. T., Interactions of the Osmolyte Glycine Betaine with Molecular Surfaces in Water: Thermodynamics, Structural Interpretation, and Prediction of m-Values. *Biochemistry* **2009,** *48*, 10372-10379.
33. Baynes, B. M.; Trout, B. L., Rational design of solution additives for the prevention of protein aggregation. *Biophysical Journal* **2004,** *87*, 1631-1639.
34. Bennion, B. J.; Daggett, V., Counteraction of urea-induced protein denaturation by trimethylamine N-oxide: A chemical chaperone at atomic resolution. *Proceedings of the National Academy of Sciences of the United States of America* **2004,** *101*, 6433-6438.
35. Vagenende, V.; Yap, M. G. S.; Trout, B. L., Mechanisms of Protein Stabilization and Prevention of Protein Aggregation by Glycerol. *Biochemistry* **2009,** *48*, 11084-11096.
36. Ma, L.; Pegram, L.; Record, M. T.; Cui, Q., Preferential Interactions between Small Solutes and the Protein Backbone: A Computational Analysis. *Biochemistry* **2010,** *49*, 1954-1962.

37. Liu, F. F.; Ji, L.; Zhang, L.; Dong, X. Y.; Sun, Y., Molecular basis for polyol-induced protein stability revealed by molecular dynamics simulations. *Journal of Chemical Physics* **2010,** *132*.
38. Shukla, D.; Schneider, C. P.; Trout, B. L., Molecular level insight into intra-solvent interaction effects on protein stability and aggregation. *Advanced Drug Delivery Reviews* **2011,** *63*, 1074-1085.
39. Wei, H. Y.; Fan, Y. B.; Gao, Y. Q., Effects of Urea, Tetramethyl Urea, and Trimethylamine N-Oxide on Aqueous Solution Structure and Solvation of Protein Backbones: A Molecular Dynamics Simulation Study. *Journal of Physical Chemistry B* **2010,** *114*, 557-568.
40. Shao, Q.; Fan, Y. B.; Yang, L. J.; Gao, Y. Q., From protein denaturant to protectant: Comparative molecular dynamics study of alcohol/protein interactions. *Journal of Chemical Physics* **2012,** *136*.
41. Chennamsetty, N.; Voynov, V.; Kayser, V.; Helk, B.; Trout, B. L., Design of therapeutic proteins with enhanced stability. *Proceedings of the National Academy of Sciences of the United States of America* **2009,** *106*, 11937-11942.
42. Kane, R. S.; Deschatelets, P.; Whitesides, G. M., Kosmotropes form the basis of protein-resistant surfaces. *Langmuir* **2003,** *19*, 2388-2391.
43. Anand, G.; Jamadagni, S. N.; Garde, S.; Belfort, G., Self-Assembly of TMAO at Hydrophobic Interfaces and Its Effect on Protein Adsorption: Insights from Experiments and Simulations. *Langmuir* **2010,** *26*, 9695-9702.
44. Silow, M.; Oliveberg, M., High concentrations of viscogens decrease the protein folding rate constant by prematurely collapsing the coil. *Journal of Molecular Biology* **2003,** *326*, 263-271.
45. Zhi, L. F.; Jiang, Y. C.; Wang, Y. S.; Hu, M. C.; Li, S. N.; Ma, Y. J., Effects of additives on the thermostability of chloroperoxidase. *Biotechnology Progress* **2007,** *23*, 729-733.
46. Jayaraman, S.; Gantz, D. L.; Gursky, O., Poly(ethylene glycol)-induced fusion and destabilization of human plasma high-density lipoproteins. *Biochemistry* **2004,** *43*, 5520-5531.
47. White, A.; Jiang, S. Y., Local and Bulk Hydration of Zwitterionic Glycine and its Analogues through Molecular Simulations. *Journal of Physical Chemistry B* **2011,** *115*, 660-667.
48. Shao, Q.; He, Y.; White, A. D.; Jiang, S. Y., Difference in Hydration between Carboxybetaine and Sulfobetaine. *Journal of Physical Chemistry B* **2010,** *114*, 16625-16631.
49. Berendsen, H. J. C.; Grigera, J. R.; Straatsma, T. P., The missing Term in Effective Pair Potentials. *Journal of Physical Chemistry* **1987,** *91*, 6269-6271.
50. Gaussian 09, Revision D.01, Frisch, M. J.; Trucks, G. W.; Schlegel, H. B.; Scuseria, G. E.; Robb, M. A.; Cheeseman, J. R.; Scalmani, G.; Barone, V.; Mennucci, B.; Petersson, G. A.; Nakatsuji, H.; Caricato, M.; Li, X.; Hratchian, H. P.; Izmaylov, A. F.; Bloino, J.; Zheng, G.; Sonnenberg, J. L.; Hada, M.; Ehara, M.; Toyota, K.; Fukuda, R.; Hasegawa, J.; Ishida, M.; Nakajima, T.; Honda, Y.; Kitao, O.; Nakai, H.; Vreven, T.; Montgomery, J. A., Jr.; Peralta, J. E.; Ogliaro, F.; Bearpark, M.; Heyd, J. J.; Brothers, E.; Kudin, K. N.; Staroverov, V. N.; Kobayashi, R.; Normand, J.; Raghavachari, K.; Rendell, A.; Burant, J. C.; Iyengar, S. S.; Tomasi, J.; Cossi, M.; Rega, N.; Millam, N. J.; Klene, M.; Knox, J. E.; Cross, J. B.; Bakken, V.; Adamo, C.; Jaramillo, J.; Gomperts, R.; Stratmann, R. E.; Yazyev, O.; Austin, A. J.; Cammi, R.; Pomelli, C.; Ochterski, J. W.; Martin, R. L.; Morokuma, K.; Zakrzewski, V. G.; Voth, G. A.; Salvador, P.; Dannenberg, J. J.; Dapprich, S.; Daniels, A. D.; Farkas, Ö.; Foresman, J. B.; Ortiz, J. V.; Cioslowski, J.; Fox, D. J. Gaussian, Inc., Wallingford CT, 2009.
51. Dooley, R.; Allen, G.; Pamidighantam, S. In *Computational Chemistry Grid: Production Cyberinfrastructure for Computational Chemistry*, Proceedings of the 13th Annual Mardi Gras Conference, Baton Rouge, LA, Feb; Baton Rouge, LA, 2005; p 83.

52. Jorgensen, W. L.; Maxwell, D. S.; TiradoRives, J., Development and testing of the OPLS all-atom force field on conformational energetics and properties of organic liquids. *Journal of the American Chemical Society* **1996,** *118*, 11225-11236.
53. Humphrey, W.; Dalke, A.; Schulten, K., VMD: Visual molecular dynamics. *Journal of Molecular Graphics* **1996,** *14*, 33-&.
54. Van der Spoel, D.; Lindahl, E.; Hess, B.; Groenhof, G.; Mark, A. E.; Berendsen, H. J. C., GROMACS: Fast, flexible, and free. *Journal of Computational Chemistry* **2005,** *26*, 1701-1718.
55. Essmann, U.; Perera, L.; Berkowitz, M. L.; Darden, T.; Lee, H.; Pedersen, L. G., A Smooth Particle Mesh Ewald Method. *Journal of Chemical Physics* **1995,** *103*, 8577-8593.
56. Berendsen, H. J. C.; Postma, J. P. M.; Vangunsteren, W. F.; Dinola, A.; Haak, J. R., Molecular-Dynamics With Coupling To An External Bath. *Journal of Chemical Physics* **1984,** *81*, 3684-3690.
57. Nose, S., A Unified Formulation Of The Constant Temperature Molecular-Dynamics Methods. *Journal of Chemical Physics* **1984,** *81*, 511-519.
58. Hoover, W. G., Canonical Dynamics - Equilibrium Phase-Space Distributions. *Physical Review A* **1985,** *31*, 1695-1697.
59. Parrinello, M.; Rahman, A., Polymorphic Transitions In Single-Crystals - A New Molecular-Dynamics Method. *Journal of Applied Physics* **1981,** *52*, 7182-7190.
60. Hess, B., P-LINCS: A parallel linear constraint solver for molecular simulation. *Journal of Chemical Theory and Computation* **2008,** *4*, 116-122.
61. Luzar, A.; Chandler, D., Hydrogen-bond kinetics in liquid water. *Nature* **1996,** *379*, 55-57.
62. Zavodszky, P.; Kardos, J.; Svingor, A.; Petsko, G. A., Adjustment of conformational flexibility is a key event in the thermal adaptation of proteins. *Proceedings of the National Academy of Sciences of the United States of America* **1998,** *95*, 7406-7411.
63. Daniel, R. M.; Dunn, R. V.; Finney, J. L.; Smith, J. C., The role of dynamics in enzyme activity. *Annual Review of Biophysics and Biomolecular Structure* **2003,** *32*, 69-92.
64. Henzler-Wildman, K. A.; Lei, M.; Thai, V.; Kerns, S. J.; Karplus, M.; Kern, D., A hierarchy of timescales in protein dynamics is linked to enzyme catalysis. *Nature* **2007,** *450*, 913-U27.
65. Alexander M, K., Why are enzymes less active in organic solvents than in water? *Trends in Biotechnology* **1997,** *15*, 97-101.
66. Bruinsma, G. M.; van der Mei, H. C.; Busscher, H. J., Bacterial adhesion to surface hydrophilic and hydrophobic contact lenses. *Biomaterials* **2001,** *22*, 3217-3224.
67. Zheng, J.; Li, L. Y.; Chen, S. F.; Jiang, S. Y., Molecular simulation study of water interactions with oligo (ethylene glycol)-terminated alkanethiol self-assembled monolayers. *Langmuir* **2004,** *20*, 8931-8938.
68. Shao, Q.; He, Y.; White, A. D.; Jiang, S. Y., Different effects of zwitterion and ethylene glycol on proteins. *Journal of Chemical Physics* **2012,** *136*.
69. Southall, N. T.; Dill, K. A.; Haymet, A. D. J., A view of the hydrophobic effect. *Journal of Physical Chemistry B* **2002,** *106*, 521-533.
70. Berne, B. J.; Weeks, J. D.; Zhou, R. H., Dewetting and Hydrophobic Interaction in Physical and Biological Systems. *Annual Review of Physical Chemistry* **2009,** *60*, 85-103.
71. Chandler, D., Interfaces and the driving force of hydrophobic assembly. *Nature* **2005,** *437*, 640-647.
72. Dyson, H. J.; Wright, P. E.; Scheraga, H. A., The role of hydrophobic interactions in initiation and propagation of protein folding. *Proceedings of the National Academy of Sciences of the United States of America* **2006,** *103*, 13057-13061.

73. Luo, Y.; Dinkel, P.; Yu, X.; Margittai, M.; Zheng, J.; Nussinov, R.; Wei, G.; Ma, B., Molecular insights into the reversible formation of tau protein fibrils. *Chemical Communications* **2013,** *49*, 3582-3584.
74. van Meer, G.; Voelker, D. R.; Feigenson, G. W., Membrane lipids: where they are and how they behave. *Nature Reviews Molecular Cell Biology* **2008,** *9*, 112-124.
75. Cozzini, P.; Fornabaio, M.; Marabotti, A.; Abraham, D. J.; Kellogg, G. E.; Mozzarelli, A., Free energy of ligand binding to protein: Evaluation of the contribution of water molecules by computational methods. *Current Medicinal Chemistry* **2004,** *11*, 3093-3118.
76. Huang, D. M.; Chandler, D., The hydrophobic effect and the influence of solute-solvent attractions. *Journal of Physical Chemistry B* **2002,** *106*, 2047-2053.
77. Zangi, R.; Hagen, M.; Berne, B. J., Effect of ions on the hydrophobic interaction between two plates. *Journal of the American Chemical Society* **2007,** *129*, 4678-4686.
78. Athawale, M. V.; Dordick, J. S.; Garde, S., Osmolyte trimethylamine-N-oxide does not affect the strength of hydrophobic interactions: Origin of osmolyte compatibility. *Biophysical Journal* **2005,** *89*, 858-866.
79. Zangi, R.; Zhou, R. H.; Berne, B. J., Urea's Action on Hydrophobic Interactions. *Journal of the American Chemical Society* **2009,** *131*, 1535-1541.
80. Jorgensen, W. L.; Chandrasekhar, J.; Madura, J. D.; Impey, R. W.; Klein, M. L., Comparison Of Simple Potential Functions For Simulating Liquid Water. *Journal of Chemical Physics* **1983,** *79*, 926-935.
81. Kast, K. M.; Brickmann, J.; Kast, S. M.; Berry, R. S., Binary phases of aliphatic N-oxides and water: Force field development and molecular dynamics simulation. *Journal of Physical Chemistry A* **2003,** *107*, 5342-5351.
82. Shao, Q.; Jiang, S. Y., Effect of Carbon Spacer Length on Zwitterionic Carboxybetaines. *Journal of Physical Chemistry B* **2013,** *117*, 1357-1366.
83. Hess, B.; Kutzner, C.; van der Spoel, D.; Lindahl, E., GROMACS 4: Algorithms for highly efficient, load-balanced, and scalable molecular simulation. *Journal of Chemical Theory and Computation* **2008,** *4*, 435-447.
84. Barducci, A.; Bussi, G.; Parrinello, M., Well-tempered metadynamics: A smoothly converging and tunable free-energy method. *Physical Review Letters* **2008,** *100*.
85. Laio, A.; Parrinello, M., Escaping free-energy minima. *Proceedings of the National Academy of Sciences of the United States of America* **2002,** *99*, 12562-12566.
86. Bussi, G.; Donadio, D.; Parrinello, M., Canonical sampling through velocity rescaling. *Journal of Chemical Physics* **2007,** *126*.
87. Bonomi, M.; Branduardi, D.; Bussi, G.; Camilloni, C.; Provasi, D.; Raiteri, P.; Donadio, D.; Marinelli, F.; Pietrucci, F.; Broglia, R. A.; Parrinello, M., PLUMED: A portable plugin for free-energy calculations with molecular dynamics. *Computer Physics Communications* **2009,** *180*, 1961-1972.
88. Lee, M. E.; van der Vegt, N. F. A., Does urea denature hydrophobic interactions? *Journal of the American Chemical Society* **2006,** *128*, 4948-4949.
89. England, J. L.; Haran, G., Role of Solvation Effects in Protein Denaturation: From Thermodynamics to Single Molecules and Back. *Annual Review of Physical Chemistry, Vol 62* **2011,** *62*, 257-277.
90. Israelachvili, J., The different faces of poly(ethylene glycol). *Proceedings of the National Academy of Sciences of the United States of America* **1997,** *94*, 8378-8379.
91. Ghosh, K.; Dill, K. A., Theory for Protein Folding Cooperativity: Helix Bundles. *Journal of the American Chemical Society* **2009,** *131*, 2306-2312.
92. Fatima, S.; Khan, R. H., Effect of polyethylene glycols on the function and structure of thiol proteases. *Journal of Biochemistry* **2007,** *142*, 65-72.

93. Kubetzko, S.; Sarkar, C. A.; Pluckthun, A., Protein PEGylation decreases observed target association rates via a dual blocking mechanism. *Molecular Pharmacology* **2005,** *68*, 1439-1454.
94. Castner, D. G.; Ratner, B. D., Biomedical surface science: Foundations to frontiers. *Surface Science* **2002,** *500*, 28-60.
95. Jiang, S. Y.; Cao, Z. Q., Ultralow-Fouling, Functionalizable, and Hydrolyzable Zwitterionic Materials and Their Derivatives for Biological Applications. *Advanced Materials* **2010,** *22*, 920-932.
96. *Poly(Ethylene Glycol) Chemistry: Biotechnical and Biomedical Applications*. Plenum Press: New York, 1992; p 408.
97. Ostuni, E.; Chapman, R. G.; Holmlin, R. E.; Takayama, S.; Whitesides, G. M., A Survey of Structure−Property Relationships of Surfaces that Resist the Adsorption of Protein. *Langmuir* **2001,** *17*, 5605-5620.
98. Gaberc-Porekar, V.; Zore, I.; Podobnik, B.; Menart, V., Obstacles and pitfalls in the PEGylation of therapeutic proteins. *Current Opinion in Drug Discovery & Development* **2008,** *11*, 242-250.
99. Zhang, Z.; Chao, T.; Chen, S. F.; Jiang, S. Y., Superlow fouling sulfobetaine and carboxybetaine polymers on glass slides. *Langmuir* **2006,** *22*, 10072-10077.
100. Zhang, Z.; Chen, S. F.; Chang, Y.; Jiang, S. Y., Surface grafted sulfobetaine polymers via atom transfer radical polymerization as superlow fouling coatings. *Journal of Physical Chemistry B* **2006,** *110*, 10799-10804.
101. Vaisocherova, H.; Yang, W.; Zhang, Z.; Cao, Z. Q.; Cheng, G.; Piliarik, M.; Homola, J.; Jiang, S. Y., Ultralow fouling and functionalizable surface chemistry based on a zwitterionic polymer enabling sensitive and specific protein detection in undiluted blood plasma. *Analytical Chemistry* **2008,** *80*, 7894-7901.
102. Yang, W.; Chen, S. F.; Cheng, G.; Vaisocherova, H.; Xue, H.; Li, W.; Zhang, J. L.; Jiang, S. Y., Film thickness dependence of protein adsorption from blood serum and plasma onto poly(sulfobetaine)-grafted surfaces. *Langmuir* **2008,** *24*, 9211-9214.
103. He, Y.; Chang, Y.; Hower, J. C.; Zheng, J.; Chen, S. F.; Jiang, S., Origin of repulsive force and structure/dynamics of interfacial water in OEG-protein interactions: a molecular simulation study. *Physical Chemistry Chemical Physics* **2008,** *10*, 5539-5544.
104. Hower, J. C.; He, Y.; Jiang, S. Y., A molecular simulation study of methylated and hydroxyl sugar-based self-assembled monolayers: Surface hydration and resistance to protein adsorption. *Journal of Chemical Physics* **2008,** *129*.
105. Hower, J. C.; Bernards, M. T.; Chen, S. F.; Tsao, H. K.; Sheng, Y. J.; Jiang, S. Y., Hydration of "Nonfouling" Functional Groups. *Journal of Physical Chemistry B* **2009,** *113*, 197-201.
106. Rasaiah, J. C.; Noworyta, J. P.; Koneshan, S., Structure of aqueous solutions of tons and neutral solutes at infinite dilution at a supercritical temperature of 683 K. *Journal of the American Chemical Society* **2000,** *122*, 11182-11193.
107. Shao, Q.; Zhou, J.; Lu, L. H.; Lu, X. H.; Zhu, Y. D.; Jiang, S. Y., Anomalous Hydration Shell Order of Na+ and K+ inside Carbon Nanotubes. *Nano Letters* **2009,** *9*, 989-994.
108. Deng, Y. Q.; Roux, B., Hydration of amino acid side chains: Nonpolar and electrostatic contributions calculated from staged molecular dynamics free energy simulations with explicit water molecules. *Journal of Physical Chemistry B* **2004,** *108*, 16567-16576.
109. Shirts, M. R.; Pande, V. S., Solvation free energies of amino acid side chain analogs for common molecular mechanics water models. *Journal of Chemical Physics* **2005,** *122*.
110. Zhou, J.; Lu, X. H.; Wang, Y. R.; Shi, J., Molecular dynamics study on ionic hydration. *Fluid Phase Equilibria* **2002,** *194*, 257-270.

111. Shao, Q.; Huang, L. L.; Zhou, J.; Lu, L. H.; Zhang, L. Z.; Lu, X. H.; Jiang, S. Y.; Gubbins, K. E.; Shen, W. F., Molecular simulation study of temperature effect on ionic hydration in carbon nanotubes. *Physical Chemistry Chemical Physics* **2008,** *10*, 1896-1906.
112. Dastidar, S. G.; Mukhopadhyay, C., Structure, dynamics, and energetics of water at the surface of a small globular protein: A molecular dynamics simulation. *Physical Review E* **2003,** *68*.
113. Chung, Y. H.; Xia, J. C.; Margulis, C. J., Diffusion and residence time of hydrogen peroxide and water in crowded protein environments. *Journal of Physical Chemistry B* **2007,** *111*, 13336-13344.
114. Noworyta, J. P.; Koneshan, S.; Rasaiah, J. C., Dynamics of aqueous solutions of ions and neutral solutes at infinite dilution at a supercritical temperature of 683 K. *Journal of the American Chemical Society* **2000,** *122*, 11194-11202.
115. Marcus, Y., Thermodynamics Of Solvation Of Ions .5. Gibbs Free-Energy Of Hydration At 298.15-K. *Journal of the Chemical Society-Faraday Transactions* **1991,** *87*, 2995-2999.
116. Hummer, G.; Pratt, L. R.; Garcia, A. E., Free energy of ionic hydration. *Journal of Physical Chemistry* **1996,** *100*, 1206-1215.
117. Chambers, C. C.; Hawkins, G. D.; Cramer, C. J.; Truhlar, D. G., Model for aqueous solvation based on class IV atomic charges and first solvation shell effects. *Journal of Physical Chemistry* **1996,** *100*, 16385-16398.
118. Iwasaki, Y.; Ishihara, K., Phosphorylcholine-containing polymers for biomedical applications. *Analytical and Bioanalytical Chemistry* **2005,** *381*, 534-546.
119. Zhang, L.; Xue, H.; Gao, C. L.; Carr, L.; Wang, J. N.; Chu, B. C.; Jiang, S. Y., Imaging and cell targeting characteristics of magnetic nanoparticles modified by a functionalizable zwitterionic polymer with adhesive 3,4-dihydroxyphenyl-L-alanine linkages. *Biomaterials* **2010,** *31*, 6582-6588.
120. Carr, L. R.; Xue, H.; Jiang, S. Y., Functionalizable and nonfouling zwitterionic carboxybetaine hydrogels with a carboxybetaine dimethacrylate crosslinker. *Biomaterials* **2011,** *32*, 961-968.
121. Georgiev, G. S.; Karnenska, E. B.; Vassileva, E. D.; Kamenova, I. P.; Georgieva, V. T.; Iliev, S. B.; Ivanov, I. A., Self-assembly, anti polyelectrolyte effect, and nonbiofouling properties of polyzwitterions. *Biomacromolecules* **2006,** *7*, 1329-1334.
122. Das, M.; Sanson, N.; Kumacheva, E., Zwitterionic Poly(betaine-N-isopropylacrylamide) Microgels: Properties and Applications. *Chemistry of Materials* **2008,** *20*, 7157-7163.
123. Kumar, R.; Fredrickson, G. H., Theory of polyzwitterion conformations. *Journal of Chemical Physics* **2009,** *131*.
124. Kunz, W.; Henle, J.; Ninham, B. W., 'Zur Lehre von der Wirkung der Salze' (about the science of the effect of salts): Franz Hofmeister's historical papers. *Current Opinion in Colloid & Interface Science* **2004,** *9*, 19-37.
125. Collins, K. D., Charge density-dependent strength of hydration and biological structure. *Biophysical Journal* **1997,** *72*, 65-76.
126. Collins, K. D.; Neilson, G. W.; Enderby, J. E., Ions in water: Characterizing the forces that control chemical processes and biological structure. *Biophysical Chemistry* **2007,** *128*, 95-104.
127. Kunz, W., Specific ion effects in colloidal and biological systems. *Current Opinion in Colloid & Interface Science* **2010,** *15*, 34-39.
128. Collins, K. D., Ions from the Hofmeister series and osmolytes: effects on proteins in solution and in the crystallization process. *Methods* **2004,** *34*, 300-311.
129. Vlachy, N.; Jagoda-Cwiklik, B.; Vacha, R.; Touraud, D.; Jungwirth, P.; Kunz, W., Hofmeister series and specific interactions of charged headgroups with aqueous ions. *Advances in Colloid and Interface Science* **2009,** *146*, 42-47.

130. Hess, B.; van der Vegt, N. F. A., Cation specific binding with protein surface charges. *Proceedings of the National Academy of Sciences of the United States of America* **2009,** *106*, 13296-13300.
131. Tobias, D. J.; Hemminger, J. C., Getting Specific About Specific Ion Effects. *Science* **2008,** *319*, 1197-1198.
132. Lund, M.; Vrbka, L.; Jungwirth, P., Specific ion binding to nonpolar surface patches of proteins. *Journal of the American Chemical Society* **2008,** *130*, 11582-+.
133. Vrbka, L.; Mucha, M.; Minofar, B.; Jungwirth, P.; Brown, E. C.; Tobias, D. J., Propensity of soft ions for the air/water interface. *Current Opinion in Colloid & Interface Science* **2004,** *9*, 67-73.
134. Jungwirth, P.; Tobias, D. J., Specific ion effects at the air/water interface. *Chemical Reviews* **2006,** *106*, 1259-1281.
135. Zangi, R., Can Salting-In/Salting-Out Ions be Classified as Chaotropes/Kosmotropes? *Journal of Physical Chemistry B* **2010,** *114*, 643-650.
136. Martinez, L.; Andrade, R.; Birgin, E. G.; Martinez, J. M., PACKMOL: A Package for Building Initial Configurations for Molecular Dynamics Simulations. *Journal of Computational Chemistry* **2009,** *30*, 2157-2164.
137. Aqvist, J., Ion Water Interaction Potentials Derived From Free-Energy Perturbation Simulations. *Journal of Physical Chemistry* **1990,** *94*, 8021-8024.
138. Schulz, D. N.; Peiffer, D. G.; Agarwal, P. K.; Larabee, J.; Kaladas, J. J.; Soni, L.; Handwerker, B.; Garner, R. T., Phase-Behavior And Solution Properties Of Sulfobetaine Polymers. *Polymer* **1986,** *27*, 1734-1742.
139. Han, D. Z.; Letteri, R.; Chan-Seng, D.; Emrick, T.; Tu, H. L., Examination of zwitterionic polymers and gels subjected to mechanical constraints. *Polymer* **2013,** *54*, 2887-2894.
140. Yang, Q.; Ulbricht, M., Novel Membrane Adsorbers with Grafted Zwitterionic Polymers Synthesized by Surface-Initiated ATRP and Their Salt-Modulated Permeability and Protein Binding Properties. *Chemistry of Materials* **2012,** *24*, 2943-2951.
141. Ning, J.; Li, G.; Haraguchi, K., Synthesis of Highly Stretchable, Mechanically Tough, Zwitterionic Sulfobetaine Nanocomposite Gels with Controlled Thermosensitivities. *Macromolecules* **2013,** *46*, 5317-5328.
142. Gauthier, M.; Carrozzella, T.; Snell, G., Sulfobetaine zwitterionomers based on n-butyl acrylate and 2-ethoxyethyl acrylate: Physical properties. *Journal of Polymer Science Part B: Polymer Physics* **2002,** *40*, 2303-2312.
143. Shao, Q.; He, Y.; Jiang, S. Y., Molecular Dynamics Simulation Study of Ion Interactions with Zwitterions. *Journal of Physical Chemistry B* **2011,** *115*, 8358-8363.
144. Fennell, C. J.; Bizjak, A.; Vlachy, V.; Dill, K. A., Ion Pairing in Molecular Simulations of Aqueous Alkali Halide Solutions. *Journal of Physical Chemistry B* **2009,** *113*, 6782-6791.
145. Zheng, J.; He, Y.; Chen, S. F.; Li, L. Y.; Bernards, M. T.; Jiang, S. Y., Molecular simulation studies of the structure of phosphorylcholine self-assembled monolayers. *Journal of Chemical Physics* **2006,** *125*.
146. Hanson, A. D.; Rathinasabapathi, B.; Rivoal, J.; Burnet, M.; Dillon, M. O.; Gage, D. A., Osmoprotective Compounds In The Plumbaginaceae - A Natural Experiment In Metabolic Engineering Of Stress Tolerance. *Proceedings of the National Academy of Sciences of the United States of America* **1994,** *91*, 306-310.
147. Carr, L. R.; Krause, J. E.; Ella-Menye, J. R.; Jiang, S. Y., Single nonfouling hydrogels with mechanical and chemical functionality gradients. *Biomaterials* **2011,** *32*, 8456-8461.
148. Weers, J. G.; Rathman, J. F.; Axe, F. U.; Crichlow, C. A.; Foland, L. D.; Scheuing, D. R.; Wiersema, R. J.; Zielske, A. G., Effect of the intramolecular charge separation distance on the solution properties of betaines and sulfobetaines. *Langmuir* **1991,** *7*, 854-867.

149. Zhou, T. H.; Zhao, J. X.; You, Y., Effect of the Interionic Distance on the Interfacial Behavior of Double-Chain Zwitterionic Amphiphiles. *Journal of Dispersion Science and Technology* **2009,** *30*, 1135-1141.
150. Zhang, Z.; Vaisocherova, H.; Cheng, G.; Yang, W.; Xue, H.; Jiang, S. Y., Nonfouling Behavior of Polycarboxybetaine-Grafted Surfaces: Structural and Environmental Effects. *Biomacromolecules* **2008,** *9*, 2686-2692.
151. Vaisocherova, H.; Zhang, Z.; Yang, W.; Cao, Z.; Cheng, G.; Taylor, A. D.; Piliarik, M.; Homola, J.; Jiang, S., Functionalizable surface platform with reduced nonspecific protein adsorption from full blood plasma-Material selection and protein immobilization optimization. *Biosensors & Bioelectronics* **2009,** *24*, 1924-1930.
152. Mi, L.; Giarmarco, M. M.; Shao, Q.; Jiang, S., Divalent cation-mediated polysaccharide interactions with zwitterionic surfaces. *Biomaterials* **2012,** *33*, 2001-2006.
153. Abraham, S.; So, A.; Unsworth, L. D., Poly(carboxybetaine methacrylamide)-Modified Nanoparticles: A Model System for Studying the Effect of Chain Chemistry on Film Properties, Adsorbed Protein Conformation, and Clot Formation Kinetics. *Biomacromolecules* **2011,** *12*, 3567-3580.
154. Bohrisch, J.; Schimmel, T.; Engelhardt, H.; Jaeger, W., Charge interaction of synthetic polycarboxybetaines in bulk and solution. *Macromolecules* **2002,** *35*, 4143-4149.
155. Favresse, P.; Laschewsky, A., New poly(carbobetaine)s made from zwitterionic diallylammonium monomers. *Macromolecular Chemistry and Physics* **1999,** *200*, 887-895.
156. Delgado, C.; Merchan, M. D.; Velazquez, M. M.; Anaya, J., Effect of surfactant structure on the adsorption of carboxybetaines at the air-water interface. *Colloids and Surfaces a-Physicochemical and Engineering Aspects* **2006,** *280*, 17-22.
157. MacDonald, A. M.; Sheppard, M. A. W.; Lucy, C. A., Enhancement of electroosmotic flow using zwitterionic additives. *Electrophoresis* **2005,** *26*, 4421-4428.
158. Bagchi, B., Water Dynamics in the Hydration Layer around Proteins and Micelles. *Chemical Reviews* **2005,** *105*, 3197-3219.
159. Chen, S.; Li, L.; Zhao, C.; Zheng, J., Surface hydration: Principles and applications toward low-fouling/nonfouling biomaterials. *Polymer* **2010,** *51*, 5283-5293.
160. Christenson, H. K.; Claesson, P. M., Direct measurements of the force between hydrophobic surfaces in water. *Advances in Colloid and Interface Science* **2001,** *91*, 391-436.
161. Meyer, E. E.; Rosenberg, K. J.; Israelachvili, J., Recent progress in understanding hydrophobic interactions. *Proceedings of the National Academy of Sciences of the United States of America* **2006,** *103*, 15739-15746.
162. He, Y.; Shao, Q.; Chen, S. F.; Jiang, S. Y., Chaotrope vs. kosmotrope: Which one has lower friction? *Journal of Chemical Physics* **2011,** *135*.
163. Chen, M.; Briscoe, W. H.; Armes, S. P.; Klein, J., Lubrication at Physiological Pressures by Polyzwitterionic Brushes. *Science* **2009,** *323*, 1698-1701.
164. Rappe, A. K.; Casewit, C. J.; Colwell, K. S.; Goddard, W. A.; Skiff, W. M., UFF, A Full Periodic-Table Force-Field For Molecular Mechanics And Molecular-Dynamics Simulations. *Journal of the American Chemical Society* **1992,** *114*, 10024-10035.
165. Miertuš S.; Scrocco E.; Tomasi J., Electrostatic Interaction of a Solute with a Continuum. A Direct Utilization of ab initio Molecular Potentials for the Prevision of Solvent Effects. *Chem. Phys.* **1981,** *55*, 117-129.
166. Chirlian, L. E.; Francl, M. M., Atomic Charges Derived From Electrostatic Potentials - A Detailed Study. *Journal of Computational Chemistry* **1987,** *8*, 894-905.
167. Bader, R., *Atoms in Molecules: A Quantum Theory*. Oxford University Press: New York, 1990.
168. Henkelman, G.; Arnaldsson, A.; Jonsson, H., A fast and robust algorithm for Bader decomposition of charge density. *Computational Materials Science* **2006,** *36*, 354-360.

169. Gallicchio, E.; Kubo, M. M.; Levy, R. M., Enthalpy−Entropy and Cavity Decomposition of Alkane Hydration Free Energies: Numerical Results and Implications for Theories of Hydrophobic Solvation. *The Journal of Physical Chemistry B* **2000,** *104*, 6271-6285.
170. Shao, Q.; White, A. D.; Jiang, S., Difference of Carboxybetaine and Oligo(ethylene glycol) Moieties in Altering Hydrophobic Interactions: A Molecular Simulation Study. *The Journal of Physical Chemistry B* **2013,** *118*, 189-194.
171. Zhang, Y. J.; Cremer, P. S., Interactions between macromolecules and ions: the Hofmeister series. *Current Opinion in Chemical Biology* **2006,** *10*, 658-663.
172. Jungwirth, P.; Winter, B., Ions at aqueous interfaces: From water surface to hydrated proteins. *Annual Review of Physical Chemistry* **2008,** *59*, 343-366.
173. Parsons, D. F.; Bostrom, M.; Lo Nostro, P.; Ninham, B. W., Hofmeister effects: interplay of hydration, nonelectrostatic potentials, and ion size. *Physical Chemistry Chemical Physics* **2011,** *13*, 12352-12367.
174. Azzaroni, O.; Brown, A. A.; Huck, W. T. S., UCST wetting transitions of polyzwitterionic brushes driven by self-association. *Angewandte Chemie-International Edition* **2006,** *45*, 1770-1774.
175. Jorgensen, W. L.; Madura, J. D., Temperature And Size Dependence For Monte-Carlo Simulations Of Tip4p Water. *Molecular Physics* **1985,** *56*, 1381-1392.
176. Sundaram, H. S.; Ella-Menye, J.-R.; Brault, N. D.; Shao, Q.; Jiang, S., Reversibly switchable polymer with cationic/zwitterionic/anionic behavior through synergistic protonation and deprotonation. *Chemical Science* **2014,** *5*, 200-205.

Qing Shao (qshao@uw.edu)
Benson Hall 337, University of Washington, Seattle, WA 98195 office: (206)616-6510, mobile:(206)434-1209

Education

2000-2004	Nanjing University of Technology, Chemical Engineering, Bachelor
2009-2011	University of Washington, Seattle, Chemical Engineering, Master
2009-present	University of Washington, Seattle, Chemical Engineering, Ph.D. candidate

Research Interests

Biomolecular Interactions Biomaterial Design Porous Materials Energy Storage
Membrane Separation Surface Science

Research Experience

2009-present Department of Chemical Engineering, University of Washington,
Advisor: Prof. Shaoyi Jiang

1. Developed the force field parameters for zwitterion molecules
2. Studied structure-hydration relationship of zwitterion molecules
3. Investigated ionic interactions of zwitterion molecules
4. Studied effects of zwitterion molecules on hydrophobic interactions
5. Studied zwitterion-protein interactions
6. Investigate conformations of polyzwitterions

2004-2009 State Key Laboratory of Material-oriented Chemical Engineering, Nanjing University of Technology

1. Studied structure of ethanol molecules in carbon nanotubes
2. Investigated ionic hydration in carbon nanotubes

Teaching Experience

Winter, 2011, Thermodynamics (CHEM E 326), Teaching Assistant
Spring, 2012, Introduction to Molecular and Nanoscale Principles (NME220), Teaching Assistant
Winter, 2013, Chemical Engineering Thermodynamics (CHEM E 326), Teaching Assistant
Spring, 2013, Process Design II (CHEM E 486), Teaching Assistant

Other Activities

Prepared research and renewal proposals for XSEDE supercomputer allocations (awarded)
Prepared NSF proposals about zwitterionic materials (awarded)
Organized the Distinguished Young Scholar Seminar Series 2013

Award

FOMMS 2012 Fellowship

Publications (cited by over 200 articles, h-index: 9)

(1) **Shao, Q.;** Jiang, S. Y., Effects of carbon spacer length on zwitterionic carboxybetaines. Journal of Physical Chemistry B 2013,117 (5), 1357–1366.
(2) **Shao, Q.;** He, Y.; White, A. D.; Jiang, S. Y., Different effects of zwitterion and ethylene glycol on proteins. Journal of Chemical Physics 2012, 136 (22) 225101.
(3) **Shao, Q.;** He, Y.; Jiang, S. Y., Molecular Dynamics Simulation Study of Ion Interactions with Zwitterions. Journal of Physical Chemistry B 2011, 115 (25), 8358-8363.
(4) **Shao, Q.;** He, Y.; White, A. D.; Jiang, S. Y., Difference in Hydration between Carboxybetaine and Sulfobetaine. Journal of Physical Chemistry B 2010, 114 (49), 16625-16631.
(5) **Shao, Q.;** White, A. D.; Jiang, S. Y., Difference of Carboxybetaine and Oligo(ethylene glycol) Moieties in Altering Hydrophobic Interactions: A Molecular Simulation Study. Journal of Physical Chemistry B, 2014, 118 (1), 189-194.
(6) **Shao, Q.;** Mi L., Bai T., Han X., Liu S., Li Y. T.; and Jiang S. Y., Similarity in Cationic and Anionic Charge Strengths Determines Zwitterionic Associations and Stimuli Responses. S*ubmitted.*

(7) **Shao, Q.;** Jiang, S. Y., Understanding Properties of Zwitterionic Materials from Their Molecular Structure. *In Preparation*.
(8) **Shao, Q.;** Jiang, S. Y., Role of Charged Groups in Properties of Zwitterionic Molecules . *In Preparation*.
(9) **Shao, Q.;** Zhou, J.; Lu, L. H.; Lu, X. H.; Zhu, Y. D.; Jiang, S. Y., Anomalous Hydration Shell Order of Na^+ and K^+ inside Carbon Nanotubes. Nano Letters 2009, 9 (3), 989-994.
(10) **Shao, Q.;** Lu, L. H.; Lu, X. H.; Wei, M. J.; Zhu, Y. D.; Shen, W. F., Molecular Simulation of Solute Hydration Structure in Nanoscale Confinement. Acta Physico-Chimica Sinica 2009, 25 (3), 583-589.
(11) **Shao, Q.;** Huang, L. L.; Zhou, J.; Lu, L. H.; Zhang, L. Z.; Lu, X. H.; Jiang, S. Y.; Gubbins, K. E.; Shen, W. F., Molecular simulation study of temperature effect on ionic hydration in carbon nanotubes. Physical Chemistry Chemical Physics 2008, 10 (14), 1896-1906.
(12) **Shao, Q.;** Huang, L. L.; Zhou, J.; Lu, L. H.; Zhang, L. Z.; Lu, X. H.; Jiang, S. Y.; Gubbins, K. E.; Zhu, Y. D.; Shen, W. F., Molecular dynamics study on diameter effect in structure of ethanol molecules confined in single-walled carbon nanotubes. Journal of Physical Chemistry C 2007, 111 (43), 15677-15685.
(13) **Shao, Q.;** Huang, L. L.; Lu, X. H.; Lu, L. H.; Zhu, Y. D.; Shen, W. F., Molecular simulation study of the structure and diffusion of ethanol molecules confined in carbon nanotubes. Acta Chimica Sinica 2007, 65 (20), 2217-2223.
(14) Sundaram, H. S.; Ella-Menye, J. R.; Brault N. D.; **Shao Q.**; Jiang S. Y., Reversibly switchable polymer with cationic/zwitterionic/anionic behavior through synergistic protonation and deprotonation. **Chem. Sci.,** 2013, **DOI:** 10.1039/C3SC52233D.
(15) White, A. D.; Keefe, A. J.; Ella-Menye, J.-R.; Nowinski, A. K.; **Shao, Q.;** Pfaendtner, J.; Jiang, S., Free Energy of Solvated Salt Bridges: A Simulation and Experimental Study. The Journal of Physical Chemistry B 2013, 117 (24), 7254-7259.
(16) White, A. D.; Keefe, A. J.; Nowinski, A. K.; **Shao, Q.;** Caldwell, K.; Jiang, S., Standardizing and Simplifying Analysis of Peptide Library Data. Journal of Chemical Information and Modeling 2013, 53 (2), 493-499.
(17) Mi, L.; Giarmarco, M. M.; **Shao, Q.;** Jiang, S. Y., Divalent cation-mediated polysaccharide interactions with zwitterionic surfaces. Biomaterials 2012, 33 (7), 2001-2006.
(18) He, Y.; **Shao, Q.;** Tsao, H. K.; Chen, S. F.; Goddard, W. A.; Jiang, S. Y., Understanding Three Hydration-Dependent Transitions of Zwitterionic Carboxybetaine Hydrogel by Molecular Dynamics Simulations. Journal of Physical Chemistry B 2011, 115 (40), 11575-11580.
(19) He, Y.; **Shao, Q.;** Chen, S. F.; Jiang, S. Y., Water Mobility: A Bridge between the Hofmeister Series of Ions and the Friction of Zwitterionic Surfaces in Aqueous Environments. Journal of Physical Chemistry C 2011, 115 (31), 15525-15531.
(20) He, Y.; **Shao, Q.;** Chen, S. F.; Jiang, S. Y., Chaotrope vs. kosmotrope: Which one has lower friction? Journal of Chemical Physics 2011, 135 (15).
(21) Zhu, Y. D.; Guo, X. J.; **Shao, Q.;** Wei, M. J.; Wu, X. M.; Lu, L. H.; Lu, X. H., Molecular simulation study of the effect of inner wall modified groups on ionic hydration confined in carbon nanotube. Fluid Phase Equilibria 2010, 297 (2), 215-220.
(22) Guo, X. J.; **Shao, Q.;** Lu, L. H.; Zhu, Y. D.; Wei, M. J.; Lu, X. H., Molecular Dynamics Simulation Study of Ionic Hydration in Negatively Charged Single-Walled Carbon Nanotubes. Journal of Nanoscience and Nanotechnology 2010, 10 (11), 7620-7624.
(23) Zhu, Y. D.; Wei, M. J.; **Shao, Q.;** Lu, L. H.; Lu, X. H.; Shen, W. F., Molecular Dynamics Study of Pore Inner Wall Modification Effect in Structure of Water Molecules Confined in Single-Walled Carbon Nanotubes. Journal of Physical Chemistry C 2009, 113 (3), 882-889.
(24) Lu, L. H.; **Shao, Q.;** Huang, L. L.; Lu, X. H., Simulation of adsorption and separation of ethanol-water mixture with zeolite and carbon nanotube. Fluid Phase Equilibria 2007, 261 (1-2), 191-198; (r) Lu, L. H.; Lu, X. H.; Chen, Y. P.; Huang, L. L.; Shao, Q.; Wang, Q., Monte Carlo simulation of adsorption of binary and quaternary alkane isomers mixtures in zeolites: Effect of pore size and structure. Fluid Phase Equilibria 2007, 259 (2), 135-145.
(25) Huang, L. L.; Zhang, L. Z.; **Shao, Q.;** Lu, L. H.; Lu, X. H.; Jiang, S. Y.; Shen, W. F., Simulations of binary mixture adsorption of carbon dioxide and methane in carbon nanotubes: Temperature, pressure, and pore size effects. Journal of Physical Chemistry C 2007, 111 (32), 11912-11920.
(26) Chen, Y. P.; Lu, L. H.; **Shao, Q.;** Huang, L. L.; Lu, X. H., Adsorption and diffusion of alkanes in mordenite. Acta Physico-Chimica Sinica 2007, 23 (6), 905-910.

(27) Huang, L. L.; Zhang, L. Z.; **Shao, Q.;** Wang, J.; Lu, L. H.; Lu, X. H.; Jiang, S. Y.; Shen, W. F., Molecular dynamics simulation study of the structural characteristics of water molecules confined in functionalized carbon nanotubes. Journal of Physical Chemistry B 2006, 110 (51), 25761-25768.
(28) Huang, L. L.; **Shao, Q.;** Lu, L. H.; Lu, X. H.; Zhang, L. Z.; Wang, J.; Jiang, S. Y., Helicity and temperature effects on static properties of water molecules confined in modified carbon nanotubes. Physical Chemistry Chemical Physics 2006, 8 (33), 3836-3844.

Presentations

(1) **Shao, Q.;** He, Y.; White, A. D.; Jiang, S. Y., "*Hydration Difference between Carboxybetaine and Sulfobetaine",* Gordon Research Conference: Water & Aqueous Solutions, Poster, August 2010, Holderness, NH.
(2) **Shao, Q.;** Jiang, S. Y., "*Molecular Dynamics Simulation Study of Hydration of Zwitterions*", 2010 AIChE Annual Meeting, Oral Presentation, October 2010, Salt Lake City, UT.
(3) **Shao, Q.;** Jiang, S. Y., "*Comparison of Poly (ethylene glycol) and Zwitterionic Materials for Their Interactions with Proteins: a Molecular Dynamics Simulation",* 2011 AIChE Annual Meeting, Oral Presentation, October 2011, Minneapolis, MN.
(4) **Shao, Q.;** He, Y.; Jiang, S. Y., "*Molecular Simulation Study of Zwitterion-Ion Association",* 2011 AIChE Annual Meeting, Oral Presentation, October 2011, Minneapolis, MN.
(5) **Shao, Q.;** Jiang, S. Y., "*Molecular Simulation of Hydration of Zwitterion Hydrophobic Association with Amphiphilic and Superhydrophilic Cosolutes"* 2012 AIChE Annual Meeting, Oral Presentation, Pittsburgh, PA.
(6) **Shao, Q.;** He, Y.; White, A. D.; Jiang, S. Y., "*Molecular Simulation of Hydration of Zwitterion"* 2012 AIChE Annual Meeting, Oral Presentation, Pittsburgh, PA
(7) **Shao, Q.;** He, Y.; White, A. D.; Jiang, S. Y., "*Molecular Simulation of Zwitterions"* FOMMS 2012, Poster, Mt. Hood, OR.
(8) **Shao, Q.;** Jiang, S. Y., "Different Self-Associations of Carboxybetaine and Sulfobetaine", AIChE Annual Meeting, Oral Presentation, November 2013, San Francisco, CA.
(9) **Shao, Q.;** Jiang, S. Y., "Molecular Understanding of the Hydration of Zwitterionic Moieties: Effect of Charged Groups", AIChE Annual Meeting, Oral Presentation, November 2013, San Francisco, CA.

Book Chapter

Liu, C.; Ji, Y.; **Shao, Q.;** Feng, X.; Lu, X. In *Molecular Therodynamics of Complex Systems*; Lu, X., Hu, Y., Eds. 2009; Vol. 131, p 193.